Published in final edited form as:

Analyst. 2018 July 21; 143(14): 3249–3283. doi:10.1039/c8an00731d.

Optical Assays Based on Colloidal Inorganic Nanoparticles

Amir Ghasemi[1,3], **Navid Rabiee**[2], **Sepideh Ahmadi**[3,4], **Shabnam Hashemzadeh**[5,6], **Farshad Lolasi**[7,8], **Mahnaz Bozorgomid**[9], **Alireza Kalbasi**[10], **Behzad Nasseri**[11,12], **Amin Shiralizadeh Dezfuli**[3,13], **Amir Reza Aref**[13], **Mahdi Karimi**[14,15,16,*], and **Michael R. Hamblin**[16,17,18,*]

[1]Department of Materials Science and Engineering, Sharif University of Technology, Tehran, Iran

[2]Department of Chemistry, Shahid Beheshti University, Tehran, Iran

[3]Advances Nanobiotechnology and Nanomedicine Research Group (ANNRG), Iran University of Medical Sciences, Tehran, Iran

[4]Department of Biology, Faculty of Basic Sciences, University of Zabol, Zabol, Iran

[5]Department of Medical Physics and Biomedical Engineering, Faculty of Medicine, Shahid Beheshti University of Medical Sciences, Tehran, Iran

[6]Research Center for Pharmaceutical Nanotechnology, Biomedicine Institute, Tabriz University of Medical Science, Tabriz, Iran

[7]Department of Biotechnology, Faculty of Advanced Sciences and Technologies, University of Isfahan, Isfahan, 81746-73441, Iran

[8]Department of Agronomy and Plant Breeding, College of Agriculture, Isfahan University of Technology, Isfahan, Iran

[9]Department of Pharmaceutical Chemistry, Islamic Azad University of Pharmaceutical Sciences Branch, Tehran, Iran

[10]Department of Medical Oncology, Dana-Farber Cancer Institute, Boston, MA, USA

[11]Departments of Microbiology and Microbial Biotechnology and Nanobiotechnology, Faculty of Life Sciences and Biotechnology, Shahid Beheshti University, Tehran, Iran

[12]Chemical Engineering Deptartment and Bioengineeing Division, Hacettepe University, 06800, Beytepe, Ankara, Turkey

[13]Belfer Center for Applied Cancer Science, Dana-Farber Cancer Institute, Harvard Medical School, Boston, MA, USA

[14]Cellular and Molecular Research Center, Iran University of Medical Sciences, Tehran, Iran

[15]Department of Medical Nanotechnology, Faculty of Advanced Technologies in Medicine, Iran University of Medical Sciences, Tehran, Iran

[*]Corresponding author: m_karimy2006@yahoo.com, karimi.m@iums.ac.ir (Mahdi Karimi). [*]Corresponding author: Hamblin@helix.mgh.harvard.edu (Michael R. Hamblin).

Transparency Declaration. The authors have declared that no competing interests exist.

[16]Wellman Center for Photomedicine, Massachusetts General Hospital, Harvard Medical School, Boston, MA, 02114, USA

[17]Department of Dermatology, Harvard Medical School, Boston, MA 02115, USA

[18]Harvard-MIT Division of Health Sciences and Technology, Cambridge, MA, 02139, USA

Abstract

Colloidal inorganic nanoparticles have wide applications in the detection of analytes and in biological assays. A large number of these assays rely on the ability of gold nanoparticles (AuNPs, in the 20-nm diameter size range) to undergo a color change from red to blue upon aggregation. AuNP assays can be based on cross-linking, non-cross linking or unmodified charge-based aggregation. Nucleic acid-based probes, monoclonal antibodies, and molecular-affinity agents can be attached by covalent or non-covalent means. Surface plasmon resonance and SERS techniques can be utilized. Silver NPs also have attractive optical properties (higher extinction coefficient). Combinations of AuNPs and AgNPs in nanocomposites can have additional advantages. Magnetic NPs and ZnO, TiO_2 and ZnS as well as insulator NPs including SiO_2 can be employed in colorimetric assays, and some can act as peroxidase mimics in catalytic applications. This review covers the synthesis and stabilization of inorganic NPs and their diverse applications in colorimetric and optical assays for analytes related to environmental contamination (metal ions and pesticides), and for early diagnosis and monitoring of diseases, using medically important biomarkers.

Keywords

Colorimetric assays; environmental contaminants; disease biomarkers; gold and silver nanoparticles; cross-linking and non-cross-linking; surface plasmon resonance

1- Introduction

Early detection of diseases such as cancer and infection is an effective way to prevent them from spreading. Diagnostic procedures based on serological, biochemical, molecular, and staining methods have been used to detect many diseases, such as cancer, infectious agents, proteins, and potentially toxic metal ions [1–6]. Such methods, however, have many disadvantages, including the need for expensive equipment, lengthy procedures, inefficient detection rates, and poor detection thresholds. Biochemical tests are usually time-consuming and expensive to implement. Moreover, they can have low sensitivity and specificity, giving false positive and negative reactions along with insufficient accuracy. Diagnosis based on serological methods, may not be suitable for early detection of disease due to inadequate production of antibodies, the required long time to obtain results, and the need for complex facilities [7–9].

Nanotechnology is concerned with the production, investigation, and application of materials at the nanometer scale. When the size of the particles is in the nanometer range, their physical and chemical properties vary markedly from the properties of the same bulk material [10]. Nanoparticles are considered to be one of the most important types of

nanomaterials, which have diameters less than 100 nm, and can take various forms depending on their material type and synthetic procedure [11]. Inorganic nanoparticles have played an important role in development of nano-biosensors [12]. The properties of inorganic nanoparticles, such as their optical (metal nanoparticles), electrical, magnetic (iron oxide or cobalt nanoparticles), and catalytic (metal nanoparticles, oxide and quantum nanoparticles) properties, depend strongly on the type of material they are composed of [13, 14]. Their optical properties, especially fluorescence-based techniques, have been investigated due to their tunable features and conditions. These techniques are based on the fluorescence resonance energy transfer (FRET), photobleaching mechanism and tuning the luminescence quantum yield. To be exact, conjugation of metallic NPs to an active fluorophore molecule (sensitizer) has led to the development of accessible, inexpensive and environmentally-friendly devices for early diagnosis and monitoring treatment procedures[15–17]. Because of these beneficial features, these devices have gathered a varied range of applications in diagnosis and treatment [18], gene therapy [19], drug delivery [20], etc. Gold nanoparticles (AuNPs) and silver nanoparticles (AgNPs), which have properties such as surface plasmon resonance (SPR), undergo visible color and spectral changes, and unique optical features, are widely used in colorimetric techniques [21]. Magnetic nanoparticles (MNPs) are also important in the setting of drug and gene delivery due to their non-toxic nature, high field irreversibility, and super-paramagnetic properties [22–24]. Metal oxide nanoparticles and semiconductor quantum dots (QDs) have unique photocatalytic properties for detection of trace contaminants, making them relevant for water purification and wastewater treatment [25].

Among mineral nanoparticles, AuNPs are widely used in colorimetric techniques because of their rapid and easy synthesis, and facile control of size and shape. AuNPs possess surfaces that can be functionalized, and are sustainable and biocompatible [26–28]

The National Institute of Standards and Technology (NIST) has discussed AuNPs as “standard nanoparticles” for biological studies and testing [28]. In the current review, we discuss the use of colorimetric techniques based on inorganic nanoparticles to detect diseases, infections, proteins, analytes, and ions. The properties, synthesis, and applications of these nanoparticles are also surveyed. Three types of approaches are discussed based on cross-linking, non-crosslinking, as well as unmodified nanoparticles. Figure 1 summarizes the properties and functionalization of inorganic nanoparticles, as well as their use in colorimetric techniques.

2- Au NPs: Synthesis, Functionalization, Properties and Application

The current method of synthesis for metal NPs relies on the reduction of cations. This leads to nanostructures with the ability to tune the size and shape. In chemical synthesis methods, ions of gold in a salt are reduced to form AuNPs. Reduction of gold salts is achieved by using reducing agents such as citrate [27, 29–33], ascorbate [32, 34], borohydride [34] or amines [35]. In these methods, the use of stabilizers is necessary to prevent aggregation of AuNPs. Among various stabilizing agents, citrate [27], and alkanethiols [36] are considered to be all-purpose agents. Since AuNPs with different sizes and shapes have diverse optical and electrical properties, size control is critical to obtain particles with uniform

characteristics. To this end, changing the pH and the ratio of chemical reagents [37] or using physical parameters in the synthetic procedure (e.g. temperature [35], microwaves [36], or UV [38] irradiation) have been deployed to control the size and shape. Recently, Alkilany and co-workers used grafted polyethylene glycol-*g*-polyvinyl alcohol as a reducing, capping and stabilizing agent combined in a one-step synthesis of AuNPs. The results of this study demonstrated that the spherical NPs produced by this method were highly stable and monodisperse with tunable size between 23-79 nm [39].

Another important method for the preparation of metal NPs is electrochemical synthesis. During this procedure, the electrolysis of an appropriate salt of the appropriate metal (usually $HAuCl_4$ for AuNP synthesis) in an electrochemical cell, leads to electro-reduction of cations on the cathode. In contrast to chemical synthesis, this method is suggested to have a better ability to control size, shape, and purity. Despite these advantages, the method suffers from two drawbacks: deposition of metal NPs on the cathode and accumulation of NPs around the proximity of the cathode. These problems however, have been solved by using stabilizers with polyfunctional groups and a rotating cathode, respectively [40].

One example of the physical synthesis of NPs is laser ablation in liquid media. AuNPs can be prepared by exposure of a gold target to pulsed laser ablation in water or an aqueous solution of an acid, base or salt. In this method, laser irradiation can result in fusion of the produced Au NPs. Because of the dependence of particle size on Zeta potential, the size of AuNPs can be adjusted using various surfactants [41].

Chemical and electrochemical synthesis methods both require and produce toxic chemicals. Physical methods, also may have high costs and a low rate of product formation [42]. To overcome these drawbacks, researchers have exploited biological systems for the synthesis of metal NPs in a so-called “green approach” [43]. In green approaches, plant leaf extracts have often been employed as reducing and stabilizing agents, for the synthesis of AuNPs with a variety of sizes and shapes [42–44].

The surface chemistry of NPs plays a critical role in their interactions. Hence, metal NP surfaces are usually modified and functionalized according to their intended usage. The general goals of functionalization include improvement of *in vivo* stability[45], prevention of aggregation, and avoidance of uptake by the reticuloendothelial system [45, 46], control of toxicity [47], and optimization for clinical diagnostic and targeting applications [48, 49]. Chemical or biological agents can attach to AuNPs by electrostatic adsorption or by chemical reactions [45–52]. Because the surface of AuNPs is negatively charged, positively charged agents such as cysteine and β-amyloid peptides in acidic pH, would be adsorbed by AuNPs [46]. Thiol groups are known to form chemical bonds with gold atoms. Therefore different chemical and biological molecules are often linked to AuNPs using thiol groups as a mediator or linker [45, 50, 52].

The ligand exchange reaction is a potential process to functionalize metal NPs with thiolated molecules [48, 51]. For instance, NPs coated with thiol-terminated polyethylene glycol (PEG) possess high stability and long blood circulation times [45]. Thiolated DNA and glucose modified AuNPs have been used to design sensing systems [50, 52]. Kloper et al.

[47] studied the effects of the type of modifier ligand and its charge on the toxicity of AuNPs. They reported that small AuNPs modified with cationic ligands displayed more acute toxicity when compared with NPs modified with negatively charged ligands.

Like all nanostructures, AuNPs have a high surface area to volume ratio. As a matter of fact, the most important feature of AuNPs is their size-tunable optical properties. In AuNPs, size confinement results in different behavior from the bulk form. When exposed to appropriate wavelengths of electromagnetic radiation, AuNPs display the surface plasmon resonance (SPR) phenomenon. SPR is the collective and coherent resonance of free electrons caused by energy absorption at a distinct wavelength of light, This wavelength depends on the particle size. This effect generates extreme electromagnetic fields at the surface of the NP and enhances the absorption and scattering of incident radiation. Spherical AuNPs with a diameter of 20 nm show an absorption peak at about 520 nm. As the size increases, it leads to the shift of the absorption peak to longer wavelengths, so the color of AuNPs changes from red to blue. Nanorods possess two absorption peaks according to their length and diameter. While the weaker peak in the visible region is not affected by size, the sharper peak in the near infrared (NIR) region shifts to longer wavelengths, with increase in aspect ratio. The aspect ratio of Au nanorods prepared by a seed-mediated synthesis method is usually controlled by the concentration of Ag ions [26, 53–55].

Due to the local SPR characteristic of AuNPs, Raman scattering by these particles can be magnified up to 12 orders of magnitude. This is called “surface enhanced Raman scattering” (SERS) [56]. AuNPs with an average size of 60-70 nm show highly efficient SERS with periodic light emission on the millisecond to second time scale [57]. The high light to heat conversion ability of AuNPs, which results from excited electron-electron collisions, is a useful property of AuNPs for applications in photothermal therapy [53]. AuNPs also can mediate redox and electrocatalytic reactions for electrochemical applications [58, 59]. Whereas electron transfer efficiency is more pronounced in smaller particles, particle size does not affect the optocatalytic activity [55]. Electrostatic interactions between these nanostructures and target cells make them potential candidates for killing pathogens and cancer cells [43, 54, 60]. Some studies have also indicated that AuNPs can have antioxidant activity [44, 54].

AuNPs have been used for diverse applications from diagnosis to therapy. The relative ease of synthesis and their biocompatibility make them excellent candidates for biological research and clinical applications. Since the properties of AuNPs depend on their size and shape, it is necessary to choose the appropriate size NPs for each specific application. For example, since the scattering to absorption ratio increases for larger NPs, these larger particles are more suitable for detection, while smaller particles are preferable for photothermal therapy. Additionally, in comparison to gold nanospheres, nanorods show longer blood duration times and may have higher cell affinity [53].

3- Colorimetric Detection Based on AuNPs

In recent years, the development of novel colorimetric techniques has attracted considerable attention thanks to the developments of nanotechnology. Recently, AuNP-based colorimetric

biosensing assays have been significantly employed in various applications due to their simplicity and versatility [61]. Because of their ability to be biologically functionalized, biological compatibility, and spectral properties, AuNPs have been used in colorimetric assay techniques [62, 63]

Functionalization is necessary for the stability, performance, and biocompatibility of AuNPs. Furthermore, functionalization is also needed to preserve the AuNPs as well to maintain the properties of surrounding biological molecules. Similarly, the AuNPs must also be stabilized to maintain their unique properties such as surface plasmon resonance and light dispersion [64, 65]. The color change of a suspension of NPs occurs when the NPs are converted from a single dispersed suspension to an aggregated state in response to the presence of specific analytes [21, 66–68]. Usually, the maximum absorption peak of 20 nm AuNPs is approximately 520 nm resulting from the SPR, and this is responsible for their red color. The aggregation of AuNPs is responsible for a color change of the colloidal solution from red to blue, and the re-dispersion of the aggregated NPs reverses the color change from blue to red [69–71]. When AuNPs aggregate, they undergo a plasmon-plasmon interaction. This causes a color change of the Au colloidal solution from red to blue, and leads to shifting of the SPR towards longer wavelengths, up to 620 nm. The exact process of aggregation has been discussed in detail [72, 73]. Moreover, assays based on AuNPs can also be monitored using UV-vis spectrophotometry [74]. In recent years, diagnostic and detection methods for analytes at trace concentrations, based on novel electrochemical systems[75], specifically AuNPs, have been widely applied as colorimetric sensors for the detection of DNA [74, 76], RNA [74, 77, 78], proteins [71, 79], ions [80], enzymes [81], pathogens [82, 83], various cancers [84, 85], parasites [86], food and water pollution [87, 88], hydrogen peroxide [89], and single nucleotide polymorphisms [90]. These colorimetric techniques based on AuNPs are quick and easy to perform. They also have many advantages including low cost and the ability to detect color changes with the naked eye [91–93]. In colorimetric detection techniques based on AuNPs, both modified and unmodified NPs can be used. Modified nanoparticles, are functionalized via connection to various biological groups, including nucleic acids fitted with thiol groups, which have strong binding affinity to the gold surface. Nanoparticles without functionalized surfaces can be also used in colorimetric technique as unmodified nanoparticles. These two techniques are described in the following sections.

3-1- Colorimetric Detection Based on Modified AuNPs

AuNPs can functionalized by various molecules including nucleic acids (DNA, RNA, and aptamers), peptides, proteins, carbohydrates, antibodies, peptide nucleic acids (PNA) etc. Several articles have been recently published describing colorimetric methods based on AuNPs functionalized with different types of molecules to detect pathogens [94] and ions [95].

In this section, we summarize different types of pathogens, cancer biomarkers, enzymes, ions, and environmental pollutants that have been detected with functionalized AuNPs. AuNPs can be functionalized with oligonucleotides; this attachment can be performed with a head-to-head, tail-to-tail, or head-to-tail arrangement of hybridization [96, 97]. Moreover,

based on the accumulation or dispersion of the NPs, colorimetric techniques can be subdivided into two types, which are “cross-linking” and “non-cross-linking” approaches.

3-1-1- Cross-Linking Approach—Cross-linking or inter-particle bond formation leads to a development of a polymeric network which results in inter-particle attachment [98]. Such connections can be formed by chemical cross-linker molecules, by direct linking between antibodies and antigens [99], via aptamer interactions with target molecules [100], or by the interaction between streptavidin and biotin [101], and so on [102].

In addition, cross-linking connections can be formed by formation of Au-S or Ag-S bonds, in which two single-stranded DNAs (ssDNA) probes are attached to the surface of the NPs and create a polymeric network. Consequently, the color of solutions containing AuNPs changes from red to blue when the target molecule binds to the probe upon salt addition [103].

The ssDNA and double-stranded DNA (dsDNA) sequences have different electrostatic properties. The basic difference is that while ssDNA can uncoil its spirals, which can be then attached to AuNPs, dsDNA molecules have a stable double helix structure which always displays a negative charge related to the phosphate groups on the exterior. Thus, a strong repulsion between the negative charges of dsDNA and AuNPs occurs; this attracts negative citrate ions and inhibits the absorption of nanoparticles by dsDNA. On the other hand ssDNA has sequence flexibility; so after the spiral opens up, the bases can bind to the AuNPs and the resulting AuNPs will be stable [104].

Oligonucleotides conjugated to AuNPs were used to detect DNA for the first time in 1996 by Mirikin et al [105]. In this study, two complementary thiolated probes were attached to AuNPs to detect the target by hydridization. The authors showed that this system created a polymeric network based on cross-linked target binding. They also observed a change in the color. In order to detect pathogens and viruses, functionalized AuNPs can be used with two complementary probes. Many nucleic acid-based targets such as RNA, genomic DNA, or amplified nucleic acid sequences can also be used in comparable approaches.

Storhoff et al. used a “spot-and-read” colorimetric detection assay for the detection of genomic DNA with high sensitivity. This technique can be easily implemented in a biological laboratory by placing hybrid NPs functionalized with a nucleic acid probe and mixed with genomic DNA on a glass surface that created chromatic dispersion. This method enables the detection of trace amounts of DNA down to the zeptomole level (10(-21) mol). This method was used to detect *Staphylococcus aureus* based on the mecA gene sequence [106]. In other studies, AuNP based colorimetric techniques have been used for pathogen detection[107]. To be more precise, a fluorescent dye can be used as a sensitizer for bioassay detection of the pathogens along with conjugation of AuNPs to the DNA or mRNA strands. In this system, a light beam introduced into the microfluidic device excites the AuNPs. The metallic NPs can provide signal amplification in smart-phone based microfluidic devices as well. Majdinasab et al. developed a novel colorimetric detection method to identify a food pathogen, *Salmonella typhimurium*, using two thiol probes for the *invA* gene with 20 nm AuNPs. In this study, both genomic and amplified DNA sequences were used. The results

demonstrated that the efficiency and sensitivity of detection of the AuNP-based assay was relatively low when non-amplified target DNA was used, as compared to Polymerase Chain Reaction (PCR) amplified DNA samples [108]. In a similar study, several pathovars of *Pseudomonas syringae* bacteria (the causal agent of different agricultural diseases) were detected using two thiol probes attached to AuNPs via cross-linked hybridization. The detection method was based on amplified DNA.

In recent years, AuNPs have been widely used to detect pathogenic viruses. Viruses can have either RNA genomes or DNA genomes, and both types can be detected by this approach. DNA viruses include human papillomavirus type 16 (HPV-16), and type 18 (HPV-18). They are major causes of cervical cancer in women. Chen et al. established a colorimetric technique based on the immobilization of two thiol probes on the surface of 13 nm AuNPs. In this *nanobiosensor*, when amplified genomic DNA and probe sequences were mixed, color variations could not be observed because of the too wide gap between the probes attached to the nanoparticles and the target DNA [109]. Influenza virus A (IAV) is one RNA virus composed of single-stranded RNA (ssRNA) and two membrane proteins HA and NA. Several colorimetric techniques were developed based on AuNPs functionalized with monoclonal antibodies (mAb) that recognized these proteins. Liu et al. showed that hybridization mAb-AuNPs with hemagglutinin type A (HA) changed the color of NPs and their absorption spectrum. These authors used also transmission electron microscopy (TEM) and also dynamic light scattering (DLS) to verify the coagulation and sedimentation of the NPs [110] .

Bacteriophage or simply “phage” is another virus that attacks bacteria and kills them. Lesniewski et al. proposed the use of AuNPs functionalized with antibodies through covalent binding, for the detection of phage *T7*. In this colorimetric approach, in presence of T7 virions, they formed an immunological complex with the antibody modified AuNPs which caused them to aggregate and color changed from red to purple. They used M13 phage as a negative control. It was also shown that this detection technique was capable of detecting all variants of phage *T7*, and not only those that were biologically active, as would be the case for a conventional biological plaque assay. They showed a detection limit of 1.08×10^{10} PFU/mL (18 pM) T7 [111] (Fig. 2A).

The incidence of cancer has increased exponentially in recent years, so rapid and accurate diagnosis followed by timely treatment has become necessary. Today, nanobiosensors based on AuNPs have been widely used for the diagnosis of cancer and malignant cells. In order to detect cancer, NPs modified with aptamers that recognized 7-MCF cells (human breast cancer cell lines) were described by Sadat Borgheia et al. [84]. These authors used aptamers in combination with other AuNPs to enhance the detection of cancer cells. In their method, two complementary thiolated ss-DNA probes were attached to AuNPs. In the presence of 7-MCF cells, binding occurred between soluble nucleolin aptamers (AS 1411) and nucleolin receptors that are over-expressed in cancer cells. As a result, binding between AS 1411 and cancer cells resulted in the removal of all aptamers from the solution. Due to the lack of aptamers in the environment no binding occurred to the ssDNA-AuNP probes, and the color of the solution did not change.

Colorimetric techniques have been developed in order to detect contamination of food and water [87, 88], factors involved in plant diseases [114], and presence of heavy metals ions [112, 115–117]. For instance, it is known that pollution due to heavy metal ions, especially Pb^{2+}, represents a threat to the environment and human health. In a new study, Chai et al. [115] demonstrated that glutathione functionalized AuNPs (GSH-AuNPs) could be exploited to develop a colorimetric sensor for Pb^{2+}detection. In this method, the presence of Pb^{2+} ions and the binding to chelating ligands on the surface of NPs, led to changes in color and wavelength. A similar study was conducted by Zhang et al. [116] to detect the metal ions Cd^{2+}, Ni^{2+} and Co^{2+} using NPs functionalized with a probe peptide (P-AuNPs) instead of chelating ligands with comparable results. Chen et al. [112] used NPs functionalized with chitosan to detect Hg^{2+}. This technique approach is illustrated in Fig. 2B. Another study based on cross-linked functionalized NPs with MMT-AuNPs (5-mercaptomethyltetrazole) was performed by Xui et al. for detection of Al^{3+} ions [117]. In all these studies listed for the recognition of metal ions, the difference in the type of cross-linker and the binding molecules on the surface of AuNPs may affect the time of detection. Another application of colorimetric technique is concerned with the detection of mutations such as single nucleotide polymorphisms [90], as well as detecting CpG methylation in genomic DNA [113]. The methylation of DNA is considered to be an indicator of DNA epigenetic modification, and occurs in a wide range of organisms ranging from eukaryotes to prokaryotes. Methylation plays a key role in the regulation of gene transcription in embryonal development, and is implicated in different diseases. A ligase chain reaction (LCR)-based colorimetric method to detect CpG methylation was developed by Su et al. [113] who used four probes, A, B, A′, and B′. In the presence of only 0.01 fM methylated DNA, probes A and B were joined together by binding to methylated DNA in order to form the AB DNA strand that was amplified by the LCR technique. Next probes A′ and B′ became connected through the DNA strand AB. Under denaturing and annealing temperature cycles, the DNA strand, AB and the methylated DNA hybridized thus connecting probe A′/B′ with probe A/B. As a result, A′B′ ssDNA was hybridized with DNA strands a and b immobilized on 13 nm AuNPs, Subsequently aggregation and change in color was observed as shown in Fig. 2C.

Colorimetric technique based on cross-linking hybridization has also been used for the detection of proteins and enzymatic activity. For example, AuNPs functionalized with peptides have been used by Wei et al. in order to detect proteins [118]. In another study, Sun et al. detected protein kinase activity using a colorimetric technique based on NPs functionalized with streptavidin (STV-GNPs). It involved binding between STV-AuNPs, and a biotinylated peptide (biotin-LRRASLG), which acts as a specific substrate for the enzyme protein kinase A (PKA). In the presence of the enzymatic activity of PKA, the biotinylated peptide was destroyed thus preventing the crosslinking of STV-GNPs and the color of AuNPs remained red [81] (Fig. 2D).

Table 1 summarizes studies where cross-linking colorimetric detection was used to identify pathogens, viruses, cancers, metal ions, proteins, etc.

3-1-2- Non-Cross-Linking Approaches—Another type of NP-based colorimetric technique is based on non-crosslinking aggregation. This technique is based on steric or

electrosteric aggregation of nanoparticles including AuNPs and AgNPs without creating cross-linked interparticle bonds (Fig. 3). Moreover, in this technique (unlike the cross-linking technique where crosslinks are created between two binding moieties attached to the NPs) a single target-binding probe attached to AuNPs is used. The outstanding pioneer scientist in this field (Pedro Baptista) for the first time, developed an inexpensive and easy-to-use assay which provided a visible change of color, blue shift, when the AuNPs bound to trace trace amounts of analyte. To achieve this result, different salt concentrations were investigated and tuned by the color changes which came from the aggregation in the presence of a complementary target, and not with mismatched targets.[62, 128–130]. Bakthavathsalam et al. [131] described a colorimetric technique based on thiol-functionalized NPs for the detection of *E.coli*. The binding of the probe to AuNPs was investigated in the presence of *E.coli* genomic DNA. The presence of genomic DNA ensures the nanoprobes remain stable and prevents them from salt-induced aggregation. In the absence of genomic DNA, the nanoprobes are unstable and the AuNPs aggregate. The authors investigated the attachment method using atomic force microscopy (AFM), and the size of the AuNPs (Fig. 4A). Ultra-sensing detection of *E. coli* was possible by conjugating specific antibodies against *E. coli* to the AuNPs for colorimetric-biosensing. In this system, the conjugation was applied in a lateral flow assay (LFA) with a pre-determined detection time. In addition, this capillary flow allowed the pathogen to increase the agglomeration of the antibodies conjugated to AuNPs which led to a red color shift. In a similar study by Castilho et al, a colorimetric technique based on non-cross-linked AuNPs functionalized with a thiol nano probe was developed to detect *Paracoccidioides brasiliensis* (a South American pathogenic fungus). In this study, DNA coding for the p27 antigen was used as the target. In the presence of the target aggregation of NPs and a color change was prevented, while in the absence of target aggregation and a color change occurred [132].

Colorimetric techniques based on non-cross-linking hybridization have been used for the initial screening of cancer. An AuNP-based colorimetric technique based on non-cross-linked aggregation and peptide substrate that could be phosphorylated by protein kinase (PKCα) was developed to detect breast cancer [133]. In the presence of the peptide substrate, phosphorylation prevented the aggregation of the AuNPs. In the absence of phosphorylation aggregation and changes in color were observed. It is known that in cancer cells there is an increase in the levels of PKCα. In target breast cancer cells where phosphorylation of substrate peptide occurred, the color red remained; while with normal cells where phosphorylation was absent, a red to purple color changes was observed (Fig. 4B).

Single nucleotide polymorphisms (SNP) occur widely across the human genome, and are related to the predisposition to several diseases, including cancers, diabetes, and allergies. Various techniques have been developed in order to detect SNPs, including AuNP-based colorimetric assays.

Wang et al. [134] used gold nano-spheres (AuNS), nanorods (AuNR) and nanostar-shaped nanoparticles (AuNT) functionalized with ssDNA to detect genotype SNPs. They used ssDNA-AuNRs with aspect ratios of 2, 3 and 4 and a different type of anisotropic gold core. In this approach, fully matched dsDNA-modified anisotropic AuNPs aggregated after salt

induction. However, in the case of a single base mismatch at the DNA level, AuNPs did not aggregate upon salt induction, and remained dispersed. The same study showed that ds-DNA AuNT aggregated faster than AuNS and AuNR, suggesting that aggregation of nanoparticles based depended on shape in addition to aspect ratio. In this investigation, individual SNPs were detected using only a single Au-nanoprobe (Fig. 2C).

AuNP-nanoprobes can also be used for the detection of small molecules relevant to toxicological investigations. In a recent study, a colorimetric assay based on non-cross-linked AuNP aggregation was developed by Sharma et al. using NPs functionalized with antibodies for the rapid detection of phenylurea herbicide. which is a harmful environmental contaminant. In the presence of antigen (Diuron), the interactions between the antigen and the antibody-functionalized AuNPs led to aggregation, and as the concentration of antigen increased, the color gradually turned blue. Upon addition of increasing salt concentrations, changes in the surface of the nanoparticles occurred and, and the nanoparticles aggregated. The conjugated hapten-protein (DCPU-BSA) was used as a control. DCPU-BSA prevented the aggregation of anti-diuron Ab–AuNPs and the color remained red. The detection limit was~5 ng/mL and the method had the advantage of not requiring washing steps. (Fig. 2D).

One of the main differences between the cross-linking and non-cross-linking approaches, is that the non-cross-linking mechanism does not require receptors and binding sites. The non-cross-linking approach is faster than the cross-linking approach, and relies on interactions between NPs due to their surface charge changing in the presence of the target analyte [135].

Studies where non-crosslinking colorimetric detection has been used for the identification of pathogens, viruses, fungi, cancer biomarkers, metal ions, etc. are summarized in Table 2.

3-2- Colorimetric Detection Based on Unmodified AuNPs

The unmodified AuNPs-based colorimetric technique utilizes nanoparticles with unmodified surfaces. In these methods, changes made to the surface of the NPs by binding of the analyte affects their electrostatic charge, leading to instability and aggregation of the NPs [145]. Attachment of single-stranded thiolated nucleic acids (RNA, DNA, and aptamers) to the AuNPs results in stabilization [146–148]. It should be noted that binding of ssDNA leads to opening of the coiled structure and exposure of the bases leads to their absorption on the surface of the AuNPs, therefore contributing to their stability. dsDNA, however, because of the repulsion between the negative phosphate charges and the surface of AuNPs, is unable to bind to the surface of nanoparticles. In the case of nucleic acid targets, however, binding to the complementary probes upon salt addition, results in accumulation of nanoparticles and a color change from red to blue (Fig. 5).

In the past years, colorimetric techniques based on unmodified nanoparticles have been widely used to detect pathogens, biomolecules, antibiotics and other drugs, metal ions, and enzyme activities, because of their simplicity, speed, and accuracy.

The surface of NPs can have a positive or negative charge depending on the method of synthesis. For example, the use of sodium citrate in the synthesis of AuNPs results in negative charges on their surface; whereas the use of hexadecyl trimethyl ammonium

bromide (CTAB) [149], sodium borohydride in the presence of cysteamine [150], HAuCl4, and polydiallyl-dimethyl ammonium chloride (PDDA) create positive charges on the surface of AuNPs [151].

Pan et al. [152] used unmodified AuNPs for detecting apoptosis based on caspase-3 enzyme activity. In this study, a specific peptide, Ac-Gly-Asp-Glu-Val-Asp-Cys-Cys-Arg-NH2 (GDEVDCCR, GR-8) was used as a substrate for the enzyme. The peptide had a negative charge and was attached via its thiol groups to the AuNP surface to stabilize them. After GR-8 was treated with caspase-3 a smaller positively charged peptide - Cys-Cys-Arg-NH2 (CCR, CR-3) - was produced by the enzymatic cleavage of GR-8. When this positively charged peptide binds to the AuNPs via thiol groups, the negative surface charge density of NPs is reduced which leads to their aggregation.

In another study, Cao et al. [150] developed unmodified AuNPs with positively charged surfaces synthesized by sodium borohydride and cysteamine to detect nuclease activity. In this study, the reaction between polyanionic ssDNA and cationic AuNPs led to electrostatic binding and AuNP aggregation and a color change. The activity of the nuclease enzyme, s1, produced smaller ssDNA fragments, thereby preventing AuNP aggregation.

One of the most important applications of unmodified nanoparticle-based colorimetric assays is the detection of bacteria and viruses. One example is provided by the report of Hussain et al.to detect *Mycobacterium tuberculosis* infection [153]. These authors developed a system based on unmodified AuNPs with an average size of 14 nm, and 21-mer oligonucleotide probes that recognized the sequence of *M. tuberculosis* IS6110 DNA duplex. The ssDNA oligo-probes underwent electrostatic binding to the AuNP surface and stabilized them. In the presence of the DNA target, the ssDNA oligo-probe hybridized to its complementary DNA and upon addition of salt aggregation occurred. In this study, the detection limit for the PCR products and genomic DNA was about 1 and 40 ng DNA respectively.

Another study reported the detection of Maize chlorotic mottle virus, which causes a lethal necrosis disease of maize. Liu et al. [154] extracted RNA virus from infected leaves and amplified it by RT-PCR. In the existence of probes, RT-PCR target products, and salt induction, color changes and aggregation of AuNPs were observed.

Biomarkers can be used to diagnose pathogens, detect various disease processes, or predict susceptibility to a certain disease as a prognostic indicator for patients. Lee et al studied a biomarker for malaria. The authors used *Plasmodium vivax* lactate dehydrogenase (*Pv*LDH) and *Plasmodium falciparum* LDH (*Pf*LDH) proteins, as well as pL1 aptamers as probes and AuNPs. When PLDH proteins were present in human serum, binding occurred between aptamers and protein. In the presence of the cationic detergent cetyltrimethyl ammonium bromide (CTAB) the negatively charged AuNPs aggregated and a color change occurred. In the absence of the target proteins, the unbound pL1 aptamers bound to the CTAB and the AuNPs remained dispersed. The serum protein detection limit of *Pv*LDH and *Pf*LDH was 1.25 PM and 2.94 pM, respectively. The authors proposed that this colorimetric aptasensor

represented a rapid, highly sensitive, and accurate biosensor for the diagnosis of *Pv*LDH and *Pf*LDH proteins [155].

Luo et al. used a thiolated aptamer as a probe for the detection of carcinoma embryonic antigen (CEA), a tumor marker. Aptamers with a thiol group can attach to the surfaces of AuNPs. In the presence of CAE that hybridizes with aptamers, the addition of NPs and salt, results in NP aggregation. A shift in the spectrum from 520 to 650 nm was observed. They concluded that the technique can be deployed to identify cancer biomarkers, given the high sensitivity and rapid detection [146].

Drug testing is performed as a forensic procedure to check for possible abuse of drugs, and to ensure patients comply with instructions and avoid addiction. For this reason, drug screening tests are required to be highly specific and rigorous. Recently, these tests have been facilitated by the introduction of AuNPs. Shi et al. [156] detected the presence of methylamphetamine (METH) using unmodified AuNPs and a METH-specific aptamer in approximately 20 minutes and with a sensitivity of 0.82 μM. The results indicated that in presence of METH in the urine, the AuNPs aggregated upon salt addition, and a change in color from red to purple was observed.

The rapid detection of antibiotics and drugs is one of the benefits of colorimetric assays based on unmodified NPs. For example, the antibiotic streptomycin was detected in milk and in animal serum because of the presence of antibiotic residues in the animal feedstuffs. Using fluorescence quenching aptasensors combined with unmodified NPs, the fluorescent dye (5',6-fluorescein) FAM-labeled double-stranded (dsDNA) and aptamers, Sarreshtehdar Emrani et al. [157] reported that, in the presence of antibiotics and aptamers, FAM-labeled complementary strands were attached to the surface of the NPs, leading to NP stability and no change in color. In the absence of a sufficient concentration of antibiotics, the complex aptamer/FAM-labeled complementary strand dsDNA remained stable and AuNPs aggregation was observed. The antibiotic detection limit in this technique was 73.1 and 47.6 nM using colorimetric and fluorescence readouts respectively. In another study, Teetoet et al. [158] used AuNPs with an average size of 13-23 nm to identify ramoplanin (an actinomycetes-derived antibiotic). After binding to the surface of the NPs, aggregation and a color change was observed. This was due to the binding of antibiotic amino groups to the AuNPs creating a positive charge and aggregation. The authors also concluded that NPs of 13 nm in size were more effective compared to 23 nm NPs. This was because the surface area of AuNPs increases with the decrease in particle size.

The advantages of unmodified AuNP assays include:

1. Addition of NPs after binding of probe to target has already occurred; the binding process sometimes employs elevated temperatures. High temperature can lead to the aggregation of NPs and to color changes, thus causing false positive or negative results.
2. No need to perform functionalization of the NP surface.
3. High rapidity with the ability to detect within minutes.

Studies on unmodified NP assays are summarized in Table 3.

4- Silver nanoparticles (AgNPs): Synthesis, Functionalization, Properties, and Application

Currently reported methods for the physical synthesis of AgNPs rely on two main approaches: (a) evaporation-condensation and (b) laser ablation. In the evaporation-condensation method, bulk silver is heated at a high temperature in a tube furnace. After evaporation, silver atoms condense from the gas phase and form Ag clusters by rapid cooling. The spherical AgNPs produced can be sorted according to their size and charge using a differential mobility analyzer and, subsequently, a narrow particle size distribution is obtained [182]. The laser ablation of Ag metal in an appropriate solvent results in formation of AgNPs with different sizes that can be controlled by the type of the solvent used and by the concentration of surfactant employed [183, 184].

The chemical synthesis of colloidal AgNPs is commonly carried out using a combination of two reductants and a stabilizing agent in a two-step process. Briefly, Ag salt is reduced by agents like $NaBH_4$ and trisodium citrate [185, 186] or by sodium citrate and tannic acid [187]; citrate also acts as a stabilizing agent. The size and shape of the particles are controlled by the reaction conditions including the type and the concentration of chemical reagents, pH, and temperature. For example, triangular NPs can be obtained using ascorbic acid as a mild reductant [186] and Ag ions reduced on Au seeds can result in the synthesis of larger and more uniform AgNPs [188]. Gamma radiation can be used to produce reactive species in solvents that act as reducing agents to form stable colloidal Ag nanoclusters from Ag cations [189].

In the electrochemical method, electro-reduction occurs at the interface of the cathode and Ag^+ solution. This method has been accomplished without any stabilizer [190] and with a polymeric stabilizer for the control of size and shape [191].

In recent years, green biosynthesis methods have attracted the attention of various workers in the field. These methods are applied to produce AgNPs using plant extracts (e.g., aloe vera) both as reducing and stabilizing agents [192–199]. Microorganisms like *Bacillus koriensis* can be utilized for the same purpose [200, 201]. These methods are eco-friendly, inexpensive and suitable for medical applications [45–54].

The surface modification of AgNPs may impact their size, stability and function. Ligand exchange is one functionalization method that is deployed for citrate stabilized AgNPs. Studies have shown that the presence of long chain molecules on these NPs decreases their catalytic activity, as a consequence of diffusion restriction [187, 191]. AgNPs have been functionalized with different molecules such as carbohydrates, in order to modulate their cellular uptake and control their toxicity to human and microbial cells [202–206]. Recent studies have shown that AgNPs embedded in multi-walled carbon nanotubes (MWCNTs) show anticancer and antibacterial properties [207]. AgNPS have been functionalized with a range of molecules to allow specific and sensitive detection of various analytes. These molecules have included macrocyclic polyammonium cations, bis-acridinium lucigenin, and

ascorbic acid [208–210]. The surface of AgNPs can be also functionalized for targeted drug delivery [211, 212].

Silver is considered to be the most conductive metal both thermally and electrically. Another important property of AgNPs is their catalytic activity [179]. AgNPs can release Ag ions as antimicrobial agents. At the nanoscale level, the antimicrobial effect is more impressive than the bulk form.

All of these properties are influenced by the size and shape of AgNPs; the smaller the size, the better the activity [187, 193–195]. Similar to AuNPs, AgNPs also have interesting optical properties. Compared to AuNPs, the SPR effect in AgNPs projects further from the surface, and is tunable over a broader range of wavelengths (350-450 nm). Larger AgNPs show effective SERS properties and are excellent candidates for the detection of single molecules [186, 188, 213].

AgNPs have been used in different fields including catalysis, sensing and optoelectronics, although the most common application still relates to their use as antibacterial, antiviral and antifungal agents [184, 185, 189, 213]. As mentioned above, it is necessary to choose NPs of appropriate shapes and sizes for the intended applications.

Table 4 compares the applications of both AuNPs and AgNPs in biology and medicine.

5-Colorimetric Detection Based on AgNPs

As mentioned above, AuNPs and AgNPs, both noble metal NPs, demonstrate LSPR (local SPR), which is the basis of label free colorimetric assays. When these NPs are exposed to light, their free electrons absorb energy at appropriate wavelengths producing high extinction coefficients. The smaller NPs show absorption peaks at shorter wavelengths; the absorption peak shifts to longer wavelengths with the increase in the size of NPs. The aggregation/dispersion of these NPs also has a similar effect to that seen with AuNPs. Researchers exploit this phenomenon for chemical and biochemical analyses when a fast response is required. The interaction between functionalized AgNPs and target molecules causes NPs aggregation or dispersion that results in a change in the color of the solution. This color change can be also detected by eye (Fig. 6). The linear relationship between absorbance and concentration is applied to quantify analytes. This method is very simple, sensitive, selective, specific and inexpensive [227–230].

The change in expression levels of specific genes might represent a disease hallmark, especially in the cancer setting. Detection of mRNAs and proteins in the early stages of disease is crucial for rapid diagnosis and treatment. Li et al. detected C-Myc mRNA using PNA oligomer functionalized AgNPs at nanomolar concentration with single base mismatch resolution [228].

Trypsin is a protease, produced from the pancreas, and changes in its concentration suggest abnormal pancreatic activity. Han and co-workers have used negatively charged AgNPs for the quantitative determination of this enzyme. Appropriate peptide chains were immobilized on the NP surface acting both as a stabilizer and as a substrate for trypsin. When exposed to

trypsin, peptide chains are cleaved so that positively charged fragments remain on the AgNP surface. Thus, the neutralization of the native negative surface charge decreases the electrostatic repulsion, with consequent NP aggregation. The resultant absorption changes provide the basis for quantitative analysis of trypsin over the range of 2.5-200 ng/mL and a detection limit of 2 ng/mL [232].

DNA modified AgNPs have been used for protein sensing. Transcription factors are proteins that bind to specific DNA sequences. Researchers at National University of Singapore modified the surfaces of two sets of AgNPs with dsDNA containing single stranded complementary sequences. These sequences also displayed good affinity for estrogen receptor α. The interaction between these DNA sequences, under certain salt concentrations, induced NP aggregation and a shift in the color of solution towards blue. Because of the high affinity, protein-DNA binding prevented NP aggregation by stabilizing transient structures via steric protection forces. The resulting accuracy was better than that achieved with colorimetric sensors based on analyte-induced aggregation mechanism [233].

Drug determination in clinical samples is an important task in analytical chemistry. Because of the affinity of sulfur atoms to Ag, unmodified AgNPs have been utilized for the detection of two different thioamide drugs. The anti-thyroid drugs, propylthiouracil and methimazole were analyzed based on covalent bond formation with AgNPs, causing aggregation and a decrease in absorbance at 400 nm. The assay response was linear in the range of 0.02-0.8 μg/mL for propylthiouracil and of 0.05-1.2 μg/mL for methimazole with corresponding LODs of 0.007 μg/mL and 0.01 μg/mL respectively [234].

Enzyme immobilization on AgNPs allows the design of nanosensors for the colorimetric determination of appropriate substrates [235]. Coralyne (a small molecule drug that intercalates into DNA) was quantitatively analyzed using homo-polyadenine adsorbed onto AgNPs in the range of 0-10 μM. In the presence of coralyne, the polyadenine chains separated from the surface of NPs to form a duplex. Consequently, the NPs aggregated and the A550/A397 (absorbance at 550nm/absorbance at 397nm) changed according to the coralyne concentration [236].

A colorimetric assay based on green synthesized AgNPs was used for the determination of ammonia in biological samples. This sensitive, selective, simple, and rapid response method showed good potential for ammonia detection at low concentrations for medical applications [237].

Anisotropic triangular AgNPs have been applied for the colorimetric detection of ascorbic acid at μM levels[238]. The surface modification of AgNPs with pH sensitive or thermosensitive chemicals can be used in order to detect the acidity or the temperature of solutions. For instance, Korean researchers utilized cytochrome c (Cyt c)-modified AgNPs for the determination of pH within a broad range (3-11). At an acidic pH, Cyt c undergoes conformational changes, inducing aggregation of NPs, and a consequent shift in the color of the solution towards blue [239].

Environmental protection is one of the most critical challenges present in the modern era. In this regard, detection of hazardous chemicals is of paramount importance. Table 5

summarizes the detection of several analytes relevant for biology and health using AgNP-based colorimetric assays.

An interesting colorimetric assay was developed based on the morphology transition of Ag nanoprisms for sensing of Hg^{2+} over a linear range from 10 to 500 nM with a LOD of 3.3 nM. Ag nanoprisms capped with 1-dodecanethiol ($C_{12}H_{25}SH$), when exposed to Hg mixed with I ions, lost the organic protective layer. The silver atoms reacted with I^- ions to form AgI. These interactions were accompanied by transformation of nanoprisms and a color change [261]. Glucose induced alteration of the nanoprism morphology in the presence of glucose oxidase, has been used for a glucose assay in the linear range 2.0×10^{-7}- 1.0×10^{-4} M [262].

An electron transfer reaction between Ag atoms and Hg ions has been used for sensing mercury. Upon this redox interaction and the conversion of AgNPs to a Ag-Hg nanoalloy, the color of solution changed according to the Hg^{2+} concentration [263, 264].

Various amino-acids and metabolites, involved in biological interactions, are chiral molecules and are present as L or D enantiomers. Differentiation of enantiomers is important especially in the drug manufacturing industry. L-cys and D-cys can be distinguished by a colorimetric assay because of their different effects on aggregation/dispersion of nucleotide capped AgNPs [265].

Aromatic ortho-trihydroxy phenols, attached by hydrogen bonding to the surface of chitosan modified AgNPs, were oxidized by reduction of Ag ions on the surface. The resulting changes in UV-Vis absorption spectra of NPs were used for quantitative analysis of gallic acid, pyrogallol, and tannic acid [266].

5-1-Colorimetric detection based on combinations of AuNPs and AgNPs

While the most important property of AuNPs is the ability for surface functionalization, AgNPs show higher extinction coefficients. The combination of these two properties can lead to a sensing system characterized by good selectivity and sensitivity. To prepare these hybrid NPs, Ag@Au and Au@Ag core-shell nanostructures, as well as NPs made of Ag-Au alloys have been developed [267–269]. Colorimetric assays based on these structures have been devised by using the changes in UV-Vis spectra caused by aggregation/dispersion of NPs or by alteration of the shell by etching. The interaction of Ag ions with organic molecules containing carbonyl groups leads to Ag^+ reduction to silver atoms. Based on this fact, both Ag^+ and organic molecules containing a carbonyl group have been detected by the formation of a Ag shell on the Au core [267, 270, 271]. In the presence of thiol terminated hyper branched polyethylenimine (HPEI), the formation of a Ag shell onto the Au core induced a color change from red to brown to green. This resulted in a significant improvement in the selectivity and sensitivity of the Ag ion assay. The graph of absorbance vs. Ag^+ concentration was linear in the range of 8.76×10^{-9}-1.27×10^{-4} M with a LOD of 8.76×10^{-9} M by UV-Vis spectra and 8.76×10^{-8}M by eye [270]. Formaldehyde and glucose, due to their carbonyl group, reduce Ag^+, this resulted in formation of a Ag shell onto the AuNP core (Fig. 7). The resultant color change was proportional to the concentration of these organic analytes [267, 271].

Anions and cations, in the presence of appropriate reagents, can etch or change the chemical composition of the shell of mixed Au-AgNPs. Variations in thickness or texture according to the concentration of analytes have been detected by colorimetry [269, 272–275].

The oxidation of some biomolecules, such as glucose and cholesterol, catalyzed by specific enzymes, is accompanied by the generation of hydrogen peroxide. H_2O_2 oxidizes and etches the Ag shell of the Au@AgNPs. The color change due to the shell etching can be used in the colorimetric assay of H_2O_2, glucose, cholesterol and other H_2O_2 producing biomolecules [276, 277].

In addition to core-shell NPs, AuAg-alloy nanoprobes have also been used in colorimetric assays. In addition to the advantages of core-shell nanostructures, these NPs are easily synthesized and show a single absorption band [268].

Tamada and co-workers designed a colorimetric biosensor composed of triple-layered AgNPs and AuNPs. AgNPs (5-nm diameter) were coated with myristates, followed by a SiO_2 coating, and labeled with biotin. Next AuNPs were prepared and their surfaces were also coated with SiO_2 and labeled with biotin. The hybrid AgNPs were attached to a gold substrate. In the presence of streptavidin (model analyte), a sandwich interaction occurred between streptavidin and biotin binding on both sides, leading to the adsorption of AuNPs on the top of the biosensor, inducing color and absorption spectral changes [278]. A marked color change could be observed at less than 30% surface coverage. The color change was attributed not only to the LSPR effect, but also to the multiple light trapping effect derived from the stratified Au and Ag NPs, as predicted by a finite-difference time-domain simulation. Table 6 summarizes some assays mediated by these hybrid NPs.

Table 6 shows that colorimetric assays based on Au-Ag hybrid nanoprobes often possess lower LODs compared with other colorimetric assays. These nanoprobes can be immobilized on a solid matrix to construct portable and user-friendly sensors and chips [278, 281].

Jin and co-workers utilized poly L-histidine modified hybrid nanoshells for colorimetric detection. They immobilized glucose oxidase enzyme on the surface of hollow Ag-Au nanoshells. Within a range of glucose concentration the enzyme produced H_2O_2 and the Ag atoms dissolved leading to shell removal. Changes of absorbance, caused by the generation of porosity, constituted the basis of this glucose analysis [282].

6- Magnetic Nanoparticles (MNPs): Synthesis, Functionalization, Properties and Applications

In recent years, many studies have been conducted with the aim of developing magnetic nanoparticles (MNPs) [283]. These MNPs have been widely used in various applications in the context of biomedicine, biotechnology, engineering, and material sciences [284]. MNPs can be synthesized using either chemical, physical or biological methods. Several of these methods are summarized in Table 7 [285].

The difficulty of controlling the particle size at the nano-scale is one of the main disadvantages of physical methods. Chemical methods (wet chemistry) are simpler, more flexible, and offer more effective control over size, composition, and in some cases, the shape of the NPs [286] . In some chemical methods such as the sonochemical decomposition method, the supercritical fluid method and the sol–gel method, the particle size can be well-controlled by adjustment of the process parameters. Functionalization is one of the more important processes that are performed on the MNPs.

MNPs have a high chemical reactivity and a large specific surface area which make them sensitive to oxidation and agglomeration [283]. Oxidation of the MNPs occurs on the surfaces, causing dramatic changes in their functional and structural properties. Agglomeration of MNPs also hinders their processing [287]. Hence, protective methods are normally used to preserve the NP-specific magnetic properties. Protection of MNPs can be accomplished using different organic and inorganic materials such as carbon and metal oxides [283].

Recently, protection methods that rely on the use of organic and inorganic coatings have been developed. The most common organic coatings are surfactants (stearic acid, elaidic acid, oleic acid, trioctylphosphonic acid and lauric acid etc.) and polymers (dextran, chitosan, starch, arabic gum and gelatin etc.) [283]. Amongst inorganic coatings, metal oxides (cobalt, titanium oxide and aluminum oxide), precious metals (gold and platinum), silica, and carbon are the most commonly used [283].

After this step, functionalization can be performed according to the specific application of MNPs. Usually, MNPs are required to be chemically stable, well dispersed in liquid media, and uniform in size [287]. Intermolecular interactions such as electrostatic chemo-adsorption and covalent conjugation are often used for the functionalization of MNPs [283]. Several studies have reported the synthesis of iron oxide nanoparticles, coated with a silica shell that can be subsequently functionalized via attachment to gold NPs[285]. Riva, et al used silica coating to prevent MNPs aggregation in aqueous environment and biological media [288]. In another study Muzio, et al. coated the MNPs by a silica shell, that were subsequently functionalized with a multi-layered conjugated linoleic acid coating [289].

One technique which is widely used for surface functionalization is silanization, which results in high stability in acidic conditions, inertness to redox reactions, and low cytotoxicity. Treccani et al used silane precursors to functionalize the surface of MNPs and then successfully used them for protein immobilization (Figure 9) [290].

One of the methods most commonly deployed for MNP surface functionalization relies on the use of thiol groups. Using this method, Huixia, et al successfully functionalized MNPs to immobilize and separate bovine serum albumin (BSA) in solution [291]. Another type of surface functionalization method that can be used for MNPs is based on the presence of amine groups (Amine-Functionalized Core-Shell MNPs). Chen, et al demonstrated that by conjugating silica to amine groups, fluorescein molecules can quickly and quantitatively associate with MNPs via electrostatic binding, leading to a significant increase in the absorption per nanoparticle [292].

An additional method to functionalize MNP surfaces relies on the use of organic and organometallic catalysts. Hu, et al reported functionalization using chiral catalysts immobilized on MNPs [293]. The immobilized catalysts were readily recycled via magnetic decantation and could be re-used up to fourteen times without any decline in activity (Figure 10)[293].

The magnetic properties of any material depend on the orbital and spin motions of its electrons [294]. There are five fundamental types of magnetic materials: diamagnetic, ferromagnetic, paramagnetic, antiferromagnetic, and ferromagnetic. The magnetic susceptibility is the main property by which a material is classified as a magnetic material. Magnetic properties can be measured using several methods, including SQUID (superconducting quantum interference device) [295] magnetometry and vibrating sample magnetometry (VSM)[296].

The most recognized technique for the study of the MNPs surface is X-ray photoelectron spectroscopy (XPS). Stabilization of MNPs with different coatings affects the surface charge of the MNPs. To study this effect, zeta potential analysis can be performed on MNPs with various coatings, It is clear that by modifying the NPs with various coated layers, the zeta potential changes can be controlled in order to achieve the optimum condition for the specific assay with regard to, pH, temperature, functional and surface groups (Figure 11) [283].

In each step of functionalization, FT-IR spectroscopy can be carried out to detect which functional group is attached to MNPs. To estimate the functionalization efficiency, the thermal gravimetric analysis (TGA) procedure can be performed on the coated MNPs [284].

A brief survey on the applications of MNPs showed that they were mostly used in industrial, biological, medical, and environmental sciences [297].

Hu, et al. developed a technique for the removal of hexavalent chromium present in the effluents of a metal-processing plant using magnetic separation based on maghemite [298]. In medical sciences, MNPs can be employed in various applications such as targeted drug delivery, biosensors, and bioimaging. MNPs are also widely used in more specialized areas such as radiotherapy, virus detection, gene therapy, enzyme catalysis, and magnetic cell separation[299]. Cole,et al reported that MNPs modified with PEG could be deployed for targeting brain tumor via external magnetic fields. They concluded that enhanced magnetic brain tumor targeting could be achieved because of the relatively long circulation lifetime of the modified NPs [300]. Hua, et al demonstrated that iron oxide nanoparticles coated with polymeric poly-[aniline-co-N-(1-one-butyric acid) aniline] (SPAnH) enhanced the therapeutic capacity and thermal stability of 1, 3-bis (2-chloroethyl)-1-nitrosourea (BCNU), which is an important chemotherapeutic agent used for the treatment of several types of brain cancer, including glioma, glioblastoma multiforme, medulloblastoma and astrocytoma [301].

7- Colorimetric Detection Based on MNPs

MNPs, due to their non-toxicity, biocompatibility and ability for remote manipulation, are interesting candidates for assays based on colorimetric detection. Liang, et al developed a technique based on the detection of organophosphorus pesticides and nerve agents using Fe_3O_4 magnetic nanoparticles as a peroxidase mimetic. The MNPs were mixed with two different enzymes acetylcholinesterase (AChE) and choline oxidase (CHO) as shown in Figure 12 [302]. The AChE and CHO enzymes catalyze the formation of H_2O_2, which in turn causes the MNP-catalyzed oxidation of a substrate, 3,3′,5,5′-tetramethylbenzidine (TMB) leading to a color reaction [302]. In this way a screening tool could be developed for ultra-sensitive detection of organophosphate compounds such as pesticides and neurotoxic nerve agents.

$$\text{Acetylcholine} + H_2O \xrightarrow{\text{Ache}} \text{choline} \quad (1)$$

$$\text{Choline} + O_2 \xrightarrow{\text{CHO}} H_2O_2 \quad (2)$$

$$H_2O_2 + \text{TMB} \xrightarrow{\text{MNP}} \text{Oxidized TMB} \quad (3)$$

Zhang, et al studied a similar assay system employing the catalytic activity of MNPs to oxidize TMB in the presence of H2O2. They employed a sandwich assay using two different aptamers that recognized thrombin. Biotinylated thrombin aptamer 1 was loaded into a 96-well plate by streptavidin binding. Next amino-terminal thrombin aptamer 2 was assembled onto the chitosan modified Fe_3O_4 MNPs (prepared via a solvothermal method) through glutaraldehyde coupling. When the thrombin sample and aptamer 2 modified MNPs were successively added the MNPs became linked to the 96-well plate and were detected by a color change ([303].

7-1 Colorimetric detection based on combinations of AuNPs and MNPs

MNPs such as nickel, cobalt, and iron can be used in various biological applications; these materials, however, rapidly oxidize in the presence of water and oxygen. One of the most effective methods to prevent oxidation relies on the generation of a protective layer of materials such as silica and gold to form a core-shell structure. Superparamagnetic iron oxide nanoparticles (SPIONs) have a pronounced tendency to accumulate and agglomerate and hence coating the nanoparticles can be an effective solution to prevent their agglomeration. Moreover, coatings also enhances properties such as biocompatibility and stability. Among the different materials used to generate a layer on the iron oxide nanoparticles (IONPs), metals such AuNPs have attracted attention due to their biocompatibility, stability and facile synthesis methods [304]. Nanoparticles coated with AuNPs show good biocompatibility and can easily react with bio-molecules such as

polypeptides, nucleic acids, and polysaccharides. The combination of IONPs and AuNPs with a core-shell structure (IONPs-AuNPs), has resulted in many applications in the biotechnology and medical fields and has proven particularly relevant for the identification of analytes, using formats such as immune-electrochemical sensors [304]. Pang,et al developed a detection method for DNA point mutations that was based on a ligase reaction between DNA sequences and Fe_3O_4/Au core/shell nanoparticle probes [305]. Using MRI and core-shell structured IONPs- AuNPs, He, et al successfully carried out *in vivo* tumor detection using dual mode contrast agents [306]. They reported covalent conjugation of lectin to Fe_2O_3@Au core@shell NPs(lectin-Fe_2O_3@AuNP) for T2-weighted magnetic resonance and X-ray computed tomography dual-modality imaging in vitro and in vivo (Figure 13) [306].

Core-shell structured IONPs-AuNPs can be covalently modified by fluorescent quantum dots. These fluorescent quantum dots need to be functionalized in order to allow better coupling of biomolecules or other probes (Figure 14) [307].

Xie, et al used Fe_3O_4/Au core-shell NPs to separate histidine-tagged (His-Tag) maltose-binding protein (MBP)[308]. The intact gold shell enabled these NPs to be modified and bio-functionalized for various biodetection and biosensing purposes. The authors concluded that Fe_3O_4/Au−NTA−Ni2+ can be used for sensitive, effective, and specific separation of His-Tag targets from a mixture of lysed cells (Figure 15) [309].

7-2 Colorimetric detection based on combinations of AgNPs and MNPs

Silver nanoparticles have been extensively used in various fields because of their antibacterial properties. The use of these particles in biosensors for the detection and treatment of diseases like cancer is also notable. AgNPs are considered to be non-toxic, non-stimulant, non-allergenic, stable in various conditions, hydrophilic, and heat-resistant [310]. Due to the simplicity of the process needed for their generation and because of the ability to control their size and shape, chemical reduction is one of the most commonly used methods to synthesize this type of NPs [311]. When comparing Ag with Au nanoparticles, Tang, et al reported the following advantages, AgNPs show a surface plasmon band in the range of 390-420 nm that is significantly different from that of Au and the extinction coefficient of the surface plasmon band for an Ag NP is almost 4 times larger than that for Au NPs of the same size [312]. The authors also described a new method to develop more advanced immunosensors to detect carcinoembryonic antigen in a clinical immunoassay using chemically functionalized core-shell Fe_3O_4@AgNPs [312]. Ranc, et al developed a method for rapid analysis of dopamine levels in artificial samples of cerebrospinal fluid [313]. Their method used a nanocomposite that consisted of magnetite and AgNPs connected by carboxymethyl chitosan (Figure 16) [313]. This method successfully showed an improvement in the detection of dopamine levels at low concentrations [313].

8- Colorimetric detection based on other inorganic nanoparticles

In addition to the noble metal and magnetic nanoparticles that have been discussed above, other mineral nanoparticles, such as semiconductor nanoparticles including ZnO, TiO_2, and ZnS, as well as insulator nanoparticles including SiO_2, have also been used in colorimetric

assays. SiO_2, due to their optical and fluorescent properties, are widely used in rapid diagnostic processes that require high sensitivity [314, 315]. These NPs can be used as coatings for other NPs due to their stability and catalytic properties [316–318]. $Ag@SiO_2$ core shell NPs were used in a study to detect pyrethroid insecticides (including lambda-cyhalothrin, LC) based on a colorimetric technique [317]. Pyrethroid insecticides can be toxic to the nervous system. $Ag@SiO_2$ core shell nanoparticles modified with amines (NH2), interacted with LC through hydrogen bond formation causing a color change from yellow to pink. The detection limit of this technique was reported to be 1.0×10^{-6} M of LC [317] (Fig. 17).

For detection of H_2O_2 and glucose, γ-Fe_2O_3/SiO_2 nanoparticles (JFSNs) were developed by Sun et al. These NPs show a peroxidase-like catalytic activity and are stable over time. JFSNs modified with glucose oxidase GOx were used to detect glucose. GOx initially catalyzes the oxidation of glucose to H_2O_2 and gluconic acid at pH 7.0. Subsequently, H_2O_2 is adsorbed on the surface of JFSNs and catalytically oxidizes TMB producing a blue color [319] (Fig. 18).

Zinc oxide (ZnO) is a non-toxic, biocompatible material with high catalytic activity. ZnO nanoparticles have been widely used in diagnostics due to their optical, chemical, and electrical properties [320–323]. The catalytic and optical properties of these ZnO-NPs have been exploited in colorimetric assays [324, 325]. In a study conducted by Hayat et al, ZnO-NPs incorporated into carbon nanotubes were synthesized for the detection of cholesterol. These NPs displayed peroxidase like activity. In the presence of cholesterol oxidase, H_2O_2 is produced as the product of cholesterol oxidation. Because of the presence of H_2O_2, catalyzed by ZnO-NPs/CNTs, a chromogenic substrate, 2,2′-azino-bis (3-ethylbenzthiazoline-6-sulfonic acid (ABTS) is oxidized and the color changes to green. The authors suggested that the use of composite nanoparticles with peroxidase-like activity is a valuable alternative to conventional enzyme assays in colorimetric procedures [324].

Another type of inorganic NPs are composed of titanium dioxide, TiO_2. TiO_2-NPs function as photocatalysts, with a high surface area, and high absorption coefficient [326–328]. A colorimetric technique based on the use of dithizone (DZ) anchored on mesoporous TiO_2-NPs was proposed for the detection and removal of Bi(III) ions. Bi(III) ions have high bacteriostatic properties and can be very dangerous to aquatic organisms. In this approach, spherical shaped TiO_2 mesoporous NPs were synthesized. Bi(III) binds with high affinity to DZ to form the [(DZ) 3-Bi] complex, with a consequent color change. In the presence of mesoporous TiO_2-NPs, a stable complex (TiO_2-[(DZ) 3-Bi]) was formed. This led to the complete disappearance of color to generate a transparent solution. This technique was used for the detection and removal of Bi(III) ions in solution [326].

Quantum dots (QDs) are semiconductor nanoparticles with tunable sizes that are widely used in optics, due to their quantum properties. In a recent study NPs composed of ZnS deposited on montmorillonite (ZnS-MMT) were produced in vacuum with high peroxidase-like activity for the detection of H_2O_2 according to the scheme in Fig. 19. In the presence of H_2O_2, ZnS-MMT composite NPs oxidize TMB due to their peroxidase-like activity

producing a color change to blue. This study reported the a H_2O_2 detection limit of 1.04838×10^{-5} M [329] (Fig. 19).

Some studies using colorimetric detection based on other inorganic nanoparticle are summarized in Table 8.

9- Conclusion and Future Outlook

In this review, the properties and application of a wide range of inorganic nanoparticles that have been used optical sensors has been discussed. Each type of nanoparticle has its own unique properties that can be used in optical diagnostic techniques, including colorimetric assays. Noble metal NPs exhibit local surface plasmon resonance and metal oxide NPs also possess extremely small size and useful potential. Quantum dots and nanocomposites exhibit fluorescence and other useful optical properties; their significant fluorescence intensity changes make them a promising choice for optical assays. Nanocomposites are made of two or more different component materials. The nanoparticles discussed in the paper have many applications in detection of a wide range of molecules and analytes due to their unique properties.

Colorimetric sensors are attractive because of their simplicity, high sensitivity and specificity and low cost. Most of them produce color changes that can simply be detected by the naked eye. Because of their properties, colorimetric sensors have attracted considerable attention. Early and timely detection of infectious and biological agents, food, and environmental contaminants are important in preventing and treating diseases. Another advantage of nanoparticles relates to their efficiency for detection of dangerous microorganisms and biomarkers of cancerous tissues both *in vivo* and *in vitro*.

AuNPs have high stability and biocompatibility and together with other molecules, they can serve as an effective sensor to detect target molecules, AgNPs are also useful for optical sensors since the nanoparticles have a higher extinction coefficient than AuNPs. Thus AgNPs can be used with DNA molecules and other recognition systems to create selective colorimetric biosensors that are used to detect important analytes.

Metal nanoparticles possessing magnetic properties including iron oxide NPs are widely used in colorimetric techniques due to their superparamagnetic properties as well as their small size and large surface area. However, these NPs tend to have high reactivity and low stability compared to metal oxide nanoparticles. They tend to agglomerate irreversibly. Therefore, it is usually necessary to protect them against the surrounding environment by coating them with a protective shell. The use of different surface coatings can improve stability and increase biocompatibility by reducing their interactions with cells or proteins.

In addition to noble metal and magnetic nanoparticles, the properties and applications of ceramic and quantum nanoparticles were also discussed. According to their unique features, such as high surface area to volume ratio, photocatalytic activity and high absorption, ceramic and quantum nanoparticles can be also deployed for removal of hazardous metal ions and a variety of toxic compounds.

SiO_2 NPs act as insulating nanoparticles with easy synthesis and good biocompatibility, and act as a coating can be used to stabilize other NPs. These NPs are very important for the formation of core-shell and other nanocomposite structures. Therefore, they can play an important role in colorimetric assays. The use of nanocomposites or multi-purpose nanoparticles allows several different analytes to be detected simultaneously. This results in increased versatility for the diagnostic techniques.

The surface plasmon resonance wavelength and absorption spectrum of the nano-shells depends on the size ratio of the core to the shell. Unlike metal NPs, the optical absorption of which remains constant at a certain wavelength, the ability to tailor the size of NPs and intensify the SPR is among their advantages as optical sensors.

Despite the importance of inorganic NPs in diagnostic sensors, there are still some problems surrounding their synthesis methods, their tendency to precipitate, and the ability to finely control the shape and size of the NPs, as well as their sustainability in environmental conditions. In order to use NPs in the development of medical and clinical diagnostic assays, efforts to optimize these parameters are essential in order to detect biomolecules and biomarkers in biological fluids and clinical samples. In order to overcome these problems, it is necessary to focus on controlling the basic parameters such as the size and shape of the NPs to make4 them suitable for applications in optics, catalysts, photonics, electronics and related fields. It is also possible to increase their biocompatibility and reduce their toxicity to individuals and also to the environment. However, due to the high performance of inorganic NPs in optical sensors, it is becoming possible to incorporate them into microarray designs, microfluidic devices and lab-on-a-chip set ups to simultaneously detect multiple pathogens or analytes. Micro-arrays and chips will be designed for the simultaneous detection of bacteria, viruses and other pathogens. Using metal NPs is much easier than other technologies for these microscale devices, and their ability to provide a range of optical read-outs including in SPR and SERS means that applications of colloidal AuNPs will continue to grow.

Acknowledgments

MRH was supported by US NIH grants R01AI050875 and R21AI121700

References

1. Cho-Chung YS. Autoantibody biomarkers in the detection of cancer. Biochimica et Biophysica Acta (BBA) - Molecular Basis of Disease. 2006; 1762(6):587–591. [PubMed: 16730166]
2. Zaenker P, Ziman MR. Serologic autoantibodies as diagnostic cancer biomarkers–a review. Cancer Epidemiol Biomarkers Prev. 2013; 22(12):2161–81. [PubMed: 24057574]
3. Suo B, et al. Development of an oligonucleotide-based microarray to detect multiple foodborne pathogens. Mol Cell Probes. 2010; 24(2):77–86. [PubMed: 19833198]
4. Steinberg TH. Protein gel staining methods: an introduction and overview. Methods Enzymol. 2009; 463:541–63. [PubMed: 19892191]
5. Mandal P, et al. Methods for Rapid Detection of Foodborne Pathogens: An Overview. 2011; 6
6. Malic L, et al. Integration and detection of biochemical assays in digital microfluidic LOC devices. Lab Chip. 2010; 10(4):418–31. [PubMed: 20126681]

7. Tay LL, et al. Silica encapsulated SERS nanoprobe conjugated to the bacteriophage tailspike protein for targeted detection ofSalmonella. Chemical Communications. 2012; 48(7):1024–1026. [PubMed: 22158658]
8. Haque QM. Evaluation of Available Diagnostic Tests for Melioidosis. Journal of Taibah University Medical Sciences. 2010; 5(2):89–97.
9. Vafajoo A, et al. Early Diagnosis of Disease Using Microbead Array Technology: A Review. Analytica Chimica Acta. 2018
10. Scholl JA, Koh AL, Dionne JA. Quantum plasmon resonances of individual metallic nanoparticles. Nature. 2012; 483(7390):421–427. [PubMed: 22437611]
11. Zamborini FP, Bao L, Dasari R. Nanoparticles in Measurement Science. Analytical Chemistry. 2012; 84(2):541–576. [PubMed: 22148733]
12. Yakoh A, et al. Biomedical Probes Based on Inorganic Nanoparticles for Electrochemical and Optical Spectroscopy Applications. Sensors. 2015; 15(9):21427–77. [PubMed: 26343676]
13. Giner-Casares JJ, et al. Inorganic nanoparticles for biomedicine: where materials scientists meet medical research. Materials Today. 2016; 19(1):19–28.
14. Tansil NC, Gao Z. Nanoparticles in biomolecular detection. Nano Today. 2006; 1(1):28–37.
15. Vellaisamy K, et al. Cell imaging of dopamine receptor using agonist labeling iridium (iii) complex. Chemical Science. 2018
16. Karimi M, et al. Smart micro/nanoparticles in stimulus-responsive drug/gene delivery systems. Chemical Society Reviews. 2016; 45(5):1457–1501. [PubMed: 26776487]
17. Hori Y, et al. Synthetic-molecule/protein hybrid probe with fluorogenic switch for live-cell imaging of DNA methylation. Journal of the American Chemical Society. 2018; 140(5):1686–1690. [PubMed: 29381073]
18. Taeho K, Taeghwan H. Applications of inorganic nanoparticles as therapeutic agents. Nanotechnology. 2014; 25(1):012001. [PubMed: 24334327]
19. Wagner DE, Bhaduri SB. Progress and outlook of inorganic nanoparticles for delivery of nucleic acid sequences related to orthopedic pathologies: a review. Tissue Eng Part B Rev. 2012; 18(1):1–14. [PubMed: 21707439]
20. Ojea-Jimenez I, et al. Engineered inorganic nanoparticles for drug delivery applications. Curr Drug Metab. 2013; 14(5):518–30. [PubMed: 23116108]
21. Vilela D, González MC, Escarpa A. Sensing colorimetric approaches based on gold and silver nanoparticles aggregation: Chemical creativity behind the assay. A review. Analytica Chimica Acta. 2012; 751(Supplement C):24–43. [PubMed: 23084049]
22. Sun C, Lee JS, Zhang M. Magnetic nanoparticles in MR imaging and drug delivery. Adv Drug Deliv Rev. 2008; 60(11):1252–65. [PubMed: 18558452]
23. Karimi M, et al. Smart micro/nanoparticles in stimulus-responsive drug/gene delivery systems. Chemical Society Reviews. 2016; 45(5):1457–1501. [PubMed: 26776487]
24. Wignarajah S, et al. Colorimetric Assay for the Detection of Typical Biomarkers for Periodontitis Using a Magnetic Nanoparticle Biosensor. Analytical Chemistry. 2015; 87(24):12161–12168. [PubMed: 26631371]
25. Qu X, Alvarez PJJ, Li Q. Applications of nanotechnology in water and wastewater treatment. Water Research. 2013; 47(12):3931–3946. [PubMed: 23571110]
26. Yeh YC, Creran B, Rotello VM. Gold Nanoparticles: Preparation, Properties, and Applications in Bionanotechnology. Nanoscale. 2012; 4(6):1871–1880. [PubMed: 22076024]
27. Ji X, et al. Size Control of Gold Nanocrystals in Citrate Reduction: The Third Role of Citrate. Journal of the American Chemical Society. 2007; 129(45):13939–13948. [PubMed: 17948996]
28. Bienert R, Emmerling F, Thunemann AF. The size distribution of ‘gold standard’ nanoparticles. Anal Bioanal Chem. 2009; 395(6):1651–60. [PubMed: 19756546]
29. Li C, et al. Facile synthesis of concentrated gold nanoparticles with low size-distribution in water: temperature and pH controls. Nanoscale Research Letters. 2011; 6(1):1–10.
30. Ojea-Jiménez I, et al. Small Gold Nanoparticles Synthesized with Sodium Citrate and Heavy Water: Insights into the Reaction Mechanism. The Journal of Physical Chemistry C. 2010; 114(4): 1800–1804.

31. Sivaraman SK, Kumar S, Santhanam V. Monodisperse sub-10 nm gold nanoparticles by reversing the order of addition in Turkevich method – The role of chloroauric acid. Journal of Colloid and Interface Science. 2011; 361(2):543–547. [PubMed: 21719021]
32. Kimling J, et al. Turkevich Method for Gold Nanoparticle Synthesis Revisited. The Journal of Physical Chemistry B. 2006; 110(32):15700–15707. [PubMed: 16898714]
33. Lee JH, et al. Production of aqueous spherical gold nanoparticles using conventional ultrasonic bath. Nanoscale Research Letters. 2012; 7(1):1–7. [PubMed: 22214494]
34. Jana NR, Gearheart L, Murphy CJ. Seed-Mediated Growth Approach for Shape-Controlled Synthesis of Spheroidal and Rod-like Gold Nanoparticles Using a Surfactant Template. Advanced Materials. 2001; 13(18):1389–1393.
35. Fleming DA, Williams ME. Size-Controlled Synthesis of Gold Nanoparticles via High-Temperature Reduction. Langmuir. 2004; 20(8):3021–3023. [PubMed: 15875823]
36. Gutierrez-Wing C, et al. Microwave-assisted synthesis of gold nanoparticles self-assembled into self-supported superstructures. Nanoscale. 2012; 4(7):2281–2287. [PubMed: 22398420]
37. Frens G. Controlled nucleation for the regulation of the particle size in monodisperse gold suspensions. Nature. 1973; 241(105):20–22.
38. Yang S, et al. UV irradiation induced formation of Au nanoparticles at room temperature: The case of pH values. Colloids and Surfaces A: Physicochemical and Engineering Aspects. 2007; 301(1–3):174–183.
39. Alkilany AM, Yaseen AIB, Kailani MH. Synthesis of monodispersed gold nanoparticles with exceptional colloidal stability with grafted polyethylene glycol-g-polyvinyl alcohol. J Nanomaterials. 2015; 16(1):51–51.
40. Ma H, et al. Synthesis of silver and gold nanoparticles by a novel electrochemical method. ChemPhysChem. 2004; 5(1):68–75. [PubMed: 14999845]
41. Riabinina D, et al. Size Control of Gold Nanoparticles Synthesized by Laser Ablation in Liquid Media. ISRN Nanotechnology. 2012; 2012:5.
42. Raliya R, Biswas P. Environmentally benign bio-inspired synthesis of Au nanoparticles, their self-assembly and agglomeration. RSC Advances. 2015; 5(52):42081–42087.
43. Bhau B, et al. Green synthesis of gold nanoparticles from the leaf extract of Nepenthes khasiana and antimicrobial assay. Adv Mater Lett. 2015; 6:55–58.
44. Kumar B, et al. Aqueous Phase Lavender Leaf Mediated Green Synthesis of Gold Nanoparticles and Evaluation of its Antioxidant Activity. Biology and Medicine. 2016; 2016
45. Manson J, et al. Polyethylene glycol functionalized gold nanoparticles: the influence of capping density on stability in various media. Gold Bulletin. 2011; 44(2):99–105.
46. Majzik A, et al. Functionalization of gold nanoparticles with amino acid, β-amyloid peptides and fragment. Colloids and Surfaces B: Biointerfaces. 2010; 81(1):235–241. [PubMed: 20674288]
47. Bozich JS, et al. Surface chemistry, charge and ligand type impact the toxicity of gold nanoparticles to Daphnia magna. Environmental Science: Nano. 2014; 1(3):260–270.
48. Capek I. Preparation and Functionalization of Gold Nanoparticles. J Surf Sci Technol. 2013; 29:1–18.
49. Gupta A, Landis R, Rotello V. Nanoparticle-Based Antimicrobials: Surface Functionality is Critical [version 1; referees: 2 approved]. 2016; 5
50. Zhang X, Servos MR, Liu J. Instantaneous and Quantitative Functionalization of Gold Nanoparticles with Thiolated DNA Using a pH-Assisted and Surfactant-Free Route. Journal of the American Chemical Society. 2012; 134(17):7266–7269. [PubMed: 22506486]
51. Pellegrino T, et al. On the development of colloidal nanoparticles towards multifunctional structures and their possible use for biological applications. Small. 2005; 1(1):48–63. [PubMed: 17193348]
52. Spampinato V, et al. Surface Analysis of Gold Nanoparticles Functionalized with Thiol-Modified Glucose SAMs for Biosensor Applications. Frontiers in chemistry. 2016; 4
53. Huang X, El-Sayed MA. Gold nanoparticles: Optical properties and implementations in cancer diagnosis and photothermal therapy. Journal of Advanced Research. 2010; 1(1):13–28.

54. Balasubramani G, et al. Structural characterization, antioxidant and anticancer properties of gold nanoparticles synthesized from leaf extract (decoction) of Antigonon leptopus Hook. & Arn. Journal of Trace Elements in Medicine and Biology. 2015; 30:83–89. [PubMed: 25432487]
55. Saxena U, Goswami P. Electrical and optical properties of gold nanoparticles: applications in gold nanoparticles-cholesterol oxidase integrated systems for cholesterol sensing. Journal of Nanoparticle Research. 2012; 14(4):1–11. [PubMed: 22448125]
56. Raghavan V, et al. Multimodal Gold Nanoprobes for SERS Bioimaging. Journal of Nanomedicine & Nanotechnology. 2015; (S6):1.
57. Krug JT, et al. Efficient Raman Enhancement and Intermittent Light Emission Observed in Single Gold Nanocrystals. Journal of the American Chemical Society. 1999; 121(39):9208–9214.
58. He J, et al. Methionine–Au Nanoparticle Modified Glassy Carbon Electrode: a Novel Platform for Electrochemical Detection of Hydroquinone. Materials Science. 2014; 20(4):381–386.
59. Pan S, Liu J, Hill CM. Observation of Local Redox Events at Individual Au Nanoparticles Using Electrogenerated Chemiluminescence Microscopy. The Journal of Physical Chemistry C. 2015; 119(48):27095–27103.
60. Yu Q, et al. Inhibition of gold nanoparticles (AuNPs) on pathogenic biofilm formation and invasion to host cells. Scientific Reports. 2016; 6:26667. [PubMed: 27220400]
61. Zhao W, Brook MA, Li Y. Design of gold nanoparticle-based colorimetric biosensing assays. Chembiochem. 2008; 9(15):2363–71. [PubMed: 18821551]
62. Baptista P, et al. Gold nanoparticles for the development of clinical diagnosis methods. Analytical and bioanalytical chemistry. 2008; 391(3):943–950. [PubMed: 18157524]
63. Medley CD, et al. Gold Nanoparticle-Based Colorimetric Assay for the Direct Detection of Cancerous Cells. Analytical Chemistry. 2008; 80(4):1067–1072. [PubMed: 18198894]
64. Jans H, et al. Dynamic Light Scattering as a Powerful Tool for Gold Nanoparticle Bioconjugation and Biomolecular Binding Studies. Analytical Chemistry. 2009; 81(22):9425–9432. [PubMed: 19803497]
65. DeLong RK, et al. Functionalized gold nanoparticles for the binding, stabilization, and delivery of therapeutic DNA, RNA, and other biological macromolecules. Nanotechnology, Science and Applications. 2010; 3:53–63.
66. Du J, et al. Optical reading of contaminants in aqueous media based on gold nanoparticles. Small. 2014; 10(17):3461–79. [PubMed: 24578321]
67. Liu D, Wang Z, Jiang X. Gold nanoparticles for the colorimetric and fluorescent detection of ions and small organic molecules. Nanoscale. 2011; 3(4):1421–1433. [PubMed: 21359318]
68. Daniel WL, et al. Colorimetric Nitrite and Nitrate Detection with Gold Nanoparticle Probes and Kinetic End Points. Journal of the American Chemical Society. 2009; 131(18):6362–6363. [PubMed: 19368386]
69. Vaseghi A, et al. Detection of Pseudomonas syringae pathovars by thiol-linked DNA–Gold nanoparticle probes. Sensors and Actuators B: Chemical. 2013; 181(Supplement C):644–651.
70. Wu Z, et al. Activity-Based DNA-Gold Nanoparticle Probe as Colorimetric Biosensor for DNA Methyltransferase/Glycosylase Assay. Analytical Chemistry. 2013; 85(9):4376–4383. [PubMed: 23544713]
71. Hu J, et al. Aptamer-based colorimetric biosensing of abrin using catalytic gold nanoparticles. Analyst. 2015; 140(10):3581–6. [PubMed: 25854313]
72. Azzazy HME, Mansour MMH. In vitro diagnostic prospects of nanoparticles. Clinica Chimica Acta. 2009; 403(1):1–8.
73. Cao X, Ye Y, Liu S. Gold nanoparticle-based signal amplification for biosensing. Analytical Biochemistry. 2011; 417(1):1–16. [PubMed: 21703222]
74. Franco R, et al. Gold nanoparticles for DNA/RNA-based diagnostics. 2015:1339–1364.
75. Rabiee N, Safarkhani M, Rabiee M. Ultra-sensitive electrochemical on-line determination of Clarithromycin based on Poly (L-Aspartic Acid)/Graphite Oxide/Pristine Graphene/Glassy Carbon Electrode. Asian Journal of Nanosciences and Materials. 2018; 1:61–70.
76. Ma Z, et al. Optical DNA detection based on gold nanorods aggregation. Anal Chim Acta. 2010; 673(2):179–84. [PubMed: 20599033]

77. Kim JH, et al. Specific and sensitive detection of nucleic acids and RNases using gold nanoparticle-RNA-fluorescent dye conjugates. Chemical Communications. 2007; (42):4342–4344. [PubMed: 17957280]

78. Alhasan AH, et al. Scanometric MicroRNA Array Profiling of Prostate Cancer Markers Using Spherical Nucleic Acid–Gold Nanoparticle Conjugates. Analytical Chemistry. 2012; 84(9):4153–4160. [PubMed: 22489825]

79. Xia F, et al. Colorimetric detection of DNA, small molecules, proteins, and ions using unmodified gold nanoparticles and conjugated polyelectrolytes. Proc Natl Acad Sci U S A. 2010; 107(24): 10837–41. [PubMed: 20534499]

80. Kim Y, Johnson RC, Hupp JT. Gold Nanoparticle-Based Sensing of "Spectroscopically Silent" Heavy Metal Ions. Nano Letters. 2001; 1(4):165–167.

81. Sun S, et al. Phosphorylation-regulated crosslinking of gold nanoparticles: a new strategy for colorimetric detection of protein kinase activity. Analyst. 2015; 140(16):5685–5691. [PubMed: 26147077]

82. Xie X, et al. Colorimetric Detection of HIV-1 Ribonuclease H Activity by Gold Nanoparticles. Small. 2011; 7(10):1393–1396. [PubMed: 21438149]

83. Sattarahmady N, et al. Gold nanoparticles biosensor of Brucella spp. genomic DNA: Visual and spectrophotometric detections. Biochemical Engineering Journal. 2015; 97(Supplement C):1–7.

84. Borghei YS, et al. Visual detection of cancer cells by colorimetric aptasensor based on aggregation of gold nanoparticles induced by DNA hybridization. Anal Chim Acta. 2016; 904:92–7. [PubMed: 26724767]

85. Valentini P, et al. Gold-Nanoparticle-Based Colorimetric Discrimination of Cancer-Related Point Mutations with Picomolar Sensitivity. ACS Nano. 2013; 7(6):5530–5538. [PubMed: 23697628]

86. Andreadou M, et al. A novel non-amplification assay for the detection of Leishmania spp. in clinical samples using gold nanoparticles. J Microbiol Methods. 2014; 96:56–61. [PubMed: 24184015]

87. Wang C, Yu C. Detection of chemical pollutants in water using gold nanoparticles as sensors: a review, in Reviews in Analytical Chemistry. 2013:1.

88. Liu X, et al. Biofunctionalized gold nanoparticles for colorimetric sensing of botulinum neurotoxin a light chain. Analytical chemistry. 2014; 86(5):2345–2352. [PubMed: 24484451]

89. Wu S, et al. Oxidation-triggered aggregation of gold nanoparticles for naked-eye detection of hydrogen peroxide. Chemical Communications. 2016; 52(17):3508–3511. [PubMed: 26839922]

90. He Y, et al. Visual Detection of Single-Nucleotide Polymorphism with Hairpin Oligonucleotide-Functionalized Gold Nanoparticles. Analytical Chemistry. 2010; 82(17):7169–7177. [PubMed: 20681563]

91. Khalil MA, et al. A sensitive colorimetric assay for identification of Acinetobacter baumannii using unmodified gold nanoparticles. J Appl Microbiol. 2014; 117(2):465–71. [PubMed: 24836820]

92. Gill P, et al. Colorimetric detection of Helicobacter pylori DNA using isothermal helicase-dependent amplification and gold nanoparticle probes. Diagn Microbiol Infect Dis. 2008; 62(2): 119–24. [PubMed: 18599249]

93. Deng H, et al. Long genomic DNA amplicons adsorption onto unmodified gold nanoparticles for colorimetric detection of Bacillus anthracis. 2012; 49

94. Verma MS, et al. Colorimetric biosensing of pathogens using gold nanoparticles. Biotechnol Adv. 2015; 33(6 Pt 1):666–80. [PubMed: 25792228]

95. Saha K, et al. Gold Nanoparticles in Chemical and Biological Sensing. Chemical Reviews. 2012; 112(5):2739–2779. [PubMed: 22295941]

96. Sliem M, Ebeid EZ, Harith MA. Selective Colorimetric Detection of Viral DNA Sequence of Hepatitis C Virus Genotype-4 Genetic Material Using Gold Nanoparticles. 2007; 3:360–366.

97. Storhoff JJ, et al. One-Pot Colorimetric Differentiation of Polynucleotides with Single Base Imperfections Using Gold Nanoparticle Probes. Journal of the American Chemical Society. 1998; 120(9):1959–1964.

98. Wang G, et al. Cross-Linking versus Non-Cross-Linking Aggregation of Gold Nanoparticles Induced by DNA Hybridization: A Comparison of the Rapidity of Solution Color Change. Bioconjugate Chemistry. 2017; 28(1):270–277. [PubMed: 27509030]

99. Wang C, et al. Biorecognition-Driven Self-Assembly of Gold Nanorods: A Rapid and Sensitive Approach toward Antibody Sensing. Chemistry of Materials. 2007; 19(24):5809–5811.

100. Huang CC, et al. Aptamer-modified gold nanoparticles for colorimetric determination of platelet-derived growth factors and their receptors. Anal Chem. 2005; 77(17):5735–41. [PubMed: 16131089]

101. Gole A, Murphy CJ. Biotin−Streptavidin-Induced Aggregation of Gold Nanorods: Tuning Rod −Rod Orientation. Langmuir. 2005; 21(23):10756–10762. [PubMed: 16262348]

102. Hone DC, Haines AH, Russell DA. Rapid, Quantitative Colorimetric Detection of a Lectin Using Mannose-Stabilized Gold Nanoparticles. Langmuir. 2003; 19(17):7141–7144.

103. Sattarahmady N, Kayani Z, Heli H. Highly simple and visual colorimetric detection of Brucella melitensis genomic DNA in clinical samples based on gold nanoparticles. Journal of the Iranian Chemical Society. 2015; 12(9):1569–1576.

104. Li H, Rothberg L. Colorimetric detection of DNA sequences based on electrostatic interactions with unmodified gold nanoparticles. Proceedings of the National Academy of Sciences of the United States of America. 2004; 101(39):14036–14039. [PubMed: 15381774]

105. Mirkin CA, et al. A DNA-based method for rationally assembling nanoparticles into macroscopic materials. Nature. 1996; 382(6592):607–609. [PubMed: 8757129]

106. Storhoff JJ, et al. Homogeneous detection of unamplified genomic DNA sequences based on colorimetric scatter of gold nanoparticle probes. Nat Biotech. 2004; 22(7):883–887.

107. Nasseri B, et al. Point-of-care microfluidic devices for pathogen detection. Biosensors and Bioelectronics. 2018

108. Majdinasab M, et al. Detection of inv A gene of Salmonella by DNA-gold nanoparticles biosensor and its comparison with PCR. Journal of Experimental Nanoscience. 2013; 8(2):223–239.

109. Chen SH, et al. Optical detection of human papillomavirus type 16 and type 18 by sequence sandwich hybridization with oligonucleotide-functionalized Au nanoparticles. IEEE Trans Nanobioscience. 2009; 8(2):120–31. [PubMed: 19651546]

110. Liu Y, et al. Colorimetric detection of influenza A virus using antibody-functionalized gold nanoparticles. Analyst. 2015; 140(12):3989–3995. [PubMed: 25899840]

111. Lesniewski A, et al. Antibody Modified Gold Nanoparticles for Fast and Selective, Colorimetric T7 Bacteriophage Detection. Bioconjugate Chemistry. 2014; 25(4):644–648. [PubMed: 24679221]

112. Chen Z, et al. Chitosan-functionalized gold nanoparticles for colorimetric detection of mercury ions based on chelation-induced aggregation. 2014; 182:611–616.

113. Su F, et al. Highly sensitive detection of CpG methylation in genomic DNA by AuNP-based colorimetric assay with ligase chain reaction. Chemical Communications. 2015; 51(16):3371–3374. [PubMed: 25621431]

114. Dharanivasan G, et al. DNA templated self-assembly of gold nanoparticle clusters in the colorimetric detection of plant viral DNA using a gold nanoparticle conjugated bifunctional oligonucleotide probe. RSC Advances. 2016; 6(14):11773–11785.

115. Chai F, et al. Colorimetric Detection of Pb2+ Using Glutathione Functionalized Gold Nanoparticles. ACS Applied Materials & Interfaces. 2010; 2(5):1466–1470. [PubMed: 20429606]

116. Zhang M, Liu YQ, Ye BC. Colorimetric assay for parallel detection of Cd2+, Ni2+ and Co2+ using peptide-modified gold nanoparticles. Analyst. 2012; 137(3):601–7. [PubMed: 22158918]

117. Xue D, Wang H, Zhang Y. Specific and sensitive colorimetric detection of Al3+ using 5-mercaptomethyltetrazole capped gold nanoparticles in aqueous solution. Talanta. 2014; 119(Supplement C):306–311. [PubMed: 24401419]

118. Wei L, et al. Colorimetric assay for protein detection based on “nano-pumpkin” induced aggregation of peptide-decorated gold nanoparticles. Biosens Bioelectron. 2015; 71:348–352. [PubMed: 25932793]

119. Soo PC, et al. A simple gold nanoparticle probes assay for identification of Mycobacterium tuberculosis and Mycobacterium tuberculosis complex from clinical specimens. Molecular and Cellular Probes. 2009; 23(5):240–246. [PubMed: 19463945]
120. Su H, et al. Gold nanoparticles as colorimetric sensor: A case study on E. coli O157:H7 as a model for Gram-negative bacteria. Sensors & Actuators: B Chemical. 2012; 161(1):298–303.
121. Lu W, et al. Multifunctional Oval-Shaped Gold-Nanoparticle-Based Selective Detection of Breast Cancer Cells Using Simple Colorimetric and Highly Sensitive Two-Photon Scattering Assay. ACS Nano. 2010; 4(3):1739–1749. [PubMed: 20155973]
122. Zhang M, Liu YQ, Ye BC. Colorimetric assay for parallel detection of Cd2+, Ni2+ and Co2+ using peptide-modified gold nanoparticles. Analyst. 2012; 137(3):601–607. [PubMed: 22158918]
123. Ma Y, et al. Colorimetric sensing strategy for mercury(II) and melamine utilizing cysteamine-modified gold nanoparticles. 2013; 138
124. Kim DY, Shinde S, Ghodake G. Colorimetric detection of magnesium (II) ions using tryptophan functionalized gold nanoparticles. Scientific Reports. 2017; 7:3966. [PubMed: 28638065]
125. Yuan Z, et al. Selective Colorimetric Detection of Hydrogen Sulfide Based on Primary Amine-Active Ester Cross-Linking of Gold Nanoparticles. Anal Chem. 2015; 87(14):7267–73. [PubMed: 26082264]
126. Wang J, et al. Selective colorimetric analysis of spermine based on the cross-linking aggregation of gold nanoparticles chain assembly. Talanta. 2017; 167(Supplement C):193–200. [PubMed: 28340710]
127. Kang J, et al. A Rapid Colorimetric Sensor of Clenbuterol Based on Cysteamine-Modified Gold Nanoparticles. ACS Applied Materials & Interfaces. 2016; 8(1):1–5. [PubMed: 26673452]
128. Doria G, Franco R, Baptista P. Nanodiagnostics: fast colorimetric method for single nucleotide polymorphism/mutation detection. Iet Nanobiotechnology. 2007; 1(4):53–57. [PubMed: 17672805]
129. Conde J, , et al. RNA quantification using noble metal nanoprobes: simultaneous identification of several different mRNA targets using color multiplexing and application to cancer diagnostics, in Nanoparticles in Biology and Medicine Springer; 2012 7187
130. Xu J, Craig SL. Thermodynamics of DNA hybridization on gold nanoparticles. Journal of the American Chemical Society. 2005; 127(38):13227–13231. [PubMed: 16173751]
131. Padmavathy B, Rajendran VK, JA BM. A direct detection of Escherichia coli genomic DNA using gold nanoprobes. 2012; 10:8.
132. Castilho ML, et al. The efficiency analysis of gold nanoprobes by FT-IR spectroscopy applied to the non-cross-linking colorimetric detection of Paracoccidioides brasiliensis. Sensors and Actuators B: Chemical. 2015; 215(Supplement C):258–265.
133. Kang JH, et al. Gold nanoparticle-based colorimetric assay for cancer diagnosis. Biosensors and Bioelectronics. 2010; 25(8):1869–1874. [PubMed: 20153162]
134. Wang G, et al. Rapid Non-Crosslinking Aggregation of DNA-Functionalized Gold Nanorods and Nanotriangles for Colorimetric Single-Nucleotide Discrimination. Chemistry. 2016; 22(1):258–63. [PubMed: 26767586]
135. Zhang H, et al. A diazirine-based photoaffinity probe for facile and efficient aptamer-protein covalent conjugation. Chemical Communications. 2014; 50(38):4891–4894. [PubMed: 24686985]
136. Priyanka D, Kumar B, Suri CR. Antibody Functionalised Gold Nanoprobes Based Colorimetric Assay for the Direct Detection of Phenylurea Herbicide. 2012; 1
137. Mollasalehi H, Yazdanparast R. An improved non-crosslinking gold nanoprobe-NASBA based on 16S rRNA for rapid discriminative bio-sensing of major salmonellosis pathogens. Biosensors and Bioelectronics. 2013; 47(Supplement C):231–236. [PubMed: 23584228]
138. Khan SA, et al. Targeted highly sensitive detection of multi-drug resistant salmonella DT104 using gold nanoparticles. Chemical Communications. 2011; 47(33):9444–9446. [PubMed: 21776500]
139. Carter JR, et al. A novel dengue virus detection method that couples DNAzyme and gold nanoparticle approaches. Virology Journal. 2013; 10:201–201. [PubMed: 23809208]

140. Phromjai J, et al. RT-LAMP detection of shrimp Taura syndrome virus (TSV) by combination with a nanogold-oligo probe. Aquaculture Research. 2015; 46(8):1902–1913.
141. Gao ZF, et al. Detection of mercury ions (II) based on non-cross-linking aggregation of double-stranded DNA modified gold nanoparticles by resonance Rayleigh scattering method. Biosensors and Bioelectronics. 2015; 65(Supplement C):360–365. [PubMed: 25461182]
142. Dwivedi C, et al. Direct Visualization of Lead Corona and Its Nanomolar Colorimetric Detection Using Anisotropic Gold Nanoparticles. ACS Applied Materials & Interfaces. 2015; 7(9):5039–5044. [PubMed: 25719820]
143. Castilho ML, et al. The efficiency analysis of gold nanoprobes by FT-IR spectroscopy applied to the non-cross-linking colorimetric detection of Paracoccidioides brasiliensis. Sensors & Actuators: B Chemical. 2015; 215:258–265. Complete.
144. Xiao N, Yu C. Rapid-Response and Highly Sensitive Noncross-Linking Colorimetric Nitrite Sensor Using 4-Aminothiophenol Modified Gold Nanorods. Analytical Chemistry. 2010; 82(9):3659–3663. [PubMed: 20373815]
145. Xia N, et al. Simple, rapid and label-free colorimetric assay for arsenic based on unmodified gold nanoparticles and a phytochelatin-like peptide. Analytical Methods. 2012; 4(12):3937–3941.
146. Luo C, et al. Simplified aptamer-based colorimetric method using unmodified gold nanoparticles for the detection of carcinoma embryonic antigen. RSC Advances. 2015; 5(15):10994–10999.
147. Hussain MM, Samir TM, Azzazy HM. Unmodified gold nanoparticles for direct and rapid detection of Mycobacterium tuberculosis complex. Clin Biochem. 2013; 46(7–8):633–7. [PubMed: 23318577]
148. Liu Z, et al. Visual detection of Listeria monocytogenes using unmodified gold nanoparticles based on a novel marker. Analytical Methods. 2015; 7(19):8159–8164.
149. Verma MS, et al. Branching and size of CTAB-coated gold nanostars control the colorimetric detection of bacteria. RSC Advances. 2014; 4(21):10660–10668.
150. Cao R, et al. Naked-eye sensitive detection of nuclease activity using positively-charged gold nanoparticles as colorimetric probes. Chemical Communications. 2011; 47(45):12301–12303. [PubMed: 22005652]
151. Chen Z, et al. A colorimetric aptamer biosensor based on cationic polymer and gold nanoparticles for the ultrasensitive detection of thrombin. Biosens Bioelectron. 2014; 56:46–50. [PubMed: 24463195]
152. Pan Y, et al. Colorimetric detection of apoptosis based on caspase-3 activity assay using unmodified gold nanoparticles. Chemical Communications. 2012; 48(7):997–999. [PubMed: 22143383]
153. Hussain MM, Samir TM, Azzazy HME. Unmodified gold nanoparticles for direct and rapid detection of Mycobacterium tuberculosis complex. Clinical Biochemistry. 2013; 46(7):633–637. [PubMed: 23318577]
154. Liu Z, et al. Visual detection of Maize chlorotic mottle virus using unmodified gold nanoparticles. RSC Advances. 2015; 5(122):100891–100897.
155. Lee S, et al. Cationic surfactant-based colorimetric detection of Plasmodium lactate dehydrogenase, a biomarker for malaria, using the specific DNA aptamer. PLoS One. 2014; 9(7)
156. Shi Q, et al. Colorimetric and bare eye determination of urinary methylamphetamine based on the use of aptamers and the salt-induced aggregation of unmodified gold nanoparticles. Microchimica Acta. 2015; 182(3):505–511.
157. Emrani AS, et al. Colorimetric and fluorescence quenching aptasensors for detection of streptomycin in blood serum and milk based on double-stranded DNA and gold nanoparticles. Food Chemistry. 2016; 190(Supplement C):115–121. [PubMed: 26212949]
158. Teepoo S, et al. Unmodified gold nanoparticles as a simple colorimetric probe for ramoplanin detection. Talanta. 2013; 117:518–522. [PubMed: 24209375]
159. Shawky SM, Bald D, Azzazy HM. Direct detection of unamplified hepatitis C virus RNA using unmodified gold nanoparticles. Clin Biochem. 2010; 43(13–14):1163–8. [PubMed: 20627095]
160. Wang L, et al. Colorimetric detection of Cucumber green mottle mosaic virus using unmodified gold nanoparticles as colorimetric probes. J Virol Methods. 2017; 243:113–119. [PubMed: 28109844]

161. Chang CC, et al. Aptamer-based colorimetric detection of proteins using a branched DNA cascade amplification strategy and unmodified gold nanoparticles. Biosens Bioelectron. 2016; 78:200–5. [PubMed: 26609945]
162. Chen C, et al. Sensitive colorimetric detection of protein by gold nanoparticles and rolling circle amplification. Analyst. 2015; 140(13):4515–20. [PubMed: 25988199]
163. Zhang L, et al. Visual chiral recognition of tryptophan enantiomers using unmodified gold nanoparticles as colorimetric probes. Analytica Chimica Acta. 2014; 809(Supplement C):123–127. [PubMed: 24418142]
164. Zhou J, et al. A gold nanoparticles colorimetric assay for label-free detection of protein kinase activity based on phosphorylation protection against exopeptidase cleavage. Biosens Bioelectron. 2014; 53:295–300. [PubMed: 24157613]
165. Chen H, et al. Sensitive colorimetric assays for alpha-glucosidase activity and inhibitor screening based on unmodified gold nanoparticles. Anal Chim Acta. 2015; 875:92–8. [PubMed: 25937110]
166. Eissa S, et al. Direct detection of unamplified hepatoma upregulated protein RNA in urine using gold nanoparticles for bladder cancer diagnosis. Clinical Biochemistry. 2014; 47(1):104–110. [PubMed: 24183881]
167. Wang Q, et al. Colorimetric detection of mercury ion based on unmodified gold nanoparticles and target-triggered hybridization chain reaction amplification. Spectrochim Acta A Mol Biomol Spectrosc. 2015; 5(136):283–7.
168. Guo Y, et al. Label-Free Colorimetric Detection of Cadmium Ions in Rice Samples Using Gold Nanoparticles. Analytical Chemistry. 2014; 86(17):8530–8534. [PubMed: 25117533]
169. Hormozi-Nezhad MR, Abbasi-Moayed S. A sensitive and selective colorimetric method for detection of copper ions based on anti-aggregation of unmodified gold nanoparticles. Talanta. 2014; 129(Supplement C):227–232. [PubMed: 25127588]
170. Li L, et al. Visual detection of melamine in raw milk using gold nanoparticles as colorimetric probe. Food Chemistry. 2010; 122(3):895–900.
171. Shen Q, et al. A simple “clickable” biosensor for colorimetric detection of copper(II) ions based on unmodified gold nanoparticles. Biosensors and Bioelectronics. 2013; 41(Supplement C):663–668. [PubMed: 23089325]
172. Memon AG, et al. Utilization of unmodified gold nanoparticles for label-free detection of mercury (II): Insight into rational design of mercury-specific oligonucleotides. J Hazard Mater. 2017; 321:417–423. [PubMed: 27669382]
173. Zhao Y, Gui L, Zhengbo Chen D. Colorimetric detection of Hg2+ based on target-mediated growth of gold nanoparticles. 2016; 241
174. Deng HH, et al. Colorimetric detection of sulfide based on target-induced shielding against the peroxidase-like activity of gold nanoparticles. Analytica Chimica Acta. 2014; 852(Supplement C):218–222. [PubMed: 25441901]
175. Deng HH, et al. Colorimetric sensor for thiocyanate based on anti-aggregation of citrate-capped gold nanoparticles. Sensors and Actuators B: Chemical. 2014; 191(Supplement C):479–484.
176. Zhang J, Wang X, Yang X. Colorimetric determination of hypochlorite with unmodified gold nanoparticles through the oxidation of a stabilizer thiol compound. Analyst. 2012; 137(12):2806–2812. [PubMed: 22573188]
177. Kumar P, Lambadi PR, Navani NK. Non-enzymatic detection of urea using unmodified gold nanoparticles based aptasensor. Biosens Bioelectron. 2015; 72:340–7. [PubMed: 26002019]
178. Liu J, et al. Highly sensitive colorimetric detection of 17beta-estradiol using split DNA aptamers immobilized on unmodified gold nanoparticles. Sci Rep. 2014; 4(7571)
179. Huo Y, et al. A sensitive aptasensor for colorimetric detection of adenosine triphosphate based on the protective effect of ATP-aptamer complexes on unmodified gold nanoparticles. Biosensors and Bioelectronics. 2016; 78(Supplement C):315–320. [PubMed: 26638040]
180. Mao Y, et al. A simple and sensitive aptasensor for colorimetric detection of adenosine triphosphate based on unmodified gold nanoparticles. Talanta. 2017; 168(Supplement C):279–285. [PubMed: 28391854]

181. Kuswandi Bambang, et al. Simple Colorimetric DNA Biosensor Based on Gold Nanoparticles for Pork Adulteration Detection in Processed Meats. Sensors & Transducers Journal. 2017; 208(1): 7–13.

182. Harra J, et al. Size-controlled aerosol synthesis of silver nanoparticles for plasmonic materials. Journal of Nanoparticle Research. 2012; 14(6):870. [PubMed: 22844206]

183. Oseguera-Galindo DO, et al. Silver nanoparticles synthesized by laser ablation confined in urea choline chloride deep-eutectic solvent. Colloid and Interface Science Communications. 2016; 12:1–4.

184. Abou El-Nour KMM, et al. Synthesis and applications of silver nanoparticles. Arabian Journal of Chemistry. 2010; 3(3):135–140.

185. Agnihotri S, Mukherji S, Mukherji S. Size-controlled silver nanoparticles synthesized over the range 5-100 nm using the same protocol and their antibacterial efficacy. RSC Advances. 2014; 4(8):3974–3983.

186. Rashid MU, Bhuiyan MKH, Quayum ME. Synthesis of Silver Nano Particles (Ag-NPs) and their uses for Quantitative Analysis of Vitamin C Tablets 2013. 2013; 12(1):5.

187. Bastús NG, et al. Synthesis of Highly Monodisperse Citrate-Stabilized Silver Nanoparticles of up to 200 nm: Kinetic Control and Catalytic Properties. Chemistry of Materials. 2014; 26(9):2836–2846.

188. Zhao Y, et al. A facile method for the synthesis of large-size Ag nanoparticles as efficient SERS substrates. Journal of Raman Spectroscopy. 2016

189. Bera A, et al. Gamma radiation synthesis of colloidal AgNPs for its potential application in antimicrobial fabrics. Radiation Physics and Chemistry. 2015; 115:62–67.

190. Khaydarov RA, et al. Electrochemical method for the synthesis of silver nanoparticles. Journal of Nanoparticle Research. 2009; 11(5):1193–1200.

191. Rold, et al. Electrochemical Method for Ag-PEG Nanoparticles Synthesis. Journal of Nanoparticles. 2013; 2013:7.

192. Shimpi G, Shirole NS, Mishra S. Biogenesis Synthesis and Characterization of Silver Nanoparticles (AgNPs) Using the Aqueous Extract of Alstonia scholaris: A Greener Approach. Micro and Nanosystems. 2015; 7(1):49–54.

193. Khatami M, et al. Synthesis of silver nanoparticles using seed exudates of Sinapis arvensis as a novel bioresource, and evaluation of their antifungal activity. Bioresources and Bioprocessing. 2015; 2(1):1–7.

194. Pani A, Lee JH, Yun S II. Autoclave mediated one-pot-one-minute synthesis of AgNPs and Au–Ag nanocomposite from Melia azedarach bark extract with antimicrobial activity against food pathogens. Chemistry Central Journal. 2016; 10(1):1–11. [PubMed: 26807144]

195. Jasuja ND, et al. Green Synthesis of AgNPs Stabilized with biowaste and their antimicrobial activities. Brazilian Journal of Microbiology. 2014; 45(4):1325–1332. [PubMed: 25763037]

196. Bankar A, et al. Banana peel extract mediated novel route for the synthesis of silver nanoparticles. Colloids and Surfaces A: Physicochemical and Engineering Aspects. 2010; 368(1–3):58–63.

197. Kumar KS, Kathireswari P. Biological synthesis of Silver nanoparticles (Ag-NPS) by Lawsonia inermis (Henna) plant aqueous extract and its antimicrobial activity against human pathogens. Int J Curr Microbiol App Sci. 2016; 5(3):926–937.

198. Tippayawat P, et al. Green synthesis of silver nanoparticles in aloe vera plant extract prepared by a hydrothermal method and their synergistic antibacterial activity. PeerJ Preprints. 2016; 4:e1912v1.

199. Anjum S, Abbasi BH. Biomimetic synthesis of antimicrobial silver nanoparticles using in vitro-propagated plantlets of a medicinally important endangered species: Phlomis bracteosa. International Journal of Nanomedicine. 2016; 11:1663–1675. [PubMed: 27217745]

200. Sharma S, et al. Synthesis of Crystalline Ag Nanoparticles (AgNPs) from Microorganisms. Materials Sciences and Applications. 2010; 1(1):7.

201. Surya M. Biocompatible synthesis of silver nanoparticles (AgNPs) using marine Vibrio sp and study their pharmacological applications 2015. 2015; 5(4):7.

202. Kennedy DC, et al. Carbohydrate functionalization of silver nanoparticles modulates cytotoxicity and cellular uptake. Journal of Nanobiotechnology. 2014; 12(1):1–8. [PubMed: 24411017]

203. Veerapandian M, et al. Glucosamine-functionalized silver glyconanoparticles: characterization and antibacterial activity. Analytical and Bioanalytical Chemistry. 2010; 398(2):867–876. [PubMed: 20623220]
204. Ashraf S, et al. Polyhexamethylene biguanide functionalized cationic silver nanoparticles for enhanced antimicrobial activity. Nanoscale Research Letters. 2012; 7(1):1–7. [PubMed: 22214494]
205. Mohamed MA. One-Step Functionalization of Silver Nanoparticles Using the Orsellinic Acid Compound Isolated From the Endophytic Fungus Epicoccum Nigrum: Characterization and Antifungal Activity. Int J Nano Chem. 2015; 1(3):103–110.
206. Oliveira E, et al. Synthesis of functionalized fluorescent silver nanoparticles and their toxicological effect in aquatic environments (Goldfish) and HEPG2 cells. Frontiers in Chemistry. 2013; 1:29. [PubMed: 24790957]
207. Yallappa S, et al. Phytochemically Functionalized Cu and Ag Nanoparticles Embedded in MWCNTs for Enhanced Antimicrobial and Anticancer Properties. Nano-Micro Letters. 2016; 8(2):120–130.
208. Misra TK, Liu CY. Surface-functionalization of spherical silver nanoparticles with macrocyclic polyammonium cations and their potential for sensing phosphates. Journal of Nanoparticle Research. 2008; 11(5):1053–1063.
209. Guerrini L, et al. Functionalization of Ag nanoparticles with the bis-acridinium lucigenin as a chemical assembler in the detection of persistent organic pollutants by surface-enhanced Raman scattering. Analytica Chimica Acta. 2008; 624(2):286–293. [PubMed: 18706335]
210. D'souza SL, Pati R, Kailasa SK. Ascorbic acid-functionalized Ag NPs as a probe for colorimetric sensing of glutathione. Applied Nanoscience. 2015; 5(6):747–753.
211. Liu C, et al. Targeted Intracellular Controlled Drug Delivery and Tumor Therapy through in Situ Forming Ag Nanogates on Mesoporous Silica Nanocontainers. ACS Applied Materials & Interfaces. 2015; 7(22):11930–11938. [PubMed: 25966745]
212. Bhardwaj V, Srinivasan S, McGoron AJ. Efficient intracellular delivery and improved biocompatibility of colloidal silver nanoparticles towards intracellular SERS immuno-sensing. Analyst. 2015; 140(12):3929–3934. [PubMed: 25939798]
213. Bankura K, et al. Dextrin-mediated synthesis of Ag NPs for colorimetric assays of Cu2+ ion and Au NPs for catalytic activity. International Journal of Biological Macromolecules. 2015; 80:309–316. [PubMed: 26143120]
214. Chen K, et al. Utilizing Gold Nanoparticle Probes to Visually Detect DNA Methylation. Nanoscale Research Letters. 2016; 11:304. [PubMed: 27325520]
215. Liu J, et al. Gold nanorods coated with a thermo-responsive poly(ethylene glycol)-b-poly(N-vinylcaprolactam) corona as drug delivery systems for remotely near infrared-triggered release. Polymer Chemistry. 2014; 5(3):799–813.
216. Zelasko-Leon DC, Fuentes CM, Messersmith PB. MUC1-Targeted Cancer Cell Photothermal Ablation Using Bioinspired Gold Nanorods. PLoS ONE. 2015; 10(7):e0128756. [PubMed: 26147830]
217. Popp MK, et al. Photothermal therapy using gold nanorods and near-infrared light in a murine melanoma model increases survival and decreases tumor volume. Journal of Nanomaterials. 2014; 2014:126.
218. Sathuluri RR, et al. Gold Nanoparticle-Based Surface-Enhanced Raman Scattering for Noninvasive Molecular Probing of Embryonic Stem Cell Differentiation. PLoS ONE. 2011; 6(8):e22802. [PubMed: 21829653]
219. Cheng Y, et al. Fluorescence Near Gold Nanoparticles for DNA Sensing. Analytical Chemistry. 2011; 83(4):1307–1314. [PubMed: 21261273]
220. Mani V, et al. A simple electrochemical platform based on pectin stabilized gold nanoparticles for picomolar detection of biologically toxic amitrole. Analyst. 2015; 140(16):5764–5771. [PubMed: 26171468]
221. Huang X, et al. Cancer Cell Imaging and Photothermal Therapy in the Near-Infrared Region by Using Gold Nanorods. Journal of the American Chemical Society. 2006; 128(6):2115–2120. [PubMed: 16464114]

222. El-Sayed IH, Huang X, El-Sayed MA. Surface Plasmon Resonance Scattering and Absorption of anti-EGFR Antibody Conjugated Gold Nanoparticles in Cancer Diagnostics: Applications in Oral Cancer. Nano Letters. 2005; 5(5):829–834. [PubMed: 15884879]

223. Sokolov K, et al. Real-time vital optical imaging of precancer using anti-epidermal growth factor receptor antibodies conjugated to gold nanoparticles. Cancer research. 2003; 63(9):1999–2004. [PubMed: 12727808]

224. Chen CH, Wu YJ, Chen JJ. Gold nanotheranostics: photothermal therapy and imaging of Mucin 7 conjugated antibody nanoparticles for urothelial cancer. BioMed research international. 2015; 2015

225. Jokerst JV, et al. Gold Nanorods for Ovarian Cancer Detection with Photoacoustic Imaging and Resection Guidance via Raman Imaging in Living Mice. ACS Nano. 2012; 6(11):10366–10377. [PubMed: 23101432]

226. Patra HK, et al. Dual role of nanoparticles as drug carrier and drug. Cancer Nanotechnology. 2011; 2(1):37–47. [PubMed: 26069483]

227. Li L, Gui L, Li W. A colorimetric silver nanoparticle-based assay for Hg(II) using lysine as a particle-linking reagent. Microchimica Acta. 2015; 182(11):1977–1981.

228. Mokarian Z, Rasuli R, Abedini Y. Facile synthesis of stable superhydrophobic nanocomposite based on multi-walled carbon nanotubes. Applied Surface Science. 2016; 369:567–575.

229. Hui S. Plasmonic nanoparticles: Towards the fabrication of biosensors. IOP Conference Series: Materials Science and Engineering. 2015; 87(1):012009.

230. Polavarapu L, et al. Optical sensing of biological, chemical and ionic species through aggregation of plasmonic nanoparticles. Journal of Materials Chemistry C. 2014; 2(36):7460–7476.

231. Qi L, Shang Y, Wu F. Colorimetric detection of lead (II) based on silver nanoparticles capped with iminodiacetic acid. Microchimica Acta. 2012; 178(1):221–227.

232. Miao P, et al. Highly sensitive, label-free colorimetric assay of trypsin using silver nanoparticles. Biosensors and Bioelectronics. 2013; 49:20–24. [PubMed: 23708813]

233. Tan YN, et al. Sensing of transcription factor through controlled-assembly of metal nanoparticles modified with segmented DNA elements. ACS nano. 2010; 4(9):5101–5110. [PubMed: 20704275]

234. Abolhasani J, et al. Colorimetric Determination of Thioamide Drugs Based on the Surface Plasmon Resonance Band of Colloidal Silver Nanoparticles. Journal of Applied Chemistry. 2014; 8(29):25–30.

235. Stasyuk N, et al. Recombinant human arginase I immobilized on gold and silver nanoparticles: preparation and properties. Nanotechnology Development. 2011; 1(1):3.

236. Xu X, et al. Label-Free Colorimetric Detection of Small Molecules Utilizing DNA Oligonucleotides and Silver Nanoparticles. Small. 2009; 5(23):2669–2672. [PubMed: 19813222]

237. Pandey S, Goswami GK, Nanda KK. Green synthesis of biopolymer–silver nanoparticle nanocomposite: An optical sensor for ammonia detection. International journal of biological macromolecules. 2012; 51(4):583–589. [PubMed: 22750580]

238. Nezhad MH, Karimi M, Shahheydari F. A sensitive colorimetric detection of ascorbic acid in pharmaceutical products based on formation of anisotropic silver nanoparticles. Sci Iran Trans F: Nanotchnol. 2010; 17(2):148–153.

239. Park JS, et al. Colorimetric Determination of pH Values using Silver Nanoparticles Conjugated with Cytochrome c. Bulletin of the Korean Chemical Society. 2011; 32(9):3433–3436.

240. Sun Z, et al. High-throughput colorimetric assays for mercury(ii) in blood and wastewater based on the mercury-stimulated catalytic activity of small silver nanoparticles in a temperature-switchable gelatin matrix. Chemical Communications. 2014; 50(65):9196–9199. [PubMed: 24995435]

241. Fan Y, et al. Synthesis of Starch-Stabilized Ag Nanoparticles and Hg(2+)Recognition in Aqueous Media. Nanoscale Research Letters. 2009; 4(10):1230–1235. [PubMed: 20596276]

242. Li Z, et al. Quantum dots loaded nanogels for low cytotoxicity, pH-sensitive fluorescence, cell imaging and drug delivery. Carbohydrate polymers. 2015; 121:477–485. [PubMed: 25659723]

243. Anambiga I, et al. Colorimetric Detection Of Lead Ions Using Glutathione Stabilized Silver Nanoparticles.

244. Ravindran A, et al. Selective colorimetric detection of nanomolar Cr (VI) in aqueous solutions using unmodified silver nanoparticles. Sensors and Actuators B: Chemical. 2012; 166–167:365–371.

245. Sharif T, et al. Isonicotinic acid hydrazide-based silver nanoparticles as simple colorimetric sensor for the detection of Cr3+ Sensors and Actuators B: Chemical. 2015; 216:402–408.

246. Shang Y, Wu F, Qi L. Highly selective colorimetric assay for nickel ion using N-acetyl-l-cysteine-functionalized silver nanoparticles. Journal of Nanoparticle Research. 2012; 14(10):1–7. [PubMed: 22448125]

247. Liu X, Wu FY, Ma LH. Colorimetric Assay for Al3+ Based on Alizarin Red S-functionalized Silver Nanoparticles. Australian Journal of Chemistry. 2014; 67(11):1700–1705.

248. Shrivas K, et al. Application of silver nanoparticles for a highly selective colorimetric assay of endrin in water and food samples based on stereoselective endo-recognition. RSC Advances. 2016; 6(35):29855–29862.

249. Ping H, et al. Visual detection of melamine in raw milk by label-free silver nanoparticles. Food Control. 2012; 23(1):191–197.

250. Song J, et al. Colorimetric detection of melamine in pretreated milk using silver nanoparticles functionalized with sulfanilic acid. Food Control. 2015; 50:356–361.

251. Kappi FA, et al. Colorimetric and visual read-out determination of cyanuric acid exploiting the interaction between melamine and silver nanoparticles. Microchimica Acta. 2014; 181(5):623–629.

252. Hajizadeh S, et al. Silver nanoparticles as a cyanide colorimetric sensor in aqueous media. Analytical Methods. 2011; 3(11):2599–2603.

253. Praveena VD, Kumar KV. A Thiocyanate Sensor Based On Ecofriendly Silver Nanoparticles Thin Film Composite.

254. Chen J, , et al. Highly sensitive and selective pymetrozine colorimetric sensor based on p-aminobenzenesulfonic acid modified Ag NPs in Applied Mechanics and Materials Trans Tech Publ; 2012

255. Liu R, et al. Metallic nanoparticles bioassay for Enterobacter cloacae P99 [small beta]-lactamase activity and inhibitor screening. Analyst. 2010; 135(5):1031–1036. [PubMed: 20419253]

256. Dungchai W, et al. Determination of aerosol oxidative activity using silver nanoparticle aggregation on paper-based analytical devices. Analyst. 2013; 138(22):6766–6773. [PubMed: 24067623]

257. Zheng LQ, et al. Rapid visual detection of quaternary ammonium surfactants using citrate-capped silver nanoparticles (Ag NPs) based on hydrophobic effect. Talanta. 2014; 118:90–95. [PubMed: 24274274]

258. Chen Z, et al. Label-free colorimetric assay for biological thiols based on ssDNA/silver nanoparticle system by salt amplification. Analyst. 2010; 135(5):1066–1069. [PubMed: 20405067]

259. Wei H, et al. Enzyme Colorimetric Assay Using Unmodified Silver Nanoparticles. Analytical Chemistry. 2008; 80(18):7051–7055. [PubMed: 18662017]

260. Jiang H, et al. Peroxidase-like activity of chitosan stabilized silver nanoparticles for visual and colorimetric detection of glucose. Analyst. 2012; 137(23):5560–5564. [PubMed: 23042152]

261. Chen L, et al. Highly Sensitive and Selective Colorimetric Sensing of Hg2+ Based on the Morphology Transition of Silver Nanoprisms. ACS Applied Materials & Interfaces. 2013; 5(2): 284–290. [PubMed: 23237272]

262. Xia Y, et al. Colorimetric Visualization of Glucose at the Submicromole Level in Serum by a Homogenous Silver Nanoprism–Glucose Oxidase System. Analytical Chemistry. 2013; 85(13): 6241–6247. [PubMed: 23706061]

263. Farhadi K, et al. Highly selective Hg2+ colorimetric sensor using green synthesized and unmodified silver nanoparticles. Sensors and Actuators B: Chemical. 2012; 161(1):880–885.

264. Bhattacharjee Y, Chakraborty A. Label-Free Cysteamine-Capped Silver Nanoparticle-Based Colorimetric Assay for Hg(II) Detection in Water with Subnanomolar Exactitude. ACS Sustainable Chemistry & Engineering. 2014; 2(9):2149–2154.

265. Zhang M, Ye BC. Colorimetric Chiral Recognition of Enantiomers Using the Nucleotide-Capped Silver Nanoparticles. Analytical Chemistry. 2011; 83(5):1504–1509. [PubMed: 21302899]
266. Chen Z, et al. Chitosan-capped silver nanoparticles as a highly selective colorimetric probe for visual detection of aromatic ortho-trihydroxy phenols. Analyst. 2013; 138(8):2343–2349. [PubMed: 23457709]
267. Zeng J-B, et al. A colorimetric agarose gel for formaldehyde measurement based on nanotechnology involving Tollens reaction. Chemical Communications. 2014; 50(60):8121–8123. [PubMed: 24846681]
268. Doria G, et al. Gold–silver-alloy nanoprobes for one-pot multiplex DNA detection. Nanotechnology. 2010; 21(25):255101. [PubMed: 20508311]
269. Li Y, et al. A convenient colorimetric method for sensitive and specific detection of cyanide using Ag@Au core–shell nanoparticles. Sensors and Actuators B: Chemical. 2016; 228:366–372.
270. Liu Y, et al. Red to brown to green colorimetric detection of Ag+ based on the formation of Au-Ag core-shell NPs stabilized by a multi-sulfhydryl functionalized hyperbranched polymer. Sensors and Actuators B: Chemical. 2016; 237:216–223.
271. Li T, et al. Sensitive detection of glucose based on gold nanoparticles assisted silver mirror reaction. Analyst. 2011; 136(14):2893–2896. [PubMed: 21611638]
272. Li T, et al. A colorimetric nitrite detection system with excellent selectivity and high sensitivity based on Ag@Au nanoparticles. Analyst. 2015; 140(4):1076–1081. [PubMed: 25564225]
273. Zeng J, et al. A colorimetric assay for measuring iodide using Au@Ag core–shell nanoparticles coupled with Cu2+ Analytica Chimica Acta. 2015; 891:269–276. [PubMed: 26388386]
274. Zeng J-B, et al. Au@Ag core/shell nanoparticles as colorimetric probes for cyanide sensing. Nanoscale. 2014; 6(17):9939–9943. [PubMed: 25054637]
275. Wang X, Chen L, Chen L. Colorimetric determination of copper ions based on the catalytic leaching of silver from the shell of silver-coated gold nanorods. Microchimica Acta. 2014; 181(1):105–110.
276. Fei K, Xiangshu H, Kun X. Highly sensitive colorimetric detection of glucose in a serum based on DNA-embeded Au@Ag core–shell nanoparticles. Nanotechnology. 2015; 26(40):405707. [PubMed: 26376788]
277. Zhang X, et al. Sensitive colorimetric detection of glucose and cholesterol by using Au@Ag core-shell nanoparticles. RSC Advances. 2016; 6(41):35001–35007.
278. Shinohara S, et al. Colorimetric plasmon sensors with multilayered metallic nanoparticle sheets. Physical Chemistry Chemical Physics. 2015; 17(28):18606–18612. [PubMed: 26113242]
279. Cao YC, et al. A two-color-change, nanoparticle-based method for DNA detection. Talanta. 2005; 67(3):449–455. [PubMed: 18970188]
280. Hao J, et al. High-Throughput Sulfide Sensing with Colorimetric Analysis of Single Au–Ag Core–Shell Nanoparticles. Analytical Chemistry. 2014; 86(10):4663–4667. [PubMed: 24809220]
281. Tao H, et al. A comparative study of different reagentless plasmon sensors based on Ag–Au alloy nanoparticles for detection of Hg. Sensors and Actuators B: Chemical. 2015; 208:43–49.
282. He H, et al. Enzymatic plasmonic engineering of Ag/Au bimetallic nanoshells and their use for sensitive optical glucose sensing. Advanced Materials. 2012; 24(13):1736–1740. [PubMed: 22388952]
283. Faraji M, Yamini Y, Rezaee M. Magnetic nanoparticles: synthesis, stabilization, functionalization, characterization, and applications. Journal of the Iranian Chemical Society. 2010; 7(1):1–37.
284. Reddy LH, et al. Magnetic nanoparticles: design and characterization, toxicity and biocompatibility, pharmaceutical and biomedical applications. Chemical reviews. 2012; 112(11): 5818–5878. [PubMed: 23043508]
285. Xu J, et al. Application of iron magnetic nanoparticles in protein immobilization. Molecules. 2014; 19(8):11465–11486. [PubMed: 25093986]
286. Gupta AK, Gupta M. Synthesis and surface engineering of iron oxide nanoparticles for biomedical applications. Biomaterials. 2005; 26(18):3995–4021. [PubMed: 15626447]

287. Lu AH, Salabas EeL, Schüth F. Magnetic nanoparticles: synthesis, protection, functionalization, and application. Angewandte Chemie International Edition. 2007; 46(8):1222–1244. [PubMed: 17278160]

288. Riva ER, et al. Plasmonic/magnetic nanocomposites: Gold nanorods-functionalized silica coated magnetic nanoparticles. Journal of Colloid and Interface Science. 2017; 502:201–209. [PubMed: 28486141]

289. Muzio G, et al. Innovative superparamagnetic iron-oxide nanoparticles coated with silica and conjugated with linoleic acid: Effect on tumor cell growth and viability. Materials Science and Engineering: C. 2017; 76(Supplement C):439–447. [PubMed: 28482548]

290. Treccani L, et al. Functionalized ceramics for biomedical, biotechnological and environmental applications. Acta biomaterialia. 2013; 9(7):7115–7150. [PubMed: 23567940]

291. Xiong H, et al. Synthesis and application of thiol-functionalized magnetic nanoparticles for studying interactions of epirubicin hydrochloride with bovine serum albumin by fluorescence spectrometry. Luminescence. 2016

292. Chen X, Organ MG, Pietro WJ. One-pot Synthesis of Size Controllable Amine-Functionalized Core-Shell Magnetic Nanoparticles for Use in Microfluidic Flow Separators. J Nanosci Adv Tech. 2016; 1(3):25–31.

293. Hu A, Yee GT, Lin W. Magnetically recoverable chiral catalysts immobilized on magnetite nanoparticles for asymmetric hydrogenation of aromatic ketones. Journal of the American Chemical Society. 2005; 127(36):12486–12487. [PubMed: 16144385]

294. Colombo M, et al. Biological applications of magnetic nanoparticles. Chemical Society Reviews. 2012; 41(11):4306–4334. [PubMed: 22481569]

295. Ney A, et al. Absolute determination of Co magnetic moments: Ultrahigh-vacuum high-T c SQUID magnetometry. Physical Review B. 2000; 62(17):11336.

296. Foner S. Versatile and sensitive vibrating-sample magnetometer. Review of Scientific Instruments. 1959; 30(7):548–557.

297. Falcaro P, et al. Application of metal and metal oxide nanoparticles@ MOFs. Coordination Chemistry Reviews. 2016; 307:237–254.

298. Hu J, Chen G, Lo IM. Removal and recovery of Cr (VI) from wastewater by maghemite nanoparticles. Water research. 2005; 39(18):4528–4536. [PubMed: 16146639]

299. Farjadian F, et al. Bacterial components as naturally inspired nano-carriers for drug/gene delivery and immunization: Set the bugs to work? Biotechnology advances. 2018

300. Cole AJ, et al. Magnetic brain tumor targeting and biodistribution of long-circulating PEG-modified, cross-linked starch-coated iron oxide nanoparticles. Biomaterials. 2011; 32(26):6291–6301. [PubMed: 21684593]

301. Hua MY, et al. The effectiveness of a magnetic nanoparticle-based delivery system for BCNU in the treatment of gliomas. Biomaterials. 2011; 32(2):516–527. [PubMed: 21030073]

302. Liang M, et al. Fe3O4 magnetic nanoparticle peroxidase mimetic-based colorimetric assay for the rapid detection of organophosphorus pesticide and nerve agent. Analytical chemistry. 2012; 85(1):308–312. [PubMed: 23153113]

303. Zhang Z, et al. Magnetic nanoparticle-linked colorimetric aptasensor for the detection of thrombin. Sensors and Actuators B: Chemical. 2010; 147(2):428–433.

304. Li J, et al. Hyaluronic acid-modified Fe 3 O 4@ Au core/shell nanostars for multimodal imaging and photothermal therapy of tumors. Biomaterials. 2015; 38:10–21. [PubMed: 25457979]

305. Pang LL, et al. A novel detection method for DNA point mutation using QCM based on Fe 3 O 4/Au core/shell nanoparticle and DNA ligase reaction. Sensors and Actuators B: Chemical. 2007; 127(2):311–316.

306. He X, et al. Lectin-conjugated Fe2O3@ Au core@ shell nanoparticles as dual mode contrast agents for in vivo detection of tumor. Molecular pharmaceutics. 2014; 11(3):738–745. [PubMed: 24472046]

307. Corr SA, Rakovich YP, Gun'ko YK. Multifunctional magnetic-fluorescent nanocomposites for biomedical applications. Nanoscale Research Letters. 2008; 3(3):87.

308. Markides H, Rotherham M, El Haj A. Biocompatibility and toxicity of magnetic nanoparticles in regenerative medicine. Journal of Nanomaterials. 2012; 2012:13.

309. Xie HY, et al. Fe3O4/Au Core/Shell Nanoparticles Modified with Ni2+− Nitrilotriacetic Acid Specific to Histidine-Tagged Proteins. The Journal of Physical Chemistry C. 2010; 114(11): 4825–4830.

310. Rai M, Yadav A, Gade A. Silver nanoparticles as a new generation of antimicrobials. Biotechnology advances. 2009; 27(1):76–83. [PubMed: 18854209]

311. Roucoux A, Schulz J, Patin H. Reduced transition metal colloids: a novel family of reusable catalysts? Chemical reviews. 2002; 102(10):3757–3778. [PubMed: 12371901]

312. Tang D, Yuan R, Chai Y. Magnetic core-shell Fe3O4@ Ag nanoparticles coated carbon paste interface for studies of carcinoembryonic antigen in clinical immunoassay. The Journal of Physical Chemistry B. 2006; 110(24):11640–11646. [PubMed: 16800458]

313. Ranc V, et al. Magnetically assisted surface-enhanced Raman scattering selective determination of dopamine in an artificial cerebrospinal fluid and a mouse striatum using Fe3O4/Ag nanocomposite. Analytical chemistry. 2014; 86(6):2939–2946. [PubMed: 24555681]

314. Tan J, et al. Aptamer-Functionalized Fluorescent Silica Nanoparticles for Highly Sensitive Detection of Leukemia Cells. Nanoscale Res Lett. 2016; 11(1):016–1512.

315. Chitra K, Annadurai G. Fluorescent Silica Nanoparticles in the Detection and Control of the Growth of Pathogen. Journal of Nanotechnology. 2013; 2013:7.

316. Gu Y, et al. R6G/8-AQ co-functionalized Fe3O4@SiO2 nanoparticles for fluorescence detection of trace Hg2+ and Zn2+ in aqueous solution. Science China Materials. 2015; 58(7):550–558.

317. Li Y, et al. Colorimetric determination of pyrethroids based on core–shell Ag@SiO2 nanoparticles. Sensors and Actuators B: Chemical. 2011; 155(2):878–883.

318. Junhui Ran, Haiying Wang, Xinjian C. Fluorescent silica nanoparticles and glass surfaces for the detection and removal of Pd(II) ions. Journal of Materials Science. 2016; 51(18):8502–8515.

319. Lu C, et al. Multifunctional Janus Hematite–Silica Nanoparticles: Mimicking Peroxidase-Like Activity and Sensitive Colorimetric Detection of Glucose. ACS Applied Materials & Interfaces. 2015; 7(28):15395–15402. [PubMed: 26110779]

320. Jiang P, et al. Hierarchical Shelled ZnO Structures Made of Bunched Nanowire Arrays. Advanced Functional Materials. 2007; 17(8):1303–1310.

321. Liu S, et al. Synthesis, characterization and enhanced photocatalytic performance of Ag2S-coupled ZnO/ZnS core/shell nanorods. Journal of Alloys and Compounds. 2013; 568(Supplement C):84–91.

322. Kazeminezhad I, Sadollahkhani A. Photocatalytic degradation of Eriochrome black-T dye using ZnO nanoparticles. Materials Letters. 2014; 120(Supplement C):267–270.

323. Sadollahkhani A, et al. Colorimetric Disposable Paper Coated with ZnO@ZnS Core–Shell Nanoparticles for Detection of Copper Ions in Aqueous Solutions. ACS Applied Materials & Interfaces. 2014; 6(20):17694–17701. [PubMed: 25275616]

324. Hayat A, et al. Colorimetric cholesterol sensor based on peroxidase like activity of zinc oxide nanoparticles incorporated carbon nanotubes. Talanta. 2015; 143(Supplement C):157–161. [PubMed: 26078143]

325. Ali MA, et al. Nanostructured zinc oxide film for urea sensor. 2009; 63:2473–2475.

326. Faisal M, et al. Highly selective colorimetric detection and preconcentration of Bi(III) ions by dithizone complexes anchored onto mesoporous TiO2. Nanoscale Research Letters. 2014; 9(1): 62. [PubMed: 24502680]

327. Gelover S, et al. A practical demonstration of water disinfection using TiO2 films and sunlight. Water Research. 2006; 40(17):3274–3280. [PubMed: 16949121]

328. Huh AJ, Kwon YJ. ”Nanoantibiotics”: a new paradigm for treating infectious diseases using nanomaterials in the antibiotics resistant era. J Control Release. 2011; 156(2):128–45. [PubMed: 21763369]

329. Ding Y, et al. A facile strategy for the preparation of ZnS nanoparticles deposited on montmorillonite and their higher catalytic activity for rapidly colorimetric detection of H2O2. Materials Science and Engineering: C. 2016; 67(Supplement C):188–194. [PubMed: 27287113]

330. Yao T, et al. SiO2 nanoparticles and diphenylcarbazide doped polymethylmethacrylate electrospun fibrous film for Cd2+ colorimetric detection. Analytical Methods. 2014; 6(12):4102–4106.

331. Idros N, et al. Colorimetric-Based Detection of TNT Explosives Using Functionalized Silica Nanoparticles. Sensors. 2015; 15(6):12891. [PubMed: 26046595]

332. Cho Y, Lee SS, Jung JH. Recyclable fluorimetric and colorimetric mercury-specific sensor using porphyrin-functionalized Au@SiO2 core/shell nanoparticles. Analyst. 2010; 135(7):1551–1555. [PubMed: 20445891]

333. Sun L, et al. Porphyrin-functionalized Fe3O4@SiO2 core/shell magnetic colorimetric material for detection, adsorption and removal of Hg2+ in aqueous solution. New Journal of Chemistry. 2011; 35(11):2697–2704.

334. Rameshkumar P, Manivannan S, Ramaraj R. Silver nanoparticles deposited on amine-functionalized silica spheres and their amalgamation-based spectral and colorimetric detection of Hg(II) ions. Journal of Nanoparticle Research. 2013; 15(5):1639.

335. Ding Y, et al. A facile strategy for the preparation of ZnS nanoparticles deposited on montmorillonite and their higher catalytic activity for rapidly colorimetric detection of H2O2. Mater Sci Eng C Mater Biol Appl. 2016; 67:188–194. [PubMed: 27287113]

336. Kim E, et al. Functionalized monolayers on mesoporous silica and on titania nanoparticles for mercuric sensing. Analyst. 2010; 135(1):149–156. [PubMed: 20024195]

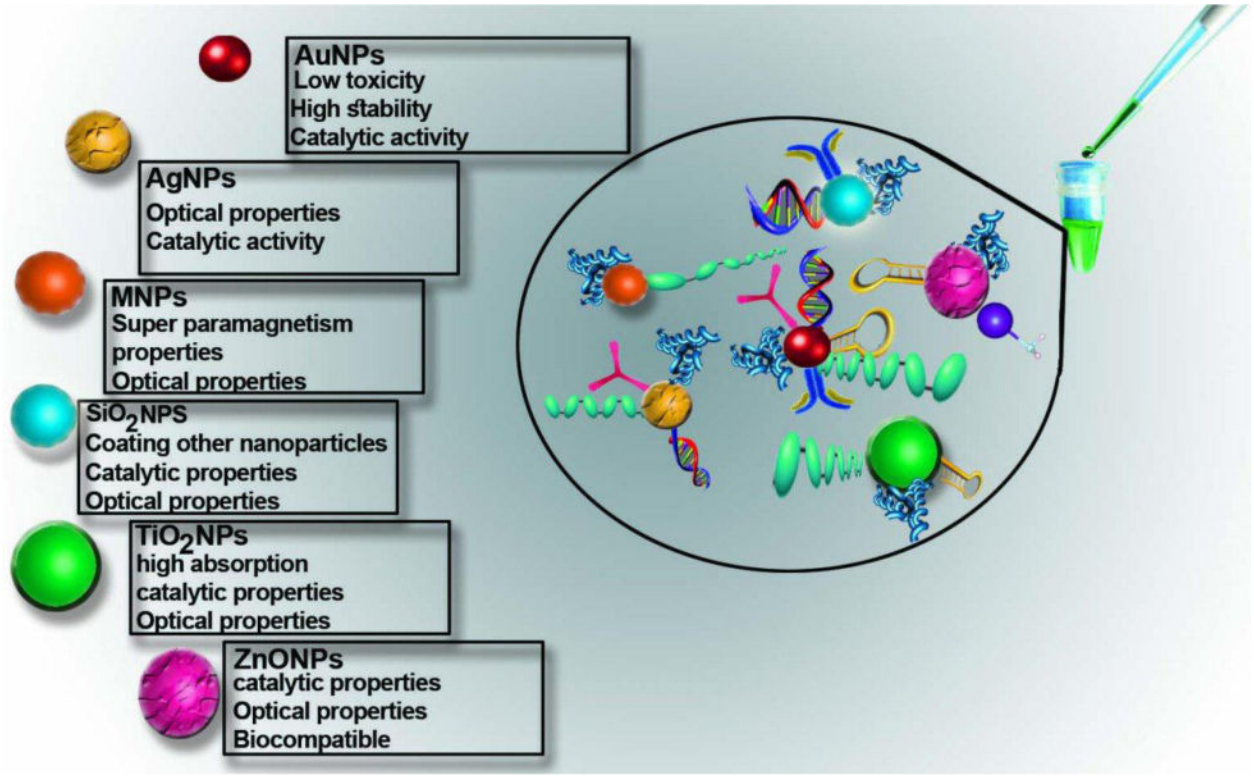

Fig. 1.
Properties and functionalization of inorganic nanoparticles in colorimetric assay.

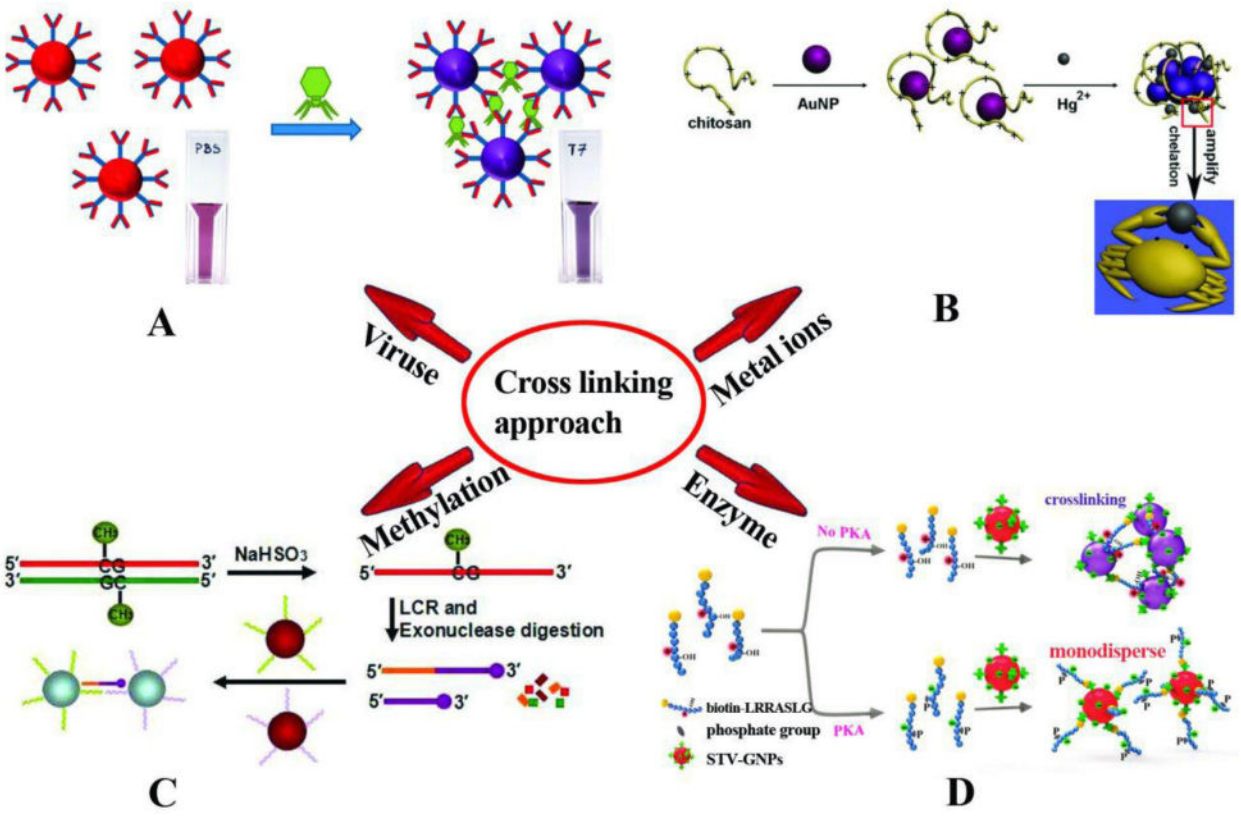

Fig. 2.

Schematic illustration of crosslinking based colorimetric assays. (A) The detection of *bacteriophage T7* using AuNPs modified with covalently bonded anti-T7 antibodies and color change based on antibody antigen interaction which causes them to aggregate [111]. (B) Colorimetric detection of Hg^{2+} based on chelation reaction between Hg^{2+} and chitosan and observed color changes in AuNPs [112]. (C) LCR amplification and colorimetric assay of CpG methylation in DNA: In the presence of methylated genomic DNA a red to purple color change can be detected [113]. (D) Colorimetric assay for detection of protein kinase activities based on hybridization between STV-AuNPs and biotinylated peptide (biotin-LRRASLG), and the PKA catalyzed phosphorylation of biotin-peptide prevented AuNPs crosslinking and the monodisperse AuNPs remained red [81]. Reprinted with Permission

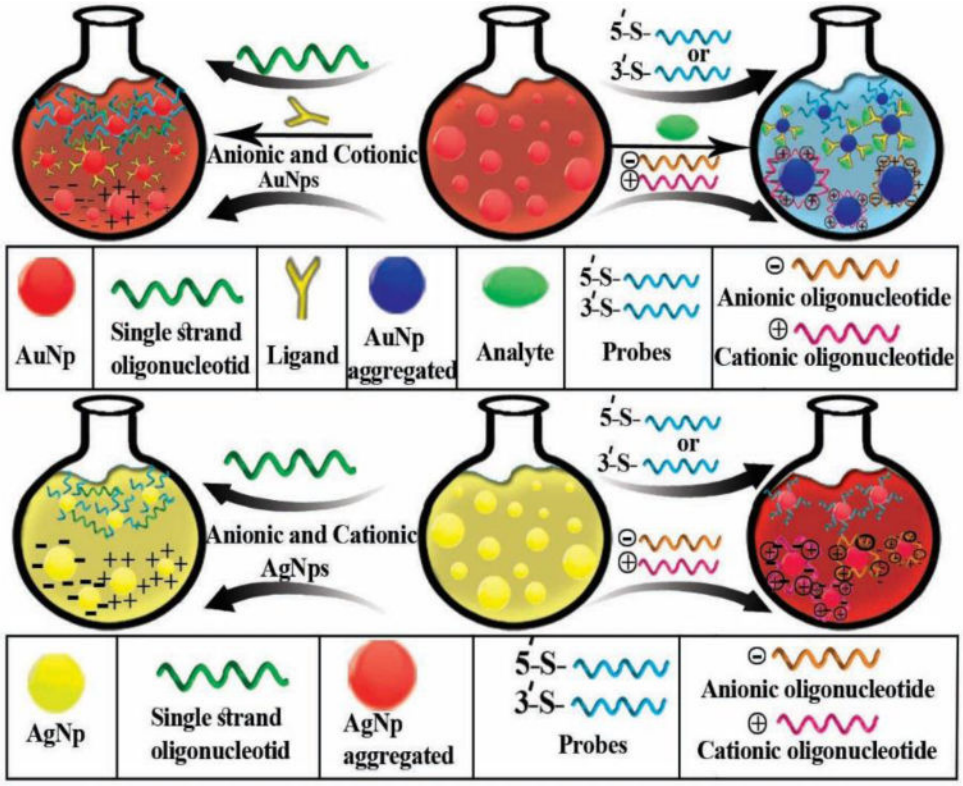

Fig. 3.

A schematic illustration of non-crosslinking AuNP and AgNP aggregation-based colorimetric detection

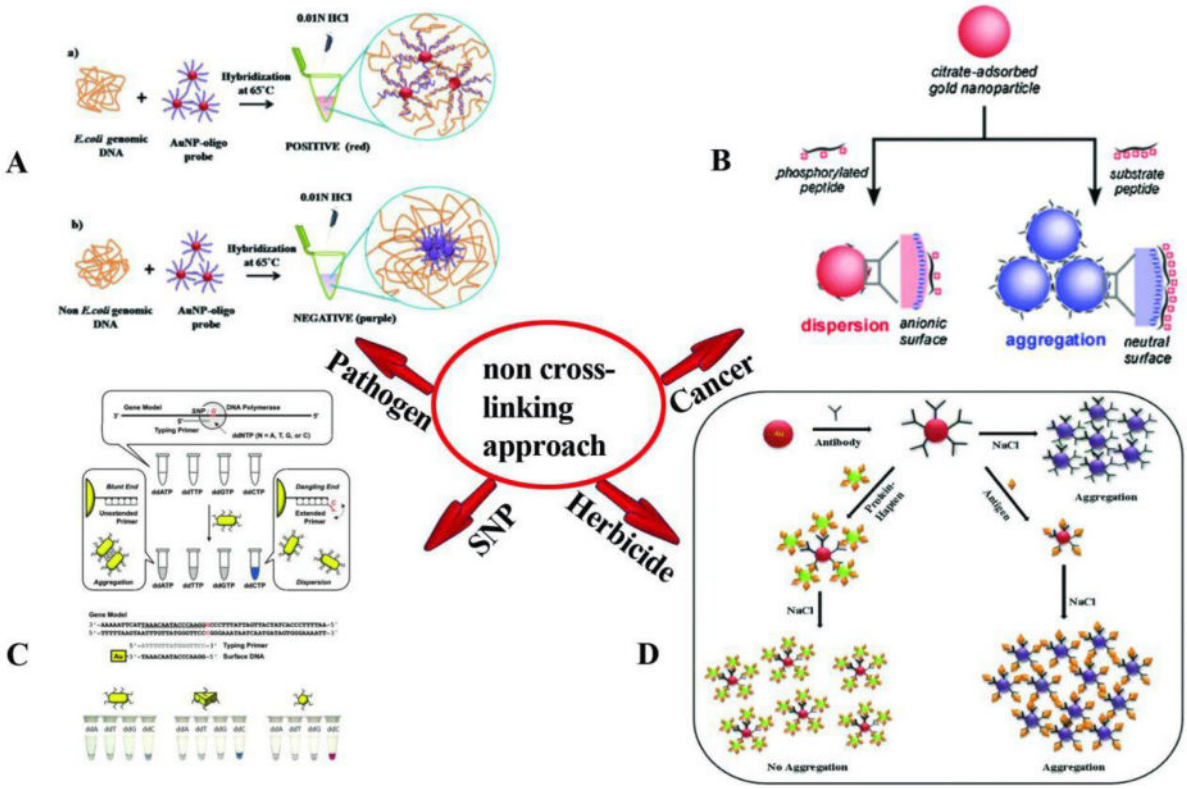

Fig. 4.

Schematic illustration of the non-crosslinking based colorimetric assay. (A) colorimetric detection of *E. coli* genomic DNA based on AuNPs probes; in presence of genomic DNA, AuNPs probes do not aggregate and the color remains red; in contrast, in the absence of genomic DNA, AuNPs probes lose stability and tend to aggregate [131]. (B) Non-crosslinking aggregation-based colorimetric detection of cancers. This assay is based on the non-crosslinking aggregation using a cationic PKC-specific peptide substrate [133]. (C) Colorimetric detection of SNP based on DNA-functionalized anisotropic AuNPs and showing a mixture of AuNR AuNT and the AuNS probe after mixing with the primer solution and color changes of NPs [134]. (D) Colorimetric detection of phenylurea herbicide, in the presence of antigen, color change is visible upon aggregation of Ab-AuNPs [136]. Reprinted with permission

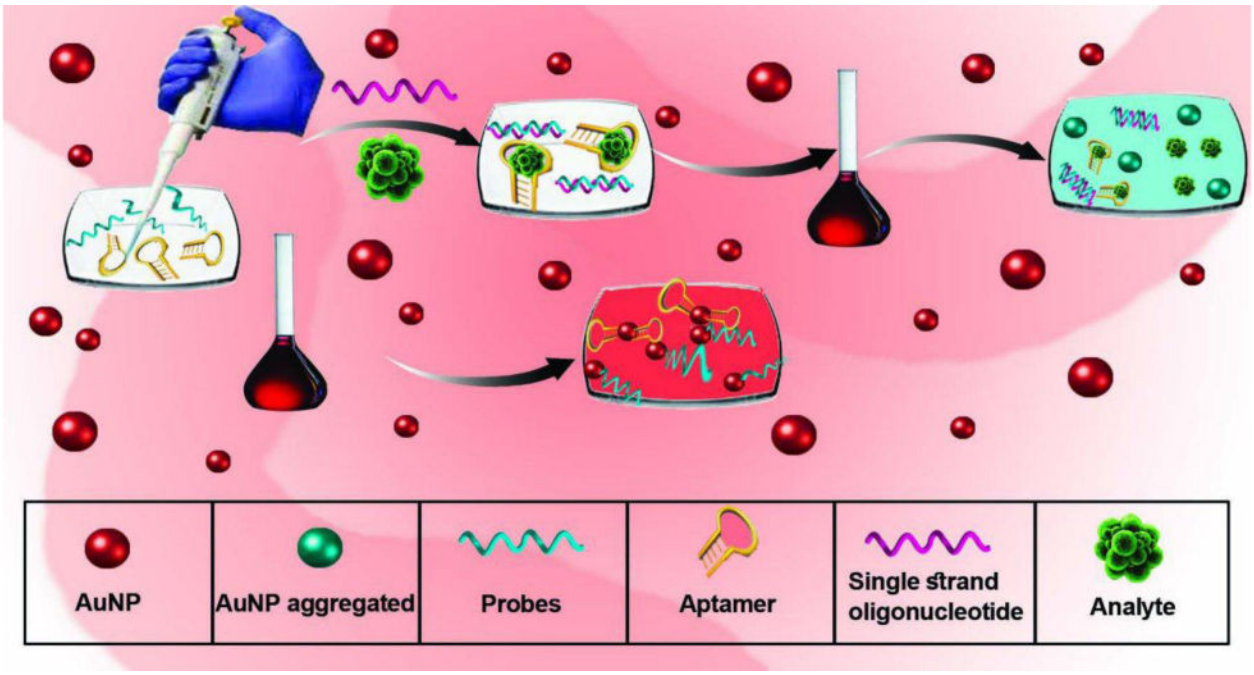

Fig. 5.
Schematic of colorimetric assays based on unmodified AuNPs

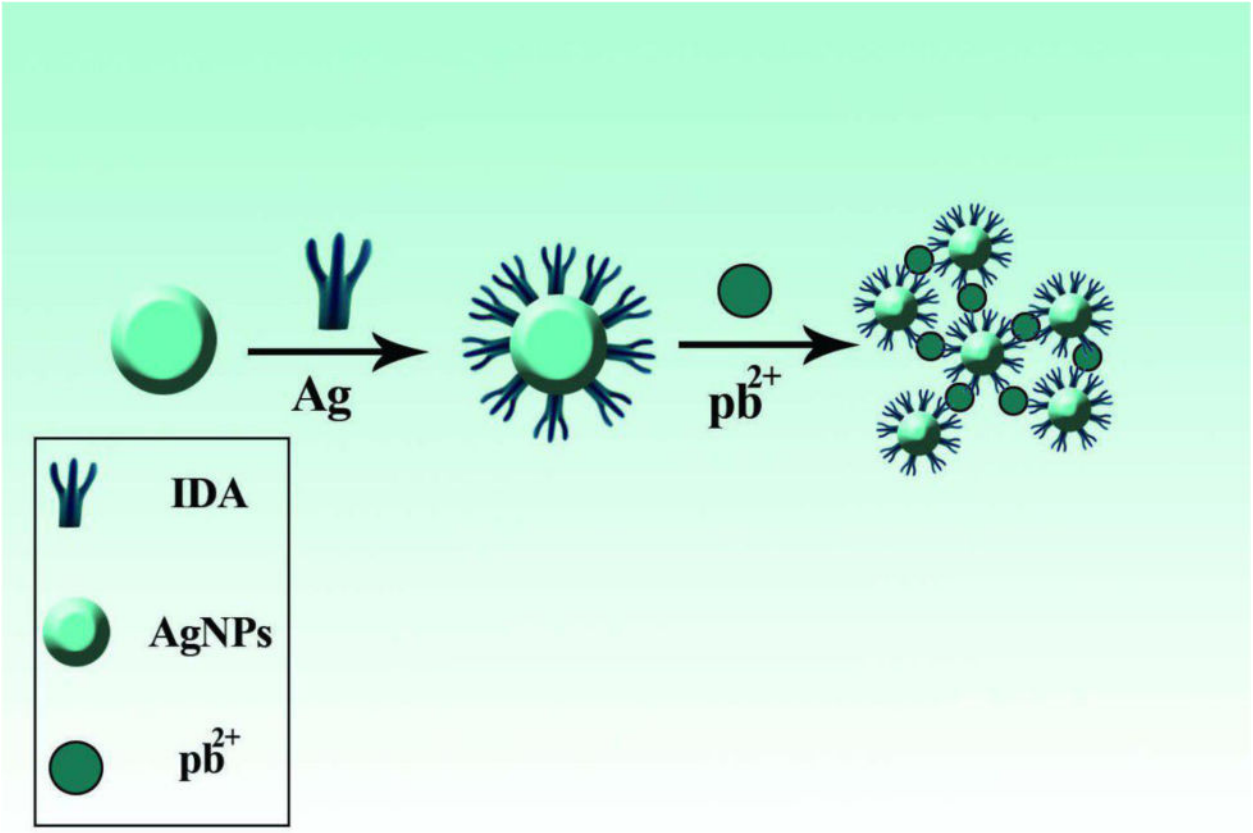

Fig. 6.
Aggregation and color change of modified AgNPs in the presence of lead ions [231]. Reprinted with permission

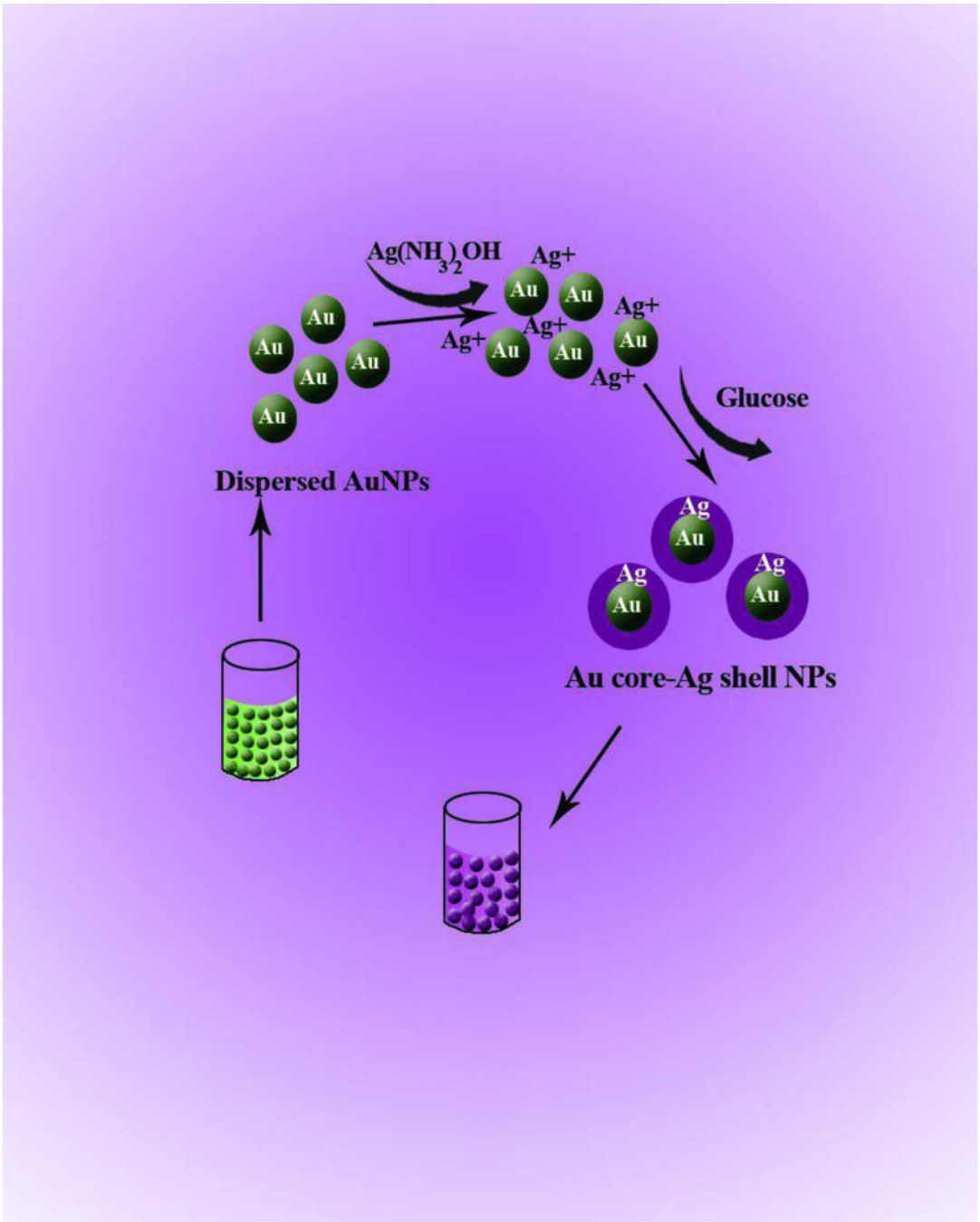

Fig. 7.

Color change induced by Ag shell formation on AuNP core. The shell thickens and the resultant color change is proportional to the glucose concentration [271]. Reprinted with permission

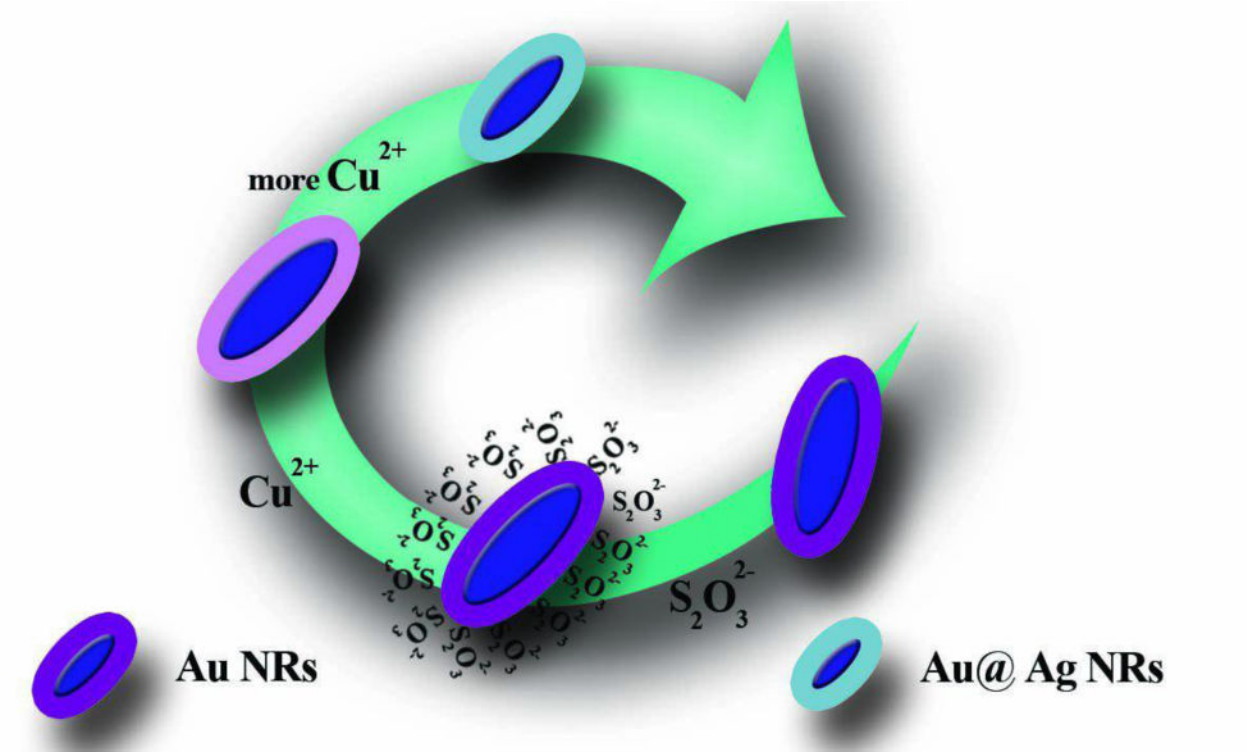

Fig. 8.
Shell etching according to the concentration of copper ions [275]. Reprinted with permission

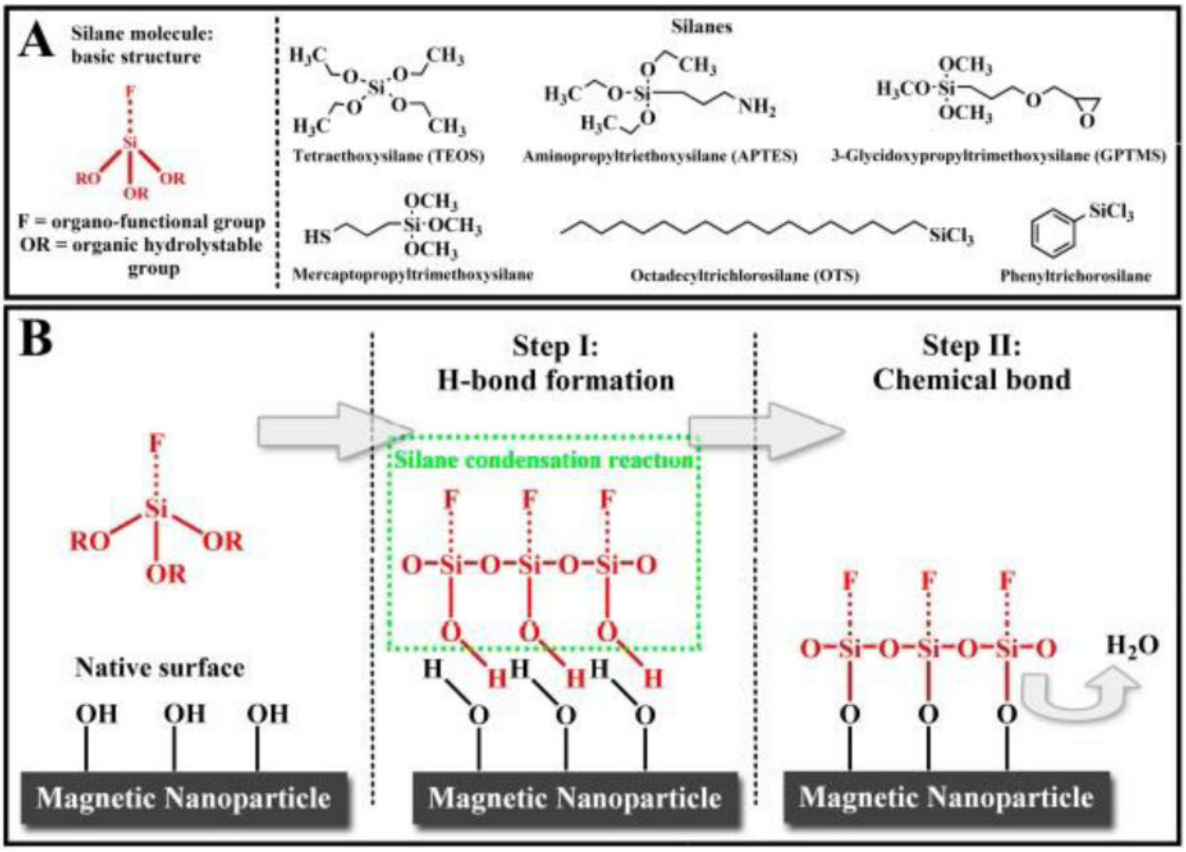

Fig. 9.

(A) Silane molecular structures. (B) Schematic of the silane condensation reaction [290]. Reprinted with permission

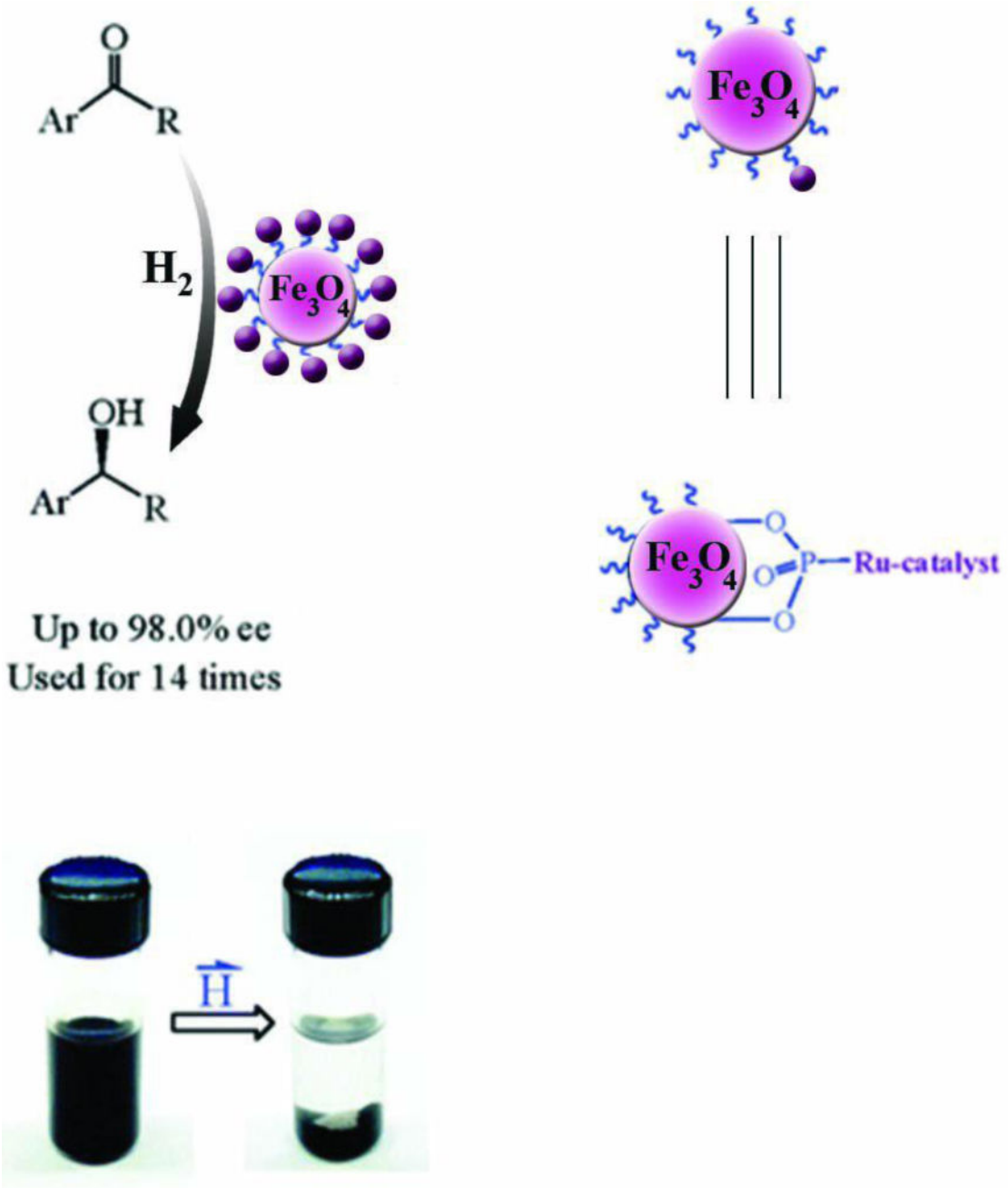

Fig. 10.

Immobilization of Chiral Ru Catalyst on MNPs. Reprinted (adapted) with permission from [293] . Copyright (2005) American Chemical Society.

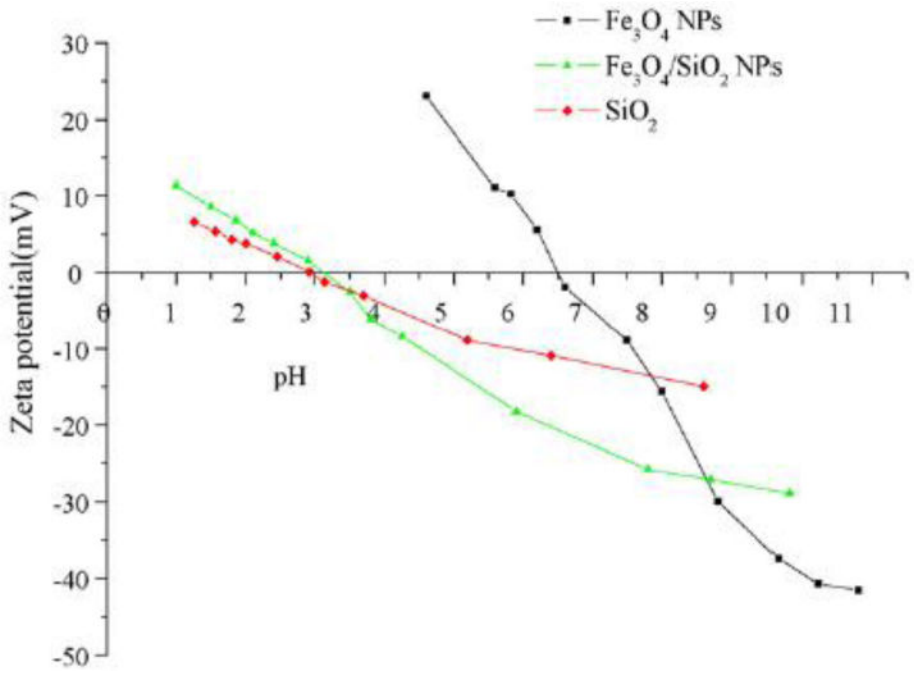

Fig. 11.

Zeta-potential of Fe_3O_4 NPs (a), Fe_3O_4/SiO_2 NPs (b) and native silica (c) [283]. Reprinted with permission

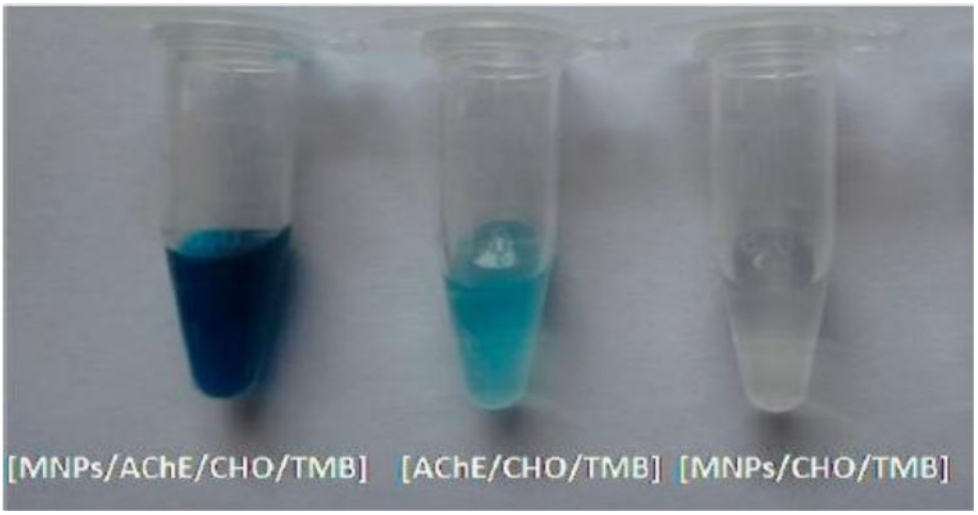

Fig. 12.

MNPs catalyze the oxidation of a colorimetric substrate, TMB, to generate a color reaction in the presence of AChE and CHO producing hydrogen peroxide after incubation in acetylcholine chloride solution. [302]. Reprinted with permission

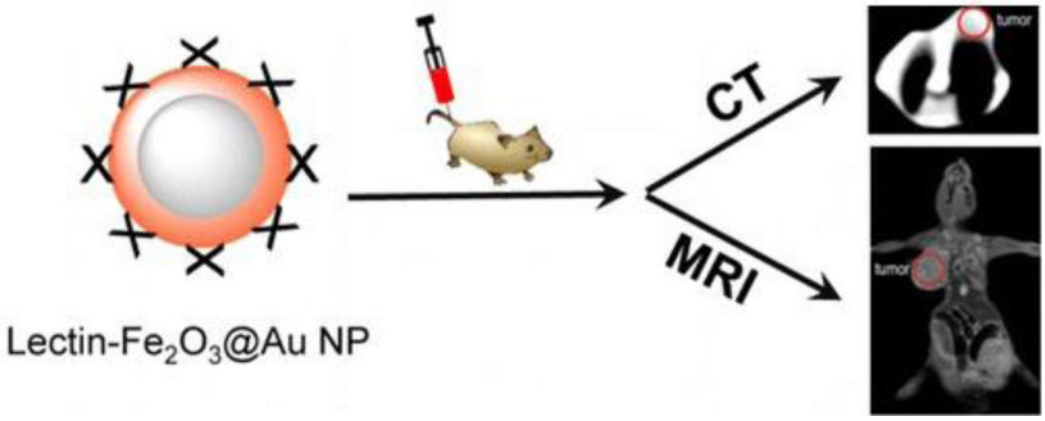

Fig. 13.

Lectin conjugated to core-shell IONPs-GNPs. Reprinted (adapted) with permission from [306]. Copyright (2014) American Chemical Society

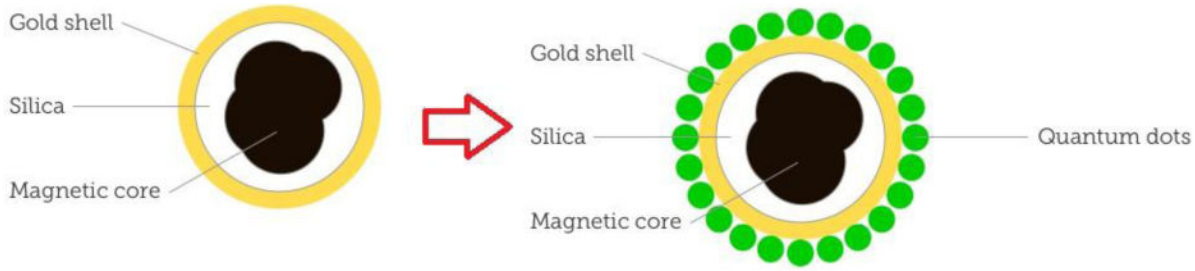

Fig. 14.

Magnetic-fluorescent composite particles consisting of a magnetic core, silica spacer, and fluorescent quantum dots covalently bonded to the silica surface.

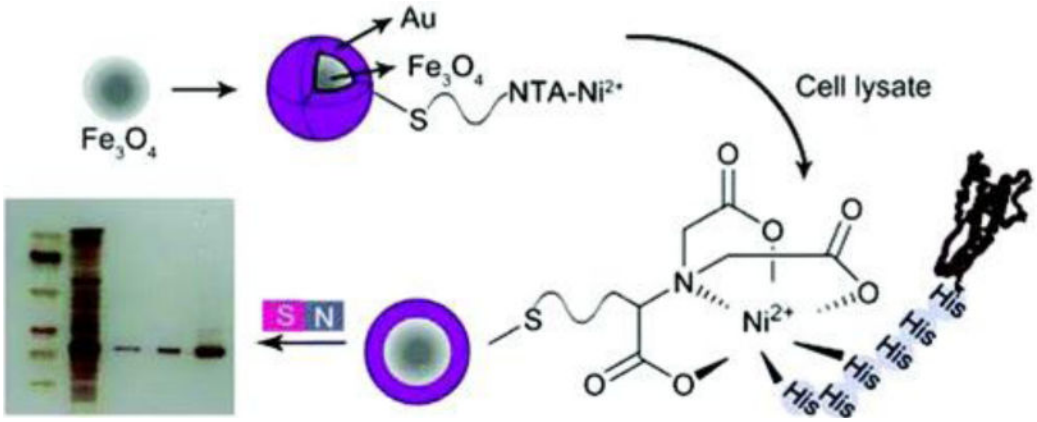

Fig. 15.

Surface modified Fe_3O_4 with mercaptopropionic acid, followed by conjugation of nitrilotriacetic acid (NTA) and subsequently chelating Ni^{2+} chelation. Reprinted (adapted) with permission from [309] Copyright (2010) American Chemical Society

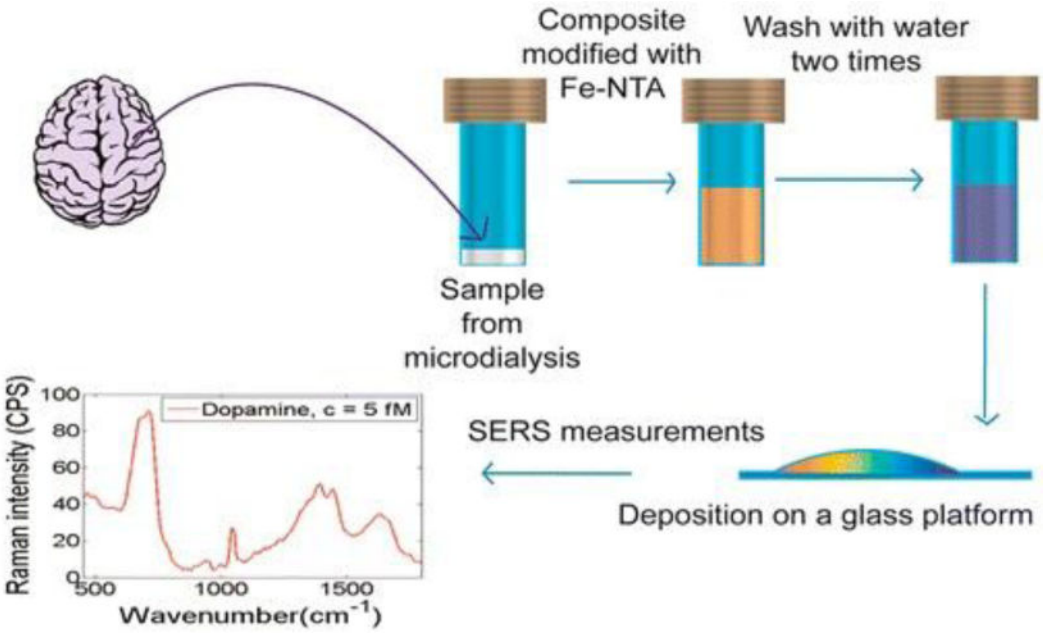

Fig. 16.

Determination of dopamine in an artificial sample of cerebrospinal fluid and in mouse striatum brain tissue using a Fe_3O_4/Ag nanocomposite. Reprinted (adapted) with permission from [313] Copyright (2014) American Chemical Society

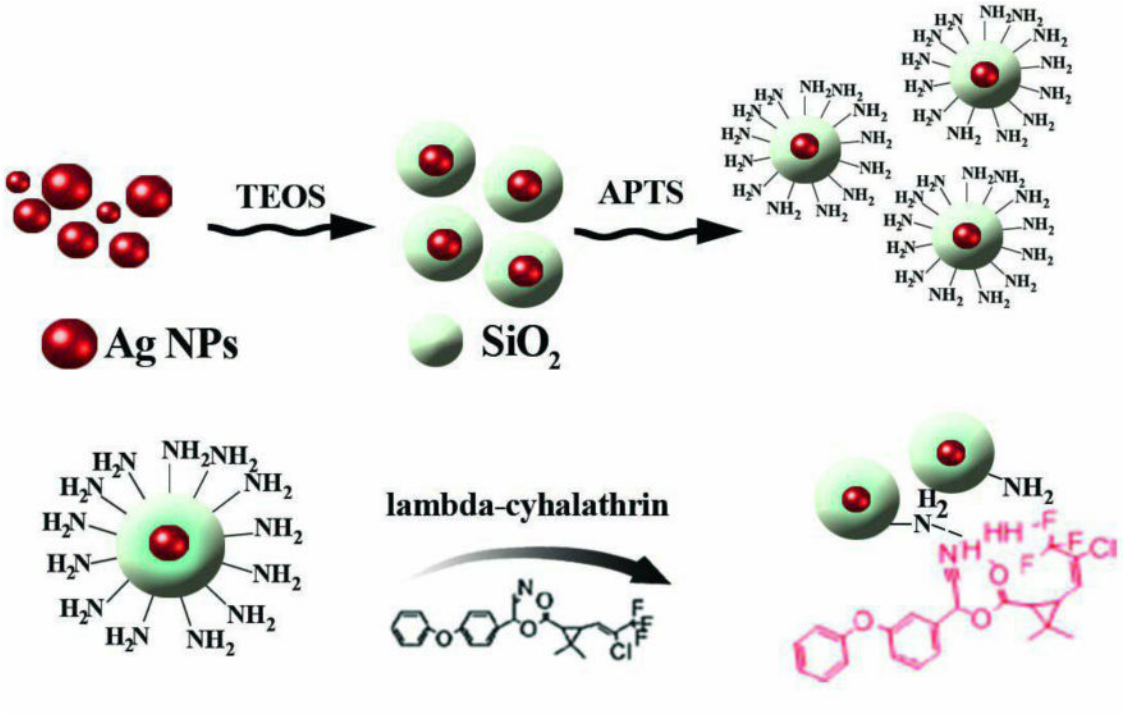

Fig. 17.

Schematic illustration of Ag@SiO_2-NH2 NPs detection of lambda-cyhalothrin (LC) [317]. Reprinted with permission

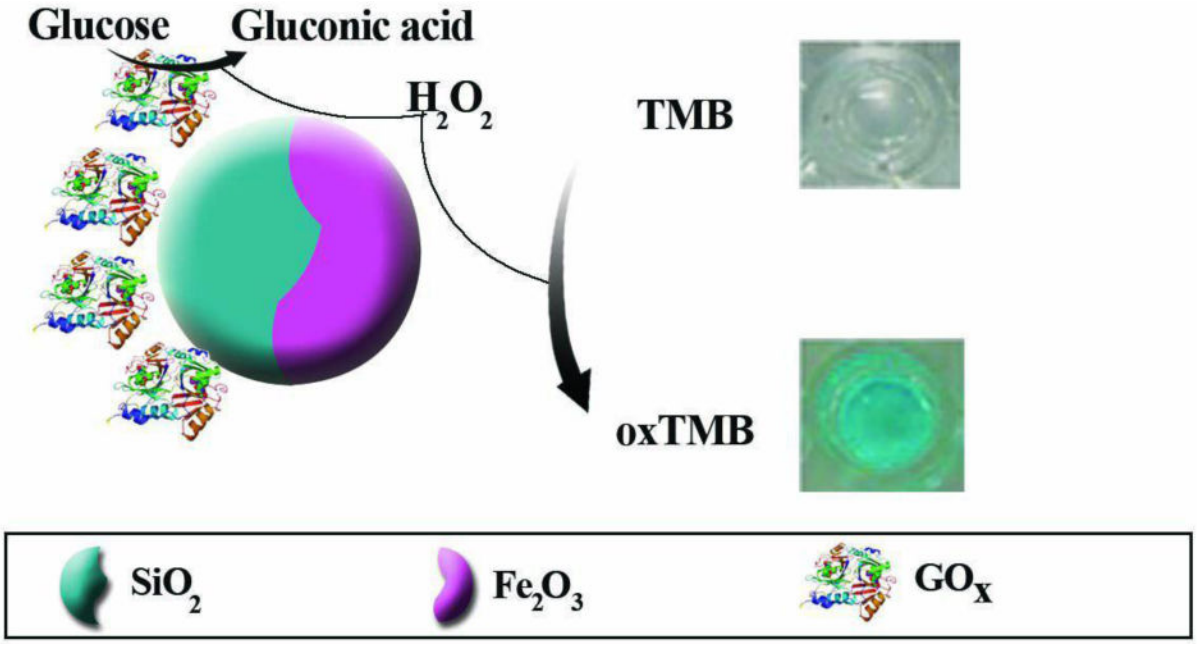

Fig. 18.

Schematic illustration of colorimetric detection of H_2O_2 and glucose by glucose oxidase and peroxidase-like activity of JFSNs. In presence of glucose, GOx catalyzes oxidation of glucose. Subsequently, glucoronic acid and H_2O_2 are produced. H_2O_2 decomposition is catalyzed by JFSNs, and if TMB is present a blue color is formed. Reprinted (adapted) with permission from [319] Copyright (2015) American Chemical Society.

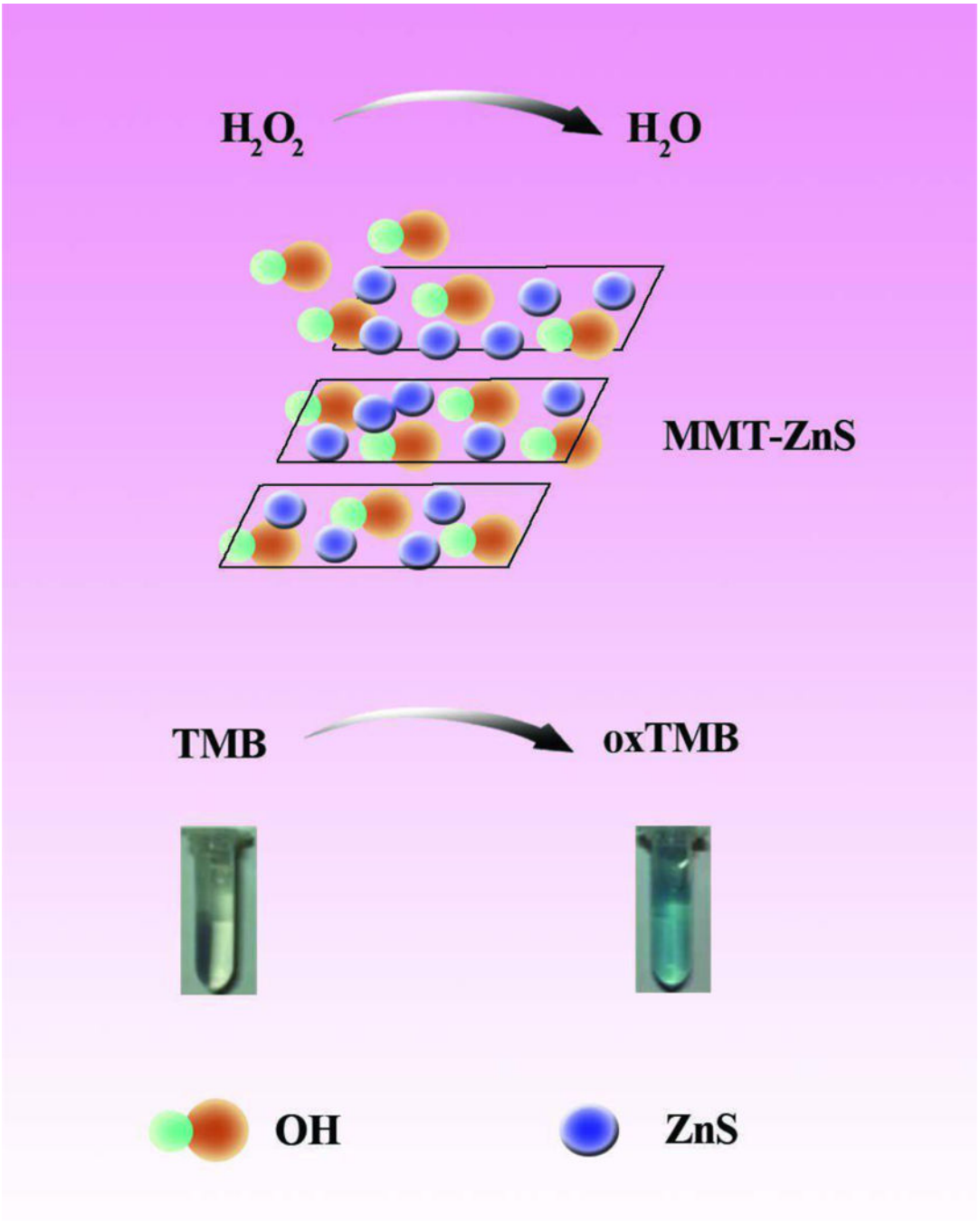

Fig. 19.

Schematic illustration of colorimetric detection of H_2O_2 by catalytic activity of ZnS-MMT nanocomposites. ZnS-MMT catalyzes the decomposition of H_2O_2 to OH radicals to oxidize TMB to form blue-colored oxTMB [329]. Reprinted with permission

Table 1

AuNP-based colorimetric detection using interparticle-crosslinking mediated aggregation

Target	Examples	Target of Nucleic Acids	Shape of AuNPs	Functionalization	Linear Range	LOD	Size of AuNPs	Ref
Pathogens	*Mycobacterium tuberculosis* (MTB) and *Mycobacterium tuberculosis* complex (MTBC)	Amplified target DNA.	NR	Thiol DNA-probe	20-0.5 pmol	1 pmol	13.7 ± 0.8 nm	[119]
	E,coli O157:H7	NR	Spherical	MEA-AuNPs	2.91×10^{8}–16×10^{8} CFU/mL^{-1}	10^{8} CFU/mL^{-1}	13 nm	[120]
	Pseudomonas syringae	Amplified target DNA.	Spherical	Thiol DNA-probe	200-2 ng/μl	15 ng/μL	13 nm	[69]
	Salmonella Typhimurium	Amplified target DNA.	Spherical	Thiol DNA-probe	NR	21.78 ng/μL	20 nm	[108]
	Helicobacter pylori	Amplified target DNA	Spherical	Thiol DNA-probe	NR	10 CFU/mL^{-1}	13 nm	[92]
Viruses	*Influenza A*	Viral RNA	Spherical	mAb-AuNPs	NR	7.8 HAU	13 nm	[110]
	Tomato leaf curl New Delhi virus (TolCNDV)	Amplified DNA target	Spherical	Thiol DNA-probe	NR	7.2 ng	19 nm	[114]
	papillomavirus type 16 and type 18	amplified DNA target	Spherical	Thiol DNAprobe	1.4×10^{0}-1.4×10^{-5} μM	1.4×10^{-4} μM	13 nm	[109]
Cancer	Cancerous Cells	-	Spherical	Ap-AuNPs	0-40000 cell	1000 cell	20, 50 and 100 nm	[63]
	MCF-7	-	Spherical	ssDNA-AuNP probes	10^{1}-10^{5} cell	10 cell	25 nm	[84]
	Breast Cancer Cells	-	Oval-shape	AuNPs- monoclonal anti-HER2/c-erb-2 antibody AuNPs- RNA aptamer	NR	100 cells/mL	14 nm length and 18 nm width	[121]
Metal Ions	Cd^{2+}, Ni^{2+} and Co^{2+}	-	Spherical	peptide- AuNPs	0-3 μM Cd^{2+}, 0-5 μM Ni^{2+}, 0-10 μM Co^{2+}	0.05 μM Cd^{2+}, 0.03 μM Ni^{2+}, 2μM Co^{2+}	NR	[122]
	pb^{2+}	-	Spherical	GSH-AuNPs	NR	100 nM	5-8 nm	[115]
	Hg^{2+}	-	Spherical	Chitosan-AuNPs	9-50 μM	1.35 μM	16 nm	[112]
	Al^{3+}	-	Spherical	MMT-AuNPs	1-10 μM	0.53 μM	12 nm	[117]
	Melamin, Hg^{2+}		Spherical	Cysteamine-AuNPs (CA-AuNPs)	0.05-3 μM Hg^{2+}, 0.08-1.6 μM Melamin	Hg^{2+}=30 nM, Melamin=80 nM	13± 2 nm	[123]
	Mg^{2+}		Spherical	Tryptophan-AuNPs	0.1-2.0 μmol L^{-1}	0.2 μmol L^{-1}	15 nm	[124]
Enzymes and Protein	Protein kinase activity		Spherical	STV-AuNPs	0.0005-0.05 U μL^{-1}.	0.0005-0.02 U μL^{-1}	13 nm	[81]
	Flt-1 protein	-	Spherical	p-AuNPs	0.2-10 nM	0.2 nM	13± 2nm	[118]
Others	Botulinum neurotoxin serotype A light chain (BoLcA)	-	Spherical	PEG –AuNPs, Eutravidin- AuNPs	NR	5-0.1 nM	20 nm	[88]
	H_2S	-	Spherical	AE-AuNPs	3–10 μM	0.2 μM	13 nm	[125]
	Spermine	-	Spherical	ctDNA-AuNPs assembly	0.1–2 μM	11.6 nM	13 nm	[126]

Analyst. Author manuscript; available in PMC 2019 July 21.

Target	Examples	Target of Nucleic Acids	Shape of AuNPs	Functionalization	Linear Range	LOD	Size of AuNPs	Ref
	Clenbuterol		Spherical	Cysteamine AuNPs	50 nM-1 μM	50 nM	10 nm	[127]

Table 2

AuNP-based colorimetric detection based on non-crosslinking aggregation mechanism

Types	Examples	Target of nucleic acids	Shape of AuNPs	Functionalization	Linear Range	LOD	Size of AuNPs	Ref
Bacteria	*E. coli*	unamplified genomic DNA	spherical	Thiolated DNA probe	215-27 ng	54 ng	20 nm	[131]
	Salmonella spp	Amplified by NASBA	_	Thiolated probe-AuNPs	10^0-0.5×10^4 CFUs/mL	5 CFUs	17-23 nm	[137]
	Salmonella typhimurium DT104	mAb-AuNPs	“Popcorn” shaped	mAb-AuNPs	NR	10^3 CFU/g	30 nm	[138]
Viruses	*Dengue virus* (DENV)	genomic RNA	-	DDZ-AuNP	1×10^1-1×10^6 TCID50 units	1×10^1 TCID50 units	15 nm	[139]
	Shrimp Taura syndrome virus (TSV)	RT LAMP Products	spherical	Thiolated-TSV oligonucleotide- AuNPs	100 pg–1 fg	1 pg total RNA	10-20 nm	[140]
Cancer biomarkerss	Breast cancer	-	spherical	peptide substrate	0-0.2 μg/mL	0.05 μg/mL	20 nm	[133]
Metal Ions	Hg^{2+}	-	spherical	Ds-DNA	. 25 nM to 1μM,	0.4 nM	12 nm	[141]
	Pb^{2+}	-	Anisotropic AuNPs and spherical AuNPs	DTT-AuNPs	1-1000 nM	~9 nM	~47nm	[142]
Fungus	*Paracoccidioides brasiliensis*	complementary DNA (cDNA)	spherical	Thiolated probe-AuNPs	NR	20 $ng/\mu L^{-1}$	23 nm	[143]
Others	SNPs and DNA mutations	complementary DNA	Nanospheres nanorods, nanotriangles	ssDNA- nanoparticles	NR	NR	AuNS: 40 (d) nm, AuNR: 20 (d)×42 nm, AuNR: 15 (d)×45 nm, AuNR: 13 (d) ×51 nm, AuNT: 20 (th)×50nm	[134]
	Nitrite	-	nanorods	4-Amino thiophenol-AuNPs (4-ATP)	0.25-5 ppm	<1 ppm	NR	[144]

Table 3

AuNP-based colorimetric detection based on unmodified AuNPs

Target	Examples	Target of Nucleic Acids	Shape of AuNPs	Linear Range	LOD	Size of AuNPs	Ref
Bacteria	*Acinetobacter baumannii*	Amplified ITS regions	Spherical	13–0.406 ng/μl^{-1}	0.8125 ng/μL	13±2 nm	[91]
	Mycobacterium, tuberculosis complex	PCR product and genomic DNA	Spherical	14.1–0.44 ng PCR product, 40–10 ng genomic DNA	1 ng for PCR product، 40 ng for genomic DNA	14±2 nm	[153]
Viruses	*Maize chlorotic mottle virus*	RT-PCR target products	Spherical	2.4 ng/μL-1.875 pg/μL	<30 pg/μL of RNA	13±2 nm	[154]
	Hepatitis C	HCV RNA	Spherical	25–2000 copies	50 copies reaction	15±2 nm	[159]
	Cucumber green mottle mosaic virus (GMMV)	RT-PCR target products	Spherical	120-3.375 pg/μL	30 pg/μL	13±2 nm	[160]
Biomarkers	*Plasmodium vivax* lactate dehydrogenase (*Pv*LDH), *Plasmodium falciparum* LDH (*Pf*LDH)	-	Spherical	0 pM–1 μM	1.25 pM and 2.94 pM	NR	[155]
	Carcinoma embryonic antigen (CEA)	-	Spherical	0-120 ng mL^{-1}	3 ng/mL	13 nm,	[146]
Proteins and Enzymes	VEGF protein	-	Spherical	NR	185 pM	-	[161]
	α-fetoprotein (AFP)	-	Spherical	50-1000 pg/mL	33.45 pg/mL	13 nm	[162]
	Tryptophan	-	Spherical	0.2-10 μM	0.1μM	13 nm	[163]
	Thrombin	-	Spherical	1 pM-5 μM	1 pM	15 nm	[151]
	Protein kinase	-	Spherical	0-1 U/μL	0.232 mU/μL	13 nm	[164]
	Caspase-3-activity	-	Spherical	0- 0.3 μg mL^{-1}	0.01 and 0.005μg/mL	13±1 nm	[152]
	α-Glucosidase activity and α-Glucosidase inhibitor	-	Spherical	0.0025-0.05 U mL^{-1}	0.001 U/mL	13nm	[165]
	hepatomaupregulated protein RNA	-	Spherical	NR	2.4 nmol/L	15nm	[166]
Drugs	Ramoplanin	-	Spherical	0.30-1.30 ppm	0.01 ppm	13nm and 23nm	[158]
	Methomphetamin	-	Spherical	2-10 μM	0.82μM	13 nm	[156]
	Steptomycin	-	Spherical	0-4000 nM	73.1 nM	15 nm	[157]
Metals Ions	Hg^{2+}		Spherical	NR	30 nM	13 nm	[167]
	Cd^{2+}	-	Spherical	0-50 μM	5 μM	~13 nm	[168]
	Cu^{2+}	-	Spherical	0.05-1.8 μmol.L^{-1}	30 nmol.L^{-1}	~13 NM	[169]
	Melamine	-	Spherical	1 mg/L-8×10^{-2} g/L	0.4 mg/L	13±1 nm	[170]
	Cu^{2+}	-	Spherical	0.5-10 μM	250 nM	13nm	[171]

Target	Examples	Target of Nucleic Acids	Shape of AuNPs	Linear Range	LOD	Size of AuNPs	Ref
	Hg^{2+}	-	Spherical	50-300 nM	15 nM	13 nm	[172]
	Hg^{2}	-	Spherical	0.5-10 nM	0.26 nM	15 nm	[173]
Others	Sulfide	-	Spherical	0-10 μM	80 nM	8.1± 1.1 nm	[174]
	Thiocyanate	-	Spherical	0-2 μM	1 μM	13 nm	[175]
	Hypochlorite	-	Spherical	NR	1.5μM	13 nm	[176]
	Urea	-	NR	20-150 mM	20 mM	NR	[177]
	17β-estradiol	-	-	$1\text{-}10^{5}$ ng/mL	0.1 ng/mL	13 nm	[178]
	Adenosine triphosphate (ATP)	-	Spherical	50-1000 nM	<50 nM	13 nm	[179]
	Adenosine triphosphate (ATP)	-	Spherical	0-5 μM	0.1 μM	14 nm	[180]
	Pork Adulteration	Genomic DNA	Spherical	NR	6 μg/mL	20 nm	[181]

Table 4

Applications of AuNPs and AgNPs

GNP/AgNP Shape/Size (nm)	Scientific base	Application	Ref.
Au Nano sphere 13 nm	SPR	DNA methylation detection	[214]
Au Nano rod Aspect Ratio(AR) = 4	SPR	Drug delivery	[215]
Au Nano rod	SPR	Photothermal therapy	[216, 217]
Au Nano sphere 40,60,100 nm	SERS	Embryonic stem cell differentiation imaging	[218]
Au Nano sphere 100 nm	Fluorescence quenching	DNA sensing	[219]
Au Nano sphere 15-100 nm	Electrochemical (voltammetry)	Hydroquinone detection, amitrole sensing	[58, 220]
Au Nano rod A.R.= 3.9	SPR, SERS	Cancer cell imaging, photothermal therapy	[221]
Au Nano sphere 35 nm	SPR, SERS	Oral cancer detection and sensing	[222]
Au Nano sphere 12 nm	Scattering and fluorescence	Cancer imaging	[223]
Au Nano sphere 47 nm	SPR, scattering and fluorescence	Tumor cell imaging, photothermal therapy	[224]
Au Nano rod AR = 3.5	Photoacoustic, SERS	Ovarian cancer detection	[225]
Au Nano sphere 13-21 nm	Electrochemical, SPR	Cholesterol sensing	[55]
Au Nano sphere 10-20 nm	Electrostatic interaction with pathogen cell, Immune response activation	Antimicrobial activity	[60]
Au Nano sphere	Electrostatic interaction with target cell	Anticancer activity, drug delivery	[226]
Ag Nano sphere 5-192 nm	Interaction with pathogen cell membrane	Antimicrobial and antifungal	[185, 189, 193–195, 197–199, 201, 203–205]
Ag Nano gate	Ag binding to thiol of GSH, fluorescence quenching	Targeted intracellular controlled drug delivery and tumor therapy, delivery monitoring	[211]
Ag Nano sphere, triangular	SPR	Ascorbic acid quantitative detection	[186]
Ag Nano sphere 2.5-28 nm	SPR	Phosphate, glutathione, Cu^{2+} assay	[208, 210, 213]
Ag Nano sphere 10-200 nm	Electron transfer	Catalyst	[187]
Ag Nano particle	SERS	Organochlorine pesticide, endosulfan sensing	[209]
Ag Nano sphere 60 nm	SERS, cell penetration	Sensing, therapeutics	[212]

Table 5

Colorimetric assays based on AgNPs

AgNP Surface modification or aggregation/dispersion agent	Analyte	Linear range	LOD	Ref.
Lysine	Hg(II)	1 nM-30 μM	1 nM	[227]
Gelatin	Hg(II)	0.5-800 nM	0.125 nM	[240]
Starch	Hg(II)	10 ppb - 1 ppm	-	[241]
Iminodiacetic Acid	Pb(II)	0.4-8 μM	13 nM	[231]
GSH	Pb(II)	0.5-4 μM	0.5 μM	[242]
GSH	Pb(II)	10^{-9}-10^{-3} M	10^{-9} M	[243]
-	Cr (VI)	10^{-9}-10^{-3} M	1 nM	[244]
Isonicotinic acid hydrazide	Cr(III)	10^{-6} -5×10^{-5} M	4.5×10^{-7} M	[245]
N-acetyl-L-cysteine	Ni(II)	2-48 μM	0.23 μM	[246]
Alizarin Red S	Al^{3+}	1-5.3 μM	0.12 μM	[247]
Dextrin	Cu(II)	50–200μM	50 μM	[213]
Sucrose	Endrin	0.05–5.00μg mL^{-1}	0.015 μg/mL	[248]
-	Melamine	0.002-0.25mM	2.32 μM	[249]
Sulfanilic acid	Melamine	0.1-3.1 μM	10.6 nM	[250]
Melamine	Cyanuric acid	1) 1.0–6.5 mg/L 2) 1-25 mg/L	1) 0.6 mg/L 2) 0.25 mg/L	[251]
SDS	Cyanide	16.7–133.3 μM	1.8 μM	[252]
Chitosan	Thiocyanate	1-14 ppm	1 ppm	[253]
p-aminobenzenesulfonic acid	Pymetrozine	0.02 to 0.09 mg/L	0.01 mg/L	[254]
-	Enterobacter cloacae P99 b-lactamase	5-600 pM	5 pM	[255]
Methylcellulose	Aerosol oxidative activity	5-25 ng	10 ng	[256]
Citrate	Quaternary ammonium surfactants	10^{-7}-5×10^{-5} M	< 5μM	[257]
ssDNA	Biological thiol	nM	nM	[258]
-	Calf intestine alkaline phosphatase Protein kinase A	-	1 unit/mL 0.022 unit/mL	[259]
Chitosan	Glucose	5.0 $\times10^{-6}$ -2.0 $\times10^{-4}$ M	100 nM	[260]

Table 6

Linear ranges and LODs of Ag-Au hybrid nanoprobes

NPs/modification	Analyte	Linear range	LOD	Detection base	Ref.
Au@Ag core-shell	HCOH	0.1–40 mM	50 nM	Shell formation	[267]
Au@Ag core-shell	Glucose	0.04 - 1 mM	10 nM	Shell formation	[271]
Ag@Au core-shell	Cyanide	0.4-32 μM	0.16 μM	Shell etching	[269]
Au@Ag core-shell	Cyanide	0.4–100 mM	0.4 mM	Shell etching	[274]
Ag@Au core-shell	Nitrite	1.0 - 20.0 μM	0.1 μM	Shell etching	[272]
Au@Agnanorod core-shell	Cu2+	3–1,000 nM	3 nM	Shell etching	[275]
Au@Ag core-shell	Iodide	0.5-80 mM	0.5 mM	Shell composition change	[273]
DNA-embedded core–shell Au@Ag	Glucose	0.00–0.20 and 1.00–100 μM	10 nM	Shell etching	[276]
Au@Ag core-shell	Glucose, cholesterol	0.5 - 400 mM 0.3-300 mM	0.24 mM 0.15 mM	Shell etching	[277]
Thiolated oligonucleotide functionalized Ag@Au core-shell	Target DNA	-	-	Aggregation	[279]
Au@Ag core-shell	H_2S	50 nM - 100 μM	50 nM	Shell composition changing	[280]
Ag-Au alloy NP	Hg	0.02–100 ppb	0.01 ppb	Shell composition changing	[281]
Oligonucleotide functionalized Ag-Au alloy NP	Target DNA	-	-	Aggregation	[268]

Table 7

Methods for the synthesis of MNPs [285]

Method	Physical	Gas-phase deposition
		Electron beam lithography
	Chemical	Sol-gel synthesis
		Oxidation Method
		Chemical co-precipitation
		Hydrothermal reaction
		Flow injection synthesis
		Electrochemical method
		Aerosol/vapor phase method
		Sonochemical decomposition reactions
		Supercritical fluid method
		Synthesis using nanoreactors
	Biological	Microbial incubation

Table 8

Colorimetric detection based on other inorganic NPs

Type of Inorganic NPs	NPs	Targets	Functionalization	Linear Range	LOD	Size of NPs	Ref
SiO_2NPs	SiO_2	Cd^{2+}	NR	10^{-1}-10^{-9} M	1×10^{-8}M	-	[330]
	Ag@SiO_2 core shell	Pyrethroids	Amine (NH2)	1.0×10^{-6}-2.0×10^{-3}	1×10^{-6}M	Ag@SiO_2 =30 nm	[317]
	SiO_2	2,4,6-trinitrotoluene (TNT)	3-aminopropyl-triethoxysilane (APTES)	500 nM-3.0 mM	100 μM	240 ± 10 nm	[331]
	Au@SiO_2 core shell	Hg^{2+}	Porphyrin	5-10 ppb	1.2 ppb for Hg^{2+}	Au@SiO_2 core/shell = 40 nm	[332]
	Fe_3O_4@SiO_2 core shell	Hg^{2+}	Porphyrin	NR	NR	core shell = 500 nm	[333]
	Ag@SiO_2 NPs	Hg^{2+}	Amine-SiO_2	NR	5 μM	AgNPs = 14 nm SiO_2 NP s = 250nm	[334]
	γ-Fe_2O_3/SiO_2	H_2O_2 and Glucose	GOX	1-100 μM of H_2O_2, 0-20 μM of glucose	10.6 nM of H_2O_2, 3.2 μM of glucose	γ-Fe_2O_3/SiO_2= ~20-120 nm	[319]
Zinc oxide and ZnS NPs	ZnO NPs/CNTs	Cholesterol	NR	0.5-500 nM	0.2 nM	NR	[324]
	ZnO/ZnS core shell nanoparticles	Cu^{2+}	NR	15-1500 μM	15 μM (~0.96 ppm)	NR	[323]
	ZnS	H_2O_2	ZnS-MMT nanocomposites	0.07-0.6 mM	1.04838×10^{-5} M	30-40 nm	[335]
Titanumoxid NPs	mesoporous TiO_2	Bi(III) ions	NR	0.001-1 ppb	1 ppb.	10 nm	[326]
	SiO_2 TiO_2	Hg^{2+}	Azobenzene-coupled receptor SiO_2 and TiO_2 (AR-SiO_2@ AR-TiO2)	NR	28 nM	mesoporous silica and the AR-SiO_2 = 2.24 and 2.15 nm TiO_2 and AR-TiO_2 = 30-60	[336]